CLRDV-AL Encoded Suppressor of RNA Silencing and its Impact on Pathogenicity

by

Mary Funmilayo Akinyuwa

A thesis submitted to the Graduate Faculty of
Auburn University
in partial fulfillment of the
requirements for the Degree of
Master of Science

Auburn, Alabama
December 9, 2023

Keywords: Polerovirus, RNA silencing, silencing suppression, host-pathogen interaction, virus protein, plant resistance

Approved by

Sung-Hwan Kang, Chair, PhD, Assistant Professor of Plant Pathology
Leonardo De La Fuente, Committee member, PhD, Professor of Plant Pathology
Sang-Wook Park, Committee member, PhD, Associate Professor of Plant Pathology

Abstract

Cotton contributes to a broad range of industries like textile, food, and healthcare industries. However, it is prone to different pests and diseases. One such is the cotton blue disease caused by the Cotton leafroll dwarf virus (CLRDV). This virus caused about 80% yield loss in South America. A new strain (CLRDV-AL) was reported for the first time in the United States. CLRDV-AL contains a resistance-breaking amino acid motif, making available resistant cultivars inefficient for its management. This poses a huge risk to the US cotton industry. Therefore, the CLRDV-AL function and virulence mechanism need to be dissected to identify candidate-resistant genes for developing resistant cotton varieties. I aim to characterize the viral suppressor of RNA silencing encoded by CLRDV-AL and its distinction from P0 proteins from other strains (Objective 1). For this, I hypothesize that CLRDV-AL VSR protein has a weak silencing suppression potency. After this, I will evaluate the risk associated with CLRV-AL virulence by introducing point mutations to significant amino acid residues of P0 (Objective 2). Here I predict that a conserved F-box-like motif affects P0 pathogenicity. Hence, host-virus interaction. To achieve this, P0 proteins from three strains and mutant derivatives will be examined for VSR potency, host response, and intracellular localization. My results will provide key information about the role of P0 in the CLRDV-AL infection cycle, and virulence propensity. This will provide a basis for developing molecular biocontrol of potential new variants of CLRDV that may pose a greater threat in cotton.

Chapter 2 of this thesis was published in Frontiers in Agronomy (Akinyuwa et al., 2023; | https://doi.org/10.3389/fagro.2023.1235168). Chapter 3 was submitted to Virus Research (Akinyuwa and Kang, 2023) and is currently under review.

Acknowledgment

Emerging with greater strength. That is the summary of my experience during this journey. While some may say, ‘There is nothing new under the sun’. For someone like me who took pride in seeing every task through to completion, this was new and unanticipated under my sun. Nevertheless, I would like to thank Dr. Sung-Hwan Kang for giving me the opportunity to pursue science in this great land of endless possibilities. Every push encouraged me to find my niche and affirmed that contributing to science while making a positive impact in people’s lives is the highest degree of fulfillment I sought.

I am deeply grateful for the unexcepted kindness, support, and continuous mentorship I was fortunate to receive from Drs. Alex Harkess, Kathy Lawrence, and Turina Massimo. Their enduring belief in my abilities and genuine commitment to my growth greatly enriched my life and bestowed upon me an unparalleled pair of opportunities. To the other members of my committee, Drs. Leonardo de Lafuente and Sang-Wook Park, I appreciate your insightful feedback, support, and constant challenge to foster critical thinking in my research endeavors. Additionally, I extend my gratitude to Drs. David Held and Arthur Appel for their attentive ears during moments of seemingly insurmountable challenges. Your wisdom and gesture left an enduring mark on my memory.

The connections I nurtured and forged during my 730-day journey at Auburn University are precious treasures and will forever occupy a special place in my heart. Therefore, I want to deeply thank my family; my parents and siblings (Damilola Akinyuwa, Elijah Akinyuwa, and David Akinyuwa) for being with me every step of the way. I am deeply grateful for your unwavering presence, even during those late-night and early-morning calls that bridged the time difference. Your love, unwavering actions, and steadfast support contributed to the pillars of stability in my life. This constancy was a source of great strength for me over the years. I consider myself truly fortunate to have you in my life. To my friends turn family, Dorcas Adejumobi, Adunola Paul, Parbati Thapa, Aliya Yagafarova, and Karamjit Kaur. Thank you for standing by me and riding with me. Finally, Seun Oladipupo, thank you for being my Proverb 18:24 man. I am grateful for your support and willingness to take a nosedive into this journey alongside me. Your cheers, encouragement, gentle push, and moments you literally carried me meant a great deal to me.

Dedication

I dedicate this achievement to God. Only He made a way and gave me the strength to complete this phase gracefully.

Table of Contents

List of Tables

Chapter 3

List of Figures

List of Abbreviations

RNA	Ribonucleic acid
VSR	Viral suppressor of RNA silencing
RNAi	RNA interference
siRNA	Small interfering RNA
CLRDV	Cotton leafroll dwarf virus
AL	Alabama
ty	Typical
at	Atypical
ROS	Reactive oxygen species
PR	Pathogenicity-related
R	Resistance
miRNA	Micro RNA
amiRNA	artificial micro-RNA
NB-LRR	Nucleotide-binding-Leucine-rich repeat
GFP	Green fluorescent protein
HC-Pro	Helper component proteinase
ORF	Open reading frame

Chapter 1

Cotton and Cotton Leafroll Dwarf Virus (CLRDV) in The United States: Menace, Threat, and Management

1.1 Cotton Production in The U.S. and Pest Emergence.

Cotton is the king of fibers. It remains one of the most comfortable and durable textiles (Hosseini Ravandi & Valizadeh, 2011). Cotton was a revolutionary tool for world industrialization. It brought continents together and has arguably been a source of disputes through religion, politics, law, art, and economics (Chabi Simin Najib et al., 2022; Estur & Gergely, 2010; Higgins, 1968; Jakes & Shokr, 2017; Kulshrestha & Agrawal, 2019; Lee & Fang, 2015). Cotton production dates back to as early as 600 B.C. in India, then spread to Europe, before becoming the most cultivated commodity in America (Gumber et al., 2014). Africa has also played a crucial role in supporting cotton accessibility for international trade (Chabi Simin Najib et al., 2022).

The United States is currently the 3rd leading cotton producer globally (Online Clothing Study, 2023). In the past 9 years, the average cotton production is 16.47 million bales (Shahbandeh, 2023). This is a 9.6% decrease from production in the last 18 years. This reduction arguably correlates with pests and pathogen incidence. Notable insects like Mexican boll weevil, whitefly, aphids inflict substantial yield loss through feeding activity (Correa et al., 2005; Cox et al., 2019; Da Silva et al., 2015; Jalloul et al., 2015; Naqvi et al., 2019; Rajendran et al., 2018; Shaban et al., 2018; Tarazi et al., 2019; Tarazi & Vaslin, 2022). Additionally, they transmit viral pathogens like Cotton leafroll dwarf virus (CLRDV) and Cotton leaf curl virus (Allen et al., 2018; Heilsnis et al., 2023; Luttrell et al., 2015; Pan et al., 2018). Also, environmental factors like extreme heat, salt, and drought stress can cause significant yield reduction in cotton (Farooq et al., 2023; Saleem et al., 2021; N. Wang et al., 2017).

1.2 CLRDV, An Emerging Threat to The Cotton Industry

Cotton leafroll dwarf virus (CLRDV) is the second most damaging viral pathogen of cotton (Agrofoglio et al., 2019; Akinyuwa et al., 2023; Conner et al., 2022; Distéfano et al., 2010). It causes a wide range of symptoms like leaf curling, distortion, leaf cupping, and discoloration of veins (Avelar et al., 2019). Sometimes, the virus maintains a cryptic status on the field, where

infected plants are mostly asymptomatic and symptomatic plants do not always test positive for the virus using an amplification-based serological detection method (Akinyuwa et al., 2023; Bag et al., 2021). CLRDV caused up to 80% yield loss in susceptible varieties in the South America (Silva et al., 2008). CLRDV has an RNA genome with seven open reading frames (ORFs) that encode proteins crucial to its host infection (Distéfano et al., 2010; King et al., 2012; Smirnova et al., 2015). CLRDV also has a high mutation rate due to the lack of proofreading activity in its RNA polymerase (Rubio et al., 2020).

There are two notable strains of CLRDV: typical (ty) and atypical (at).These strains have varying levels of virulence propensity and ability to break host resistance (Agrofoglio et al., 2019; Da Silva et al., 2015; Nishiguchi & Kobayashi, 2011). CLRDV-AL, an isolate found in Alabama was the first reported case of CLRDV in The U.S. and has since spread to other cotton growing region of the United States known as US Cotton Belt (Aboughanem-Sabanadzovic et al., 2019; Alabi et al., 2020; A. Ali & Mokhtari, 2020; Avelar et al., 2019; Faske et al., 2020; Tabassum et al., 2019). Hence, there is need to find an effective and environmentally sustainable management strategy before it becomes a ‘CLRDV Pandemic’.

1.3 Managing Viral Pathogens

Curing viral infection is not feasible (Rubio et al., 2020). However, plants have evolved to utilize various defensive strategies to minimize the damage by virus invasion. These include RNA silencing, protein degradation, receptor signaling, and hormone-mediated defense (Calil & Fontes, 2017; Mandadi & Scholthof, 2013; Schwessinger & Ronald, 2012; Wu et al., 2019). As a result, virus infection is managed by optimizing these defense processes. Some techniques used are prophylaxis, immunization with antiviral compounds or peptides, and cross-protection (Cong et al., 2019; Manjunatha et al., 2022; Rubio et al., 2020).

Prophylaxis involves the use of legislative measures to restrict the movement and spread of infected propagative materials and vectors to manage plant viruses (Rubio et al., 2020). Immunization involves breeding for resistance using active resistance proteins which could reduce virus virulence and movement or passive resistance involving host factors. A good example is the introduction of artificial micro-RNA (amiRNAs) into a plant to create a resistant or tolerant variety (Fahim et al., 2012). Endogenous micro-RNAs (miRNAs) are naturally involved in triggering the activation of resistance (R) genes by Nucleotide-binding-Leucine-rich repeat (NB-LRR) receptor

signaling upon detecting exogenous invasion. They have been utilized to target messenger RNAs (mRNAs) for degradation or translation suppression. Endogenous or exogenous stimuli could trigger the production of miRNAs, and it can protect a plant upon viral infection (Khalid et al., 2017; Lu et al., 2008; Voinnet, 2009; Zhai et al., 2011).

Artificial miRNAs function by either directly cleaving viral RNAs or aiding the production of siRNA as an antiviral response in the host and as a viral counter-defense tool (S.-R. Liu et al., 2017; Roberts et al., 2011). It has been effective for the management of *Plum Pox virus* (PPV), *Tobacco mosaic virus* (TMV), *Turnip yellow mosaic virus* (TYMV), *Rice black streaked dwarf virus* (RBSDV), *Rice stripe virus* (RSV), *Wheat streak mosaic virus* (WSMV), *Tomato leaf curl virus* (ToLCV), *Grapevine fanleaf virus* (GFLV), and *Turnip mosaic virus* (TuMV) in *Arabidopsis thaliana*, *Nicotiana benthamiana*, *N. tabacum*, tomato, potato, rice, grapevine, and maize (Amin et al., 2011; Jelly et al., 2012; F. Li et al., 2012; S.-R. Liu et al., 2017; Pacheco et al., 2012; Simón-Mateo & García, 2006; Sun et al., 2016; Vu et al., 2013; Xuan et al., 2015).

Mild virus strains can also provide cross-protection by priming plants against virulent strains (Pechinger et al., 2019). This method is used to manage economically important diseases in the absence of other effective measures (Rubio et al., 2020). Putting together, understanding the infection cycle of a virus by characterizing the function of its protein will help identify utilizable components for sustainable management tactics of novel viruses.

1.4 Developing Novelty and Preliminary Characterization of CLRDV-AL Proteins

It is imperative to dissect the molecular components of a virus for its sustainable management. This can be achieved through the molecular characterization of viral proteins and host-virus interaction. Some crucial observation involves subcellular localization of virus protein in plant, colocalization with host proteins, protein-protein interaction among virus-encoded proteins / virus-host protein interaction, and host responses (S. Ali et al., 2018; Komatsu et al., 2010; H. Li et al., 2020; Paape et al., 2006; Rodriguez-Peña et al., 2021; Schoelz et al., 2011; Widana Gamage & Dietzgen, 2017). Self-interaction of viral proteins is sometimes required for certain viral functions. For example, self-interaction of the 2b protein of *Cucumber mosaic virus* (CMV) and HC-Pro in *Turnip mosaic virus* (TMV) are responsible for viral suppressor of RNA silencing (VSR) activity; a viral protein involved in the counter defense against host's RNA silencing defense pathway (Han et al., 2016; Xu et al., 2013). Also, interaction among encoded

proteins like CMV 1a and 2b protein selectively regulates the function of viral suppressors of RNA silencing (VSRs) (Watt et al., 2020).

CLRDV-AL has seven ORFs that encode its proteins (as shown in Appendices Figure 1). ORF 0; encodes P0, a viral suppressor of RNA silencing. ORF1 and ORF2 encode P1 and P1-P2, involved in RNA dependent RNA polymerase (RdRp), ORF 3a and ORF 4 encode P3a and P4 responsible for virus movement. Finally, ORF 3 and ORF3-5 encode P3 and P3-5 proteins involved in major and minor coat proteins (Avelar et al., 2020; Delfosse et al., 2021). Initial screening of some selected CLRDV-AL proteins indicated that only the major coat protein P3 which is encoded by ORF3 undergoes self–interaction (Appendices Figure 2). Also, the overexpression of these recombinant proteins in host (Appendices Figure 3) showed that P0 which is encoded by ORF 0 upregulated *pathogenicity-related (PR)-2* and *PR-6* while P3, and P4 encoded by ORF 3, and 4 respectively upregulated only *PR-2* in *N. benthamiana* (Appendices Figure 4). Furthermore, the expression of individual CLRDV-AL protein resulted in the burst of reactive oxygen species (ROS) in infiltrated patches on leaves. Although, patches infiltrated with P0 showed a strong dark brown stain. Putting together, this suggests the involvement of P0 in CLRDV-AL pathogenicity (Appendices figure 5).

Viral proteins or RNAs often hijack host proteins, and traffick them to other subcellular locations where they support the virus infection by stimulating negative-strand RNA synthesis, promoting translation, formation of replication compartment, downregulating antiviral response or increasing reactive oxygen species (ROS) (Chen et al., 2013; Hyodo et al., 2019; Jungfleisch et al., 2015; Mathioudakis et al., 2013; R. Y.-L. Wang & Nagy, 2008). TAV protein of *Cauliflower mosaic virus* (CaMV) hijacks *A. thaliana* RISP protein into cytoplasmic and nuclear inclusion bodies where it stimulates the viral translation (Thiébeauld et al., 2009). Preliminary observation of CLRDV-AL proteins demonstrated a similar localization pattern as other Poleroviruses (Appendices Figure 6). However, P3, P4, and P0 formed inclusion bodies along the membrane or in the cytoplasm. Exploring the function of such localization patterns and identifying host proteins interacting with CLRDV-AL proteins at these locations would be important to understand the infection cycle of this virus and, potentially, the innovative management strategies.

Viral suppressors of RNA silencing (VSRs), a viral protein used to counteract the host antiviral defense, RNA silencing, which degrades viral genomes often inhibit miRNA-directed processes.

Hence, contribute to viral pathogenicity and disease severity of many viruses (Chapman et al., 2004; Kasschau et al., 2003; F. Liu et al., 2008; Shen et al., 2012). These influences plant gene expression, metabolism, and development. For example, CMV 2b protein regulates auxin response pathways. The 2b protein from a severe strain reduces plant root elongation. However, the mixture of 2b protein from a mild and severe strain increases root elongation (Verchot-Lubicz & Carr, 2008). Similarly, P1/HC-Pro, a VSR of TuMV triggers flower development defects, stunting, and reduced internodal distances due to ectopic cell division on non-meristematic tissues, interference with hormone production, and defense signaling (Kasschau et al., 2003). Thus, the characterization of CLRDV-AL VSR will provide information about its functions, interacting host partners, and mechanism as a basis in understanding its role in viral pathogenicity. This will serve as preliminary information for developing resistant varieties and other innovative biotechnological resources for managing CLRV in the United States.

1.5 Study Objectives

The objectives of this study were to characterize the CLRDV-AL encoded suppressor of RNA silencing and its impact on pathogenicity. Specifically,

a) Characterization of a Viral Suppressor of RNA silencing encoded by CLRDV AL and its distinction from P0 proteins from other strains.

The goal of objective a) is to understand the cryptic nature and level of pathogenicity of CLRDV-AL strain in the United States.

b) Evaluate the risk associated with CLRV-AL virulence by introducing point mutations to significant amino acid residues of P0.

The goal of objective b) is to determine if any mutation within the critical protein domain can aggravate the virulent potency of CLRDV.

Long term, the identified important molecular traits of CLRDV VSR proteins can be exploited for the development of resistant cotton varieties to manage CLRDV in the U.S.

1.6 References

Aboughanem-Sabanadzovic, N., Allen, T. W., Wilkerson, T. H., Conner, K. N., Sikora, E. J., Nichols, R. L., & Sabanadzovic, S. (2019). First report of Cotton Leafroll Dwarf Virus in upland cotton (*Gossypium hirsutum*) in Mississippi. *Plant Disease*, *103*(7), 1798. doi: 10.1094/PDIS-01-19-0017-PDN

Agrofoglio, Y. C., Delfosse Ab, V. C., Casse, M. F., Hopp, H. E., Bonacic Kresic, I., Ziegler-Graff, V., & Dist Efano, A. J. (2019). P0 protein of Cotton Leafroll Dwarf Virus-atypical isolate is a weak RNA silencing suppressor and the avirulence determinant that breaks the cotton Cbd gene-based resistance. *Plant Pathology*, 68(6). doi: 10.1016/j.virusres.2013.12.018

Akinyuwa, M. F., Price, B. K., Martin, K. M., & Kang, S.-H. (2023). A newly isolated cotton-infecting Polerovirus with cryptic pathogenicity encodes a weak suppressor of RNA silencing. *Frontiers in Agronomy* doi: 10.3389/fagro.2023.1235168

Alabi, O. J., Isakeit, T., Vaughn, R., Stelly, D., Conner, K. N., Gaytán, B. C., Villegas, C., Hitzelberger, C., De Santiago, L., Monclova-Santana, C., & Brown, J. K. (2020). First report of Cotton Leafroll Dwarf Virus infecting upland cotton (*Gossypium hirsutum*) in Texas. *Plant Disease*, *104*(3), 998. doi: 10.1094/PDIS-09-19-2008-PDN

Ali, A., & Mokhtari, S. (2020). First report of Cotton Leafroll Dwarf Virus infecting cotton (*Gossypium hirsutum*) in Kansas. *Plant Disease*, *104*(6), 1880. doi: 10.1094/PDIS-12-19-2589-PDN

Ali, S., Ganai, B. A., Kamili, A. N., Bhat, A. A., Mir, Z. A., Bhat, J. A., Tyagi, A., Islam, S. T., Mushtaq, M., Yadav, P., Rawat, S., & Grover, A. (2018). Pathogenesis-related proteins and peptides as promising tools for engineering plants with multiple stress tolerance. *Microbiological Research*, *212–213*, 29–37. doi: 10.1016/j.micres.2018.04.008

Allen, K. C., Luttrell, R. G., Sappington, T. W., Hesler, L. S., & Papiernik, S. K. (2018). Frequency and abundance of selected early-season insect pests of cotton. *Journal of Integrated Pest Management*, *9*(1), 20. doi: 10.1093/jipm/pmy010

Amin, I., Patil, B. L., Briddon, R. W., Mansoor, S., & Fauquet, C. M. (2011). A common set of developmental miRNAs are upregulated in *Nicotiana benthamiana* by diverse begomoviruses. *Virology Journal*, *8*(1), 143. doi: 10.1186/1743-422X-8-143

Avelar, S., Ramos-Sobrinho, R., Conner, K., Nichols, R. L., Lawrence, K., & Brown, J. K. (2020). Characterization of the complete genome and P0 protein for a previously unreported genotype of Cotton Leafroll Dwarf Virus, an introduced polerovirus in the United States. *Plant Disease*, *104*(3), 780–786. doi: 10.1094/PDIS-06-19-1316-RE/ASSET/IMAGES/LARGE/PDIS-06-19-1316-RE_T2

Avelar, S., Schrimsher, D. W., Lawrence, K., & Brown, J. K. (2019). First report of Cotton Leafroll Dwarf Virus associated with Cotton Blue Disease symptoms in Alabama. doi: 10.1094/PDIS-09-18-1550-PDN, 103(3), 592–592.

Bag, S., Roberts, P. M., & Kemerait, R. C. (2021). Cotton Leafroll Dwarf Disease: An emerging virus disease on cotton in the U.S. *Crops & Soils*, *54*(2), 18–22. doi: 10.1002/crso.20105

Calil, I. P., & Fontes, E. P. B. (2017). Plant immunity against viruses: Antiviral immune receptors in focus. *Annals of Botany*, *119*(5), 711–723. doi: 10.1093/aob/mcw200

Chabi Simin Najib, D., Fei, C., Dilanchiev, A., & Romaric, S. (2022). Modeling the impact of cotton production on economic development in Benin: A technological innovation perspective. *Frontiers in Environmental Science*, *10*. doi: 10.3389/fenvs.2022.926350

Chapman, E. J., Prokhnevsky, A. I., Gopinath, K., Dolja, V. V., & Carrington, J. C. (2004). Viral RNA silencing suppressors inhibit the microRNA pathway at an intermediate step. *Genes & Development*, *18*(10), 1179–1186. doi: 10.1101/gad.1201204

Chen, I.-H., Chiu, M.-H., Cheng, S.-F., Hsu, Y.-H., & Tsai, C.-H. (2013). The glutathione transferase of *Nicotiana benthamiana* NbGSTU4 plays a role in regulating the early replication of Bamboo mosaic virus. *The New Phytologist*, *199*(3), 749–757. doi: 10.1111/nph.12304

Cong, Q. Q., Wang, Y., Liu, J., Lan, Y. F., Guo, Z. K., Yang, J. G., Li, X.-D., & Tian, Y. P. (2019). Evaluation of Potato Virus X mild mutants for cross protection against severe infection in China. *Virology Journal*, *16*(1), 36. doi: 10.1186/s12985-019-1143-7

Conner, K., Sikora, E., Koebernick, J., & Zaccaron, M. (2022). Interdisciplinary Team Addresses Cotton Leafroll Dwarf Virus in Alabama. *Journal of Extension*, *60*(2). doi: 10.34068/joe.60.02.09

Correa, R., Silva, T., Simoes-Araujo, J., Barroso, P., Vidal, M., & Vaslin, M. (2005). Molecular characterization of a virus from the family *Luteoviridae* associated with cotton blue disease. *Archives of Virology*, *150*, 1357–1367. doi: 10.1007/s00705-004-0475-8

Cox, K. L., Babilonia, K., Wheeler, T., He, P., & Shan, L. (2019). Return of old foes—Recurrence of bacterial blight and Fusarium wilt of cotton. *Current Opinion in Plant Biology*, *50*, 95–103. doi: 10.1016/j.pbi.2019.03.012

Da Silva, A. K. F., Romanel, E., Silva, T. da F., Castilhos, Y., Schrago, C. G., Galbieri, R., Bélot, J.-L., & Vaslin, M. F. S. (2015). Complete genome sequences of two new virus isolates associated with cotton blue disease resistance breaking in Brazil. *Archives of Virology*, *160*(5), 1371–1374. doi: 10.1007/s00705-015-2380-8

Delfosse, V. C., Barrios Barón, M. P., & Distéfano, A. J. (2021). What we know about poleroviruses: Advances in understanding the functions of polerovirus proteins. *Plant Pathology*, *70*(5), 1047–1061. doi: 10.1111/ppa.13368

Distéfano, A. J., Bonacic Kresic, I., & Hopp, H. E. (2010). The complete genome sequence of a virus associated with cotton blue disease, cotton leafroll dwarf virus, confirms that it is a new member of the genus Polerovirus. *Archives of Virology*, *155*(11), 1849–1854. doi: 10.1007/s00705-010-0764-3

Estur, G., & Gergely, N. (2010). *The Economics of Roller Ginning Technology and Implications for African Cotton Sector*. World Bank. doi: 10.1596/27585

Fahim, M., Millar, A. A., Wood, C. C., & Larkin, P. J. (2012). Resistance to Wheat Streak Mosaic Virus generated by expression of an artificial polycistronic microRNA in wheat. *Plant Biotechnology Journal*, *10*(2), 150–163. doi: 10.1111/j.1467-7652.2011.00647.x

Farooq, M. A., Chattha, W. S., Shafique, M. S., Karamat, U., Tabusam, J., Zulfiqar, S., & Shakeel, A. (2023). Transgenerational impact of climatic changes on cotton production. *Frontiers in Plant Science*, *14*. doi: 10.3389/fpls.2023.987514

Faske, T. R., Stainton, D., Aboughanem-Sabanadzovic, N., & Allen, T. W. (2020). First Report of Cotton Leafroll Dwarf Virus from upland cotton (*Gossypium hirsutum*) in Arkansas. *Plant Disease*, *104*(10), 2742. doi: 10.1094/PDIS-12-19-2610-PDN

Gumber, R., S, G., Rathore, P., Pathak, D., S, G., P, S., Singh, K., Singh, S., P, P., Kour, A., & Sarlach, R. (2014). *History and status of cotton* (pp. 1–10).

Guo, W. L., Chen, B. H., Guo, Y. Y., Yang, H. L., Mu, J. Y., Wang, Y. L., Li, X. Z., & Zhou, J. G. (2019). Improved Powdery Mildew resistance of transgenic *Nicotiana benthamiana* overexpressing the *Cucurbita moschata* CmSGT1 Gene. *Frontiers in Plant Science*, *10*, 955–955. doi: 10.3389/FPLS.2019.00955/BIBTEX

Han, J.-Y., Chung, J., Kim, J., Seo, E.-Y., Kilcrease, J. P., Bauchan, G. R., Lim, S., Hammond, J., & Lim, H.-S. (2016). Comparison of helper component-protease RNA silencing suppression activity, subcellular localization, and aggregation of three Korean isolates of Turnip mosaic virus. *Virus Genes*, *52*(4), 592–596. doi: 10.1007/s11262-016-1330-1

Heilsnis, B., Mahas, J. B., Conner, K., Pandey, S., Clark, W., Koebernick, J., Srinivasan, R., Martin, K., & Jacobson, A. L. (2023). Characterizing the vector competence of Aphis gossypii, Myzus persicae and Aphis craccivora (Hemiptera: Aphididae) to transmit cotton leafroll dwarf virus to cotton in the United States. *Journal of Economic Entomology*, *116*(3), 719–725. doi: 10.1093/jee/toad080

Higgins, J. P. P. (1968). S. Shapiro. Capital and the cotton industry in the industrial revolution. *The Economic Journal*, *78*(311), 705–707. doi: 10.2307/2229412

Hosseini Ravandi, S. A., & Valizadeh, M. (2011). 2—Properties of fibers and fabrics that contribute to human comfort. In G. Song (Ed.), *Improving Comfort in Clothing* (pp. 61–78). Woodhead Publishing. doi: 10.1533/9780857090645.1.61

Hyodo, K., Suzuki, N., & Okuno, T. (2019). Hijacking a host scaffold protein, RACK1, for replication of a plant RNA virus. *New Phytologist*, *221*(2), 935–945. doi: 10.1111/nph.15412

Jakes, A. G., & Shokr, A. (2017). Finding value in empire of cotton. *Critical Historical Studies*, *4*(1), 107–136. doi: 10.1086/691060

Jalloul, A., Sayegh, M., Champion, A., & Nicole, M. (2015). Bacterial blight of cotton. *Phytopathologia Mediterranea*, *54*(1), 3–20. doi: 10.14601/Phytopathol_Mediterr-14690

Jelly, N. S., Schellenbaum, P., Walter, B., & Maillot, P. (2012). Transient expression of artificial microRNAs targeting Grapevine Fanleaf Virus and evidence for RNA silencing in grapevine somatic embryos. *Transgenic Research*, *21*(6), 1319–1327. doi: 10.1007/s11248-012-9611-5

Jiang, Y., Zheng, W., Li, J., Liu, P., Zhong, K., Jin, P., Xu, M., Yang, J., & Chen, J. (2021). NbWRKY40 Positively regulates the response of *Nicotiana benthamiana* to Tomato Mosaic Virus via salicylic acid signaling. *Frontiers in Plant Science*, *11*, 2090–2090. doi: 10.3389/FPLS.2020.603518/BIBTEX

Jungfleisch, J., Chowdhury, A., Alves-Rodrigues, I., Tharun, S., & Díez, J. (2015). The Lsm1-7-Pat1 complex promotes viral RNA translation and replication by differential mechanisms. *RNA*, *21*(8), 1469–1479. doi: 10.1261/rna.052209.115

Kasschau, K. D., Xie, Z., Allen, E., Llave, C., Chapman, E. J., Krizan, K. A., & Carrington, J. C. (2003). P1/HC-Pro, a Viral suppressor of RNA silencing, interferes with Arabidopsis development and miRNA function. *Developmental Cell*, *4*(2), 205–217. doi: 10.1016/S1534-5807(03)00025-X

Khalid, A., Zhang, Q., Yasir, M., & Li, F. (2017). Small RNA based genetic engineering for plant viral resistance: Application in crop protection. *Frontiers in Microbiology*, *8*, 43. doi: 10.3389/fmicb.2017.00043

King, A. M. Q., Adams, M. J., Carstens, E. B., & Lefkowitz, E. J. (Eds.). (2012). Family—Luteoviridae. In *Virus Taxonomy* (pp. 1045–1053). Elsevier. doi: 10.1016/B978-0-12-384684-6.00090-2

Komatsu, K., Hashimoto, M., Ozeki, J., Yamaji, Y., Maejima, K., Senshu, H., Himeno, M., Okano, Y., Kagiwada, S., & Namba, S. (2010). Viral-induced systemic necrosis in plants involves both programmed cell death and the inhibition of viral multiplication, which are regulated by independent pathways. *Molecular Plant-Microbe Interactions: MPMI*, *23*(3), 283–293. doi: 10.1094/MPMI-23-3-0283

Kulshrestha, D., & Agrawal, K. K. (2019). An Econometric Analysis of Agricultural Production and Economic Growth in India. *Indian Journal of Marketing*, *49*(11), Article 11. doi: 10.17010/ijom/2019/v49/i11/148276

Lee, J. A., & Fang, D. D. (2015). Cotton as a world crop: origin, history, and current status. In *Cotton* (pp. 1–23). John Wiley & Sons, Ltd. doi: 10.2134/agronmonogr57.2013.0019

Li, F., Pignatta, D., Bendix, C., Brunkard, J. O., Cohn, M. M., Tung, J., Sun, H., Kumar, P., & Baker, B. (2012). MicroRNA regulation of plant innate immune receptors. *Proceedings of the National Academy of Sciences*, *109*(5), 1790–1795. doi: 10.1073/pnas.1118282109

Li, H., Li, F., Zhang, M., Gong, P., & Zhou, X. (2020). Dynamic subcellular localization, accumulation, and interactions of proteins from Tomato Yellow Leaf Curl China Virus and its associated Betasatellite. *Frontiers in Plant Science*, *11*. doi: 10.3389/fpls.2020.00840

Liu, F., Zhao, Q., Ruan, X., He, Y., & Li, H. (2008). Suppressor of RNA silencing encoded by Rice gall dwarf virus genome segment 11. *Chinese Science Bulletin*, *53*(3), 362–369. doi: 10.1007/s11434-008-0095-x

Liu, S.-R., Zhou, J.-J., Hu, C.-G., Wei, C.-L., & Zhang, J.-Z. (2017). MicroRNA-mediated gene silencing in plant defense and viral counter-defense. *Frontiers in Microbiology*, *8*. doi: 10.3389/fmicb.2017.01801

Lu, Y., Gan, Q., Chi, X., & Qin, S. (2008). Roles of microRNA in plant defense and virus offense interaction. *Plant Cell Reports*, *27*(10), 1571–1579. doi: 10.1007/s00299-008-0584-z

Luttrell, R. G., Teague, T. G., & Brewer, M. J. (2015). Cotton Insect Pest Management. In *Cotton* (pp. 509–546). John Wiley & Sons, Ltd. doi: 10.2134/agronmonogr57.2014.0072

Mandadi, K. K., & Scholthof, K.-B. G. (2013). Plant Immune Responses Against Viruses: How Does a Virus Cause Disease?[OA]. *The Plant Cell*, *25*(5), 1489–1505. doi: 10.1105/tpc.113.111658

Manjunatha, L., Rajashekara, H., Uppala, L. S., Ambika, D. S., Patil, B., Shankarappa, K. S., Nath, V. S., Kavitha, T. R., & Mishra, A. K. (2022). Mechanisms of microbial plant protection and control of plant viruses. *Plants*, *11*(24), 3449. doi: 10.3390/plants11243449

Mathioudakis, M. M., Veiga, R. S. L., Canto, T., Medina, V., Mossialos, D., Makris, A. M., & Livieratos, I. (2013). Pepino mosaic virus triple gene block protein 1 (TGBp1) interacts with and increases tomato catalase 1 activity to enhance virus accumulation. *Molecular Plant Pathology*, *14*(6), 589–601. doi: 10.1111/mpp.12034

Naqvi, R. Z., Zaidi, S. S.-A., Mukhtar, M. S., Amin, I., Mishra, B., Strickler, S., Mueller, L. A., Asif, M., & Mansoor, S. (2019). Transcriptomic analysis of cultivated cotton *Gossypium hirsutum* provides insights into host responses upon whitefly-mediated transmission of cotton leaf curl disease. *PLOS ONE*, *14*(2), e0210011. doi: 10.1371/journal.pone.0210011

Nie, J., Zhou, W., Liu, J., Tan, N., Zhou, J. M., & Huang, L. (2021). A receptor-like protein from *Nicotiana benthamiana* mediates VmE02 PAMP-triggered immunity. *New Phytologist*, *229*(4), 2260–2272. doi: 10.1111/NPH.16995

Nishiguchi, M., & Kobayashi, K. (2011). Attenuated plant viruses: Preventing virus diseases and understanding the molecular mechanism. *Journal of General Plant Pathology*, *77*(4), 221–229. doi: 10.1007/s10327-011-0318-x

Online Clothing Study. (2023, May 21). Top 10 cotton producing countries in the world. *Online Clothing Study*. https://www.onlineclothingstudy.com/2023/05/top-10-cotton-producing-countries-in.html

Paape, M., Solovyev, A. G., Erokhina, T. N., Minina, E. A., Schepetilnikov, M. V., Lesemann, D.-E., Schiemann, J., Morozov, S. Yu., & Kellmann, J.-W. (2006). At-4/1, an Interactor of the Tomato Spotted Wilt Virus movement protein, belongs to a new family of plant proteins capable of directed intra- and intercellular trafficking. *Molecular Plant-Microbe Interactions®*, *19*(8), 874–883. doi: 10.1094/MPMI-19-0874

Pacheco, R., García-Marcos, A., Barajas, D., Martiáñez, J., & Tenllado, F. (2012). PVX–potyvirus synergistic infections differentially alter microRNA accumulation in *Nicotiana benthamiana*. *Virus Research*, *165*(2), 231–235. doi: 10.1016/j.virusres.2012.02.012

Pan, L.-L., Cui, X.-Y., Chen, Q.-F., Wang, X.-W., & Liu, S.-S. (2018). Cotton Leaf Curl Disease: Which Whitefly Is the Vector? *Phytopathology*, *108*(10), 1172–1183. doi: 10.1094/PHYTO-01-18-0015-R

Pechinger, K., Chooi, K. M., MacDiarmid, R. M., Harper, S. J., & Ziebell, H. (2019). A new era for mild strain cross-protection. *Viruses*, *11*(7), Article 7. doi: 10.3390/v11070670

Rajendran, T. P., Birah, A., & Burange, P. (2018). Insect pests of cotton. In *Pests and Their Management* (pp. 361–411). doi: 10.1007/978-981-10-8687-8_11

Roberts, A. P. E., Lewis, A. P., & Jopling, C. L. (2011). The role of microRNAs in viral infection. In D. Grimm (Ed.), *Progress in Molecular Biology and Translational Science* (Vol. 102, pp. 101–139). Academic Press. doi: 10.1016/B978-0-12-415795-8.00002-7

Rodriguez-Peña, R., Mounadi, K. E., & Garcia-Ruiz, H. (2021). Changes in subcellular localization of host proteins induced by plant viruses. *Viruses*, *13*(4), 677. doi: 10.3390/v13040677

Rubio, L., Galipienso, L., & Ferriol, I. (2020). Detection of plant viruses and disease management: Relevance of genetic diversity and evolution. *Frontiers in Plant Science*, *11*. doi: 10.3389/fpls.2020.01092

Saleem, M. A., Malik, W., Qayyum, A., Ul-Allah, S., Ahmad, M. Q., Afzal, H., Amjid, M. W., Ateeq, M. F., & Zia, Z. U. (2021). Impact of heat stress responsive factors on growth and physiology of cotton (*Gossypium hirsutum* L.). *Molecular Biology Reports*, *48*(2), 1069–1079. doi: 10.1007/s11033-021-06217-z

Schoelz, J. E., Harries, P. A., & Nelson, R. S. (2011). Intracellular transport of plant viruses: Finding the door out of the cell. *Molecular Plant*, *4*(5), 813–831. doi: 10.1093/mp/ssr070

Schwessinger, B., & Ronald, P. C. (2012). Plant innate immunity: Perception of conserved microbial signatures. *Annual Review of Plant Biology*, *63*, 451–482. doi: 10.1146/annurev-arplant-042811-105518

Shaban, M., Miao, Y., Ullah, A., Khan, A. Q., Menghwar, H., Khan, A. H., Ahmed, M. M., Tabassum, M. A., & Zhu, L. (2018). Physiological and molecular mechanism of defense in cotton against *Verticillium dahliae*. *Plant Physiology and Biochemistry*, *125*, 193–204. doi: 10.1016/j.plaphy.2018.02.011

Shahbandeh, M. (2023). *Cotton production in the U.S. 2022*. Statista. https://www.statista.com/statistics/191500/cotton-production-in-the-us-since-2000/

Shen, W.-J., Ruan, X.-L., Li, X.-S., Zhao, Q., & Li, H.-P. (2012). RNA silencing suppressor Pns11 of Rice Gall Dwarf Virus induces virus-like symptoms in transgenic rice. *Archives of Virology*, *157*(8), 1531–1539. doi: 10.1007/s00705-012-1339-2

Silva, T., Corrêa, R., Castilho, Y., Silvie, P., Bélot, J.-L., & Vaslin, M. (2008). Widespread distribution and a new recombinant species of Brazilian virus associated with cotton blue disease. *Virology Journal*, *5*(1), 123. doi: 10.1186/1743-422X-5-123

Simón-Mateo, C., & García, J. A. (2006). MicroRNA-guided processing impairs Plum Pox Virus replication, but the virus readily evolves to escape this silencing mechanism. *Journal of Virology*, *80*(5), 2429–2436. doi: 10.1128/jvi.80.5.2429-2436.2006

Smirnova, E., Firth, A. E., Miller, W. A., Scheidecker, D., Brault, V., Reinbold, C., Rakotondrafara, A. M., Chung, B. Y. W., & Ziegler-Graff, V. (2015). Discovery of a small non-AUG-initiated ORF in Poleroviruses and Luteoviruses that is required for long-distance movement. *PLOS Pathogens*, *11*(5), e1004868–e1004868. doi: 10.1371/journal.ppat.1004868

Sun, L., Lin, C., Du, J., Song, Y., Jiang, M., Liu, H., Zhou, S., Wen, F., & Zhu, C. (2016). Dimeric artificial microRNAs mediate high resistance to RSV and RBSDV in transgenic rice plants. *Plant Cell, Tissue and Organ Culture (PCTOC)*, *126*(1), 127–139. doi: 10.1007/s11240-016-0983-8

Tabassum, A., Bag, S., Roberts, P., Suassuna, N., Chee, P., Whitaker, J. R., Conner, K. N., Brown, J., Nichols, R. L., & Kemerait, R. C. (2019). First report of Cotton Leafroll Dwarf Virus infecting cotton in Georgia, U.S.A. *Plant Disease*, *103*(7), 1803. doi: 10.1094/PDIS-12-18-2197-PDN

Tarazi, R., Jimenez, J. L. S., & Vaslin, M. F. S. (2019). Biotechnological solutions for major cotton (*Gossypium hirsutum*) pathogens and pests. *Biotechnology Research and Innovation*, *3*, 19–26. doi: 10.1016/j.biori.2020.01.001

Tarazi, R., & Vaslin, M. F. S. (2022). The viral threat in cotton: How new and emerging technologies accelerate virus identification and virus resistance breeding. *Frontiers in Plant Science*, *13*. doi: 10.3389/fpls.2022.851939

Thiébeauld, O., Schepetilnikov, M., Park, H.-S., Geldreich, A., Kobayashi, K., Keller, M., Hohn, T., & Ryabova, L. A. (2009). A new plant protein interacts with eIF3 and 60S to enhance virus-

activated translation re-initiation. *The EMBO Journal*, *28*(20), 3171–3184. doi: 10.1038/emboj.2009.256

Verchot-Lubicz, J., & Carr, J. P. (2008). Viral suppressors of gene silencing. *Encyclopedia of Virology*, 325–332. doi: 10.1016/B978-012374410-4.00718-4

Voinnet, O. (2009). Origin, biogenesis, and activity of plant microRNAs. *Cell*, *136*(4), 669–687. doi: 10.1016/j.cell.2009.01.046

Vu, T. V., Roy Choudhury, N., & Mukherjee, S. K. (2013). Transgenic tomato plants expressing artificial microRNAs for silencing the pre-coat and coat proteins of a begomovirus, Tomato Leaf Curl New Delhi Virus, show tolerance to virus infection. *Virus Research*, *172*(1), 35–45. doi: 10.1016/j.virusres.2012.12.008

Wang, N., Qiao, W., Liu, X., Shi, J., Xu, Q., Zhou, H., Yan, G., & Huang, Q. (2017). Relative contribution of Na+/K+ homeostasis, photochemical efficiency and antioxidant defense system to differential salt tolerance in cotton (*Gossypium hirsutum* L.) cultivars. *Plant Physiology and Biochemistry*, *119*, 121–131. doi: 10.1016/j.plaphy.2017.08.024

Wang, R. Y.-L., & Nagy, P. D. (2008). Tomato Bushy Stunt Virus Co-opts the RNA-binding function of a host metabolic enzyme for viral genomic RNA synthesis. *Cell Host & Microbe*, *3*(3), 178–187. doi: 10.1016/j.chom.2008.02.005

Watt, L. G., Crawshaw, S., Rhee, S.-J., Murphy, A. M., Canto, T., & Carr, J. P. (2020). The cucumber mosaic virus 1a protein regulates interactions between the 2b protein and ARGONAUTE 1 while maintaining the silencing suppressor activity of the 2b protein. *PLoS Pathogens*, *16*(12), e1009125. doi: 10.1371/journal.ppat.1009125

Widana Gamage, S. M. K., & Dietzgen, R. G. (2017). Intracellular localization, interactions and functions of Capsicum Chlorosis Virus proteins. *Frontiers in Microbiology*, *8*. doi: 10.3389/fmicb.2017.00612

Wu, X., Valli, A., García, J. A., Zhou, X., & Cheng, X. (2019). The Tug-of-War between plants and viruses: Great progress and many remaining questions. *Viruses*, *11*(3), 203. doi: 10.3390/v11030203

Xu, A., Zhao, Z., Chen, W., Zhang, H., Liao, Q., Chen, J., Carr, J. P., & Du, Z. (2013). Self-interaction of the Cucumber Mosaic Virus 2b protein plays a vital role in the suppression of RNA silencing and the induction of viral symptoms. *Molecular Plant Pathology*, *14*(8), 803–812. doi: 10.1111/mpp.12051

Xuan, N., Zhao, C., Peng, Z., Chen, G., Bian, F., Lian, M., Liu, G., Wang, X., & Bi, Y. (2015). Development of transgenic maize with anti-rough dwarf virus artificial miRNA vector and their disease resistance. *Sheng wu gong cheng xue bao = Chinese journal of biotechnology*, *31*(9), 1375–1386.

Zhai, J., Jeong, D.-H., De Paoli, E., Park, S., Rosen, B. D., Li, Y., González, A. J., Yan, Z., Kitto, S. L., Grusak, M. A., Jackson, S. A., Stacey, G., Cook, D. R., Green, P. J., Sherrier, D. J., & Meyers, B. C. (2011). MicroRNAs as master regulators of the plant NB-LRR defense gene family via the production of phased, trans-acting siRNAs. *Genes & Development*, *25*(23), 2540–2553 doi: 10.1101/gad.177527.111

Chapter 2

A Newly Isolated Cotton-infecting Polerovirus with Cryptic Pathogenicity Encodes a Weak Suppressor of RNA Silencing

2.1 Abstract

Cotton leafroll dwarf virus (CLRDV), a phloem limited Polerovirus (Family: Solemoviridae) transmitted by aphids, causes significant economic losses to cotton cultivation. CLRDV strains (CLRDV-ty and CLRDV-at) previously prevalent in other countries cause severe symptoms leading to high yield loss. Recently, a new isolate of CLRDV (CLRDV-AL) has been characterized from infected cotton plants in Alabama that are often asymptomatic and difficult to detect, implying a low titer and pathogenicity within the host. Different pathogenicity among certain strains within the same species often correlates with environmental and molecular factors. Thus, better management and control of the vector-borne disease can be achieved by elucidating host-pathogen interaction, such as host immune response and pathogen counter-response. In this chapter, the ability of CLRDV-AL to suppress a major host defense response known as RNA silencing was demonstrated and the potency of silencing suppression to other strains of the same virus was compared. Also, the difference in pathogenicity among them by evaluating the observations based on the amino acid variation within the functional domain was discussed. The result from the study shown in this chapter provides and suggests a future direction for specifying the strategy to mitigate potential cotton disease severity.

2.2 Introduction

Cotton is a multipurpose agricultural resource cultivated in most continents, including Africa, Asia, and the Americas. In 2021, 12.8% of the global cotton harvested area was in the United States, and the production was valued at $7.4 billion (reviewed in Tarazi and Vaslin, 2022; Edula et al., 2023). Similarly, like many other crops, cotton is prone to damage from pests and diseases (Xiao et al., 2019; Chohan et al., 2020). Among them, viruses are major pests affecting the yield (Ziegler-Graff, 2020; Tarazi and Vaslin, 2022). Cotton leafroll dwarf virus (CLRDV) is the second most damaging virus to commercial cotton worldwide, reported in all cotton-growing continents (Distéfano et al., 2010; Agrofoglio et al., 2019; Conner et al., 2021). CLRDV is a member of the genus Polerovirus (family Solemoviridae) and the causal agent for the cotton blue disease (Parkash et al., 2021; Sõmera et al., 2021). This disease has caused about 80% yield loss in commercial cotton in South America (Silva et al., 2008). To manage CLRDV and mitigate the loss, the growers' remedy was increasing the application of pesticides to reduce the population level of the insect vector, *Aphis gossypii* (Ellis et al., 2016; Galbieri et al., 2017). However, it has not been effective (Galbieri et al., 2017; Mahas et al., 2022).

A resistant cotton variety was developed with a dominant resistant gene (Cbd) (Fang et al., 2010). Although this variety showed absolute resistance to CLRDV by restricting systemic virus replication, it was not long before a new strain that broke the resistance was identified in South America (Silva et al., 2008). This resistance-breaking strain was called CLRDV-atypical (CLRDV-at) in contrast to the previous strain CLRDV-typical (CLRDV-ty) (Da Silva et al., 2015). In 2017, CLRDV was reported first time in the United States in Alabama, and the genome sequence analysis identified it as a new strain (CLRDV-AL) (Avelar et al., 2019). Since the first incidence, CLRDV has been reported in many other cotton-growing states (Aboughanem-Sabanadzovic et al., 2019; Alabi et al., 2020; Ali and Mokhtari, 2020; Ali et al., 2020; Faske et al., 2020; Iriarte et al., 2020; Price et al., 2020; Tabassum et al., 2020; Thiessen et al., 2020; Wang et al., 2020; Ramos-Sobrinho et al., 2021; Ferguson and Ali, 2022). All cotton varieties grown in the United States are susceptible to this virus (Edula et al., 2023), and the presence of this pathogen poses a considerable threat. Plants infected in the early season show stunted leaves. During a late season infection, the symptoms include leaf distortion, cupping of leaves, and discoloration of veins (Avelar et al., 2019). However, CLRDV-AL-infected plants are also cryptic as they are often detected in

asymptomatic plants, and infected plants do not always test positive for the virus using an amplification-based detection method (Tabassum et al., 2020; Bag et al., 2021; Tabassum et al., 2021).

CLRDV has seven open reading frames (ORFs) that encode proteins necessary for the virus infection cycle (Distéfano et al., 2010; King et al., 2012; Delfosse et al., 2014; Smirnova et al., 2015). Genome analysis has revealed that ORF 0, which encodes a viral suppressor of RNA silencing suppressor (VSR) protein (P0), and is the most divergent region among CLRDV strains (Cascardo et al., 2015; Avelar et al., 2020). Like other plant viruses, certain poleroviral proteins function as VSRs (Almasi et al., 2015; Cascardo et al., 2015; Clavel et al., 2021; Wang et al., 2021; Xiao- Yan et al., 2021). VSRs are virus-encoded proteins to prevent the antiviral mechanism employed by their hosts, which degrades the viral RNA molecules (reviewed in Li and Wang, 2019). Thus, VSRs are considered to play key roles in determining the pathogenicity, virulence, and disease severity of viral pathogens (Sharma and Ikegami, 2010; Wang et al., 2021). Previous studies have shown that CLRDV-ty has a more potent suppression of RNA silencing activity than CLRDV-at and correlated this difference to their symptom severity (Nishiguchi and Kobayashi, 2011; Agrofoglio et al., 2019). Although the difference in amino acid (aa) sequence of CLRDV-AL encoded P0 protein from the other two strains' P0 proteins was identified (Avelar et al., 2020), its effect on the VSR potency has not yet compared with that of the other strains. This chapter demonstrated the VSR activity of CLRDV-AL encoded P0 protein via Agrobacterium-mediated transient expression and compared VSR potency to the P0 proteins encoded by two other strains (CLRDV-ty and CLRDV-at).

2.3 Materials and Methods

2.3.1 Generation of cDNA Constructs

The cDNAs of ORF 0 from three different strains of CLRDV were synthesized and cloned into a pUC57mini plasmid (Genscript, Piscataway, NJ, USA) using the reference genome sequences; CLRDV-ty (GenBank accession number: GU167940), CLRDV-at (GenBank accession number: KF359946), and CLRDV-AL (GenBank accession number: MN071395.1). pAI-P0AL, pAI-P0at, and pAI-P0ty, constructs of ORF 0 placed under the CaMV 35S promoter sequence, were generated using these pUC57mini clones as templates. Fragments encompassing the ORF 0 from three different strains of CLRDV were amplified using a Phusion® High-Fidelity DNA polymerase (New England BioLab, Ipswich, MA, USA) by a pair of oligomers, P0-AL.FW.ApaI (5`- ACTAGGGCCCAACAATGTTGAATTTGATCATCTGC-3`) and P0-AL.RV.XbaI (5`-GGACTCTAGATCAACTGCTTTCTT CTTCAC-3`). The amplified product was separated in 0.8% agarose gel by electrophoresis, and the target DNAs were purified from the gel using Zymoclean Gel DNA Recovery Kit (Zymo Research, Irvine, CA, USA).

The purified DNAs were digested using *Apa*I and *Xba*I restriction endonucleases (New England BioLab) and ligated into the corresponding region of the binary plasmid pAIDEE (pAI; Lin et al., 2014), which was digested with the same restriction endonucleases using T4 DNA ligase (Promega, Madison, WI, USA). Constructs were transformed into *E. coli* JM109 competent cells (Promega) and the resulting transformants were screened on Luria–Bertani (LB) agar plates containing kanamycin (100 mg/ml). Sequence analysis was performed at Psomagen Inc. (Rockville, MD, USA). pAI-GFP, a construct expressing ´green fluorescent protein (GFP) within the same vector background, was generated in a similar way using a pair of oligomers GFP.FW.ApaI (5`-ACTAGGGCCCAACAATGGCTAG CAAAGGAGAAG-3`) and GFP.RV.XbaI (5`-GTACTCTAGA CTATTTGTAGAGCTCATCC-3`) for the amplification.

2.3.2 Sequence Analysis

Multisequence alignment of amino acid sequence for P0 ORFs of CLRDV-ty, CLRDV-at, and CLRDV-AL was performed using CLUSTAL multiple sequence alignment by MUSCLE (Multiple Sequence Comparison by Log- Expectation at

https://www.ebi.ac.uk/Tools/msa/muscle/) (Edgar, 2004). The GenBank accession number for each strain is identified above.

2.3.3 Agroinfiltration

Agroinfiltration of the constructs was conducted as previously described (Kang et al., 2015). Briefly, *Agrobacterium tumefaciens* strain GV3101 was transformed with the cloned plasmids by the heat shock method. The resulting transformants were screened on LB agar plates containing kanamycin and rifampicin (100 mg/ml and 50 mg/ml, respectively). A single colony was selected and inoculated in 3 ml liquid LB media containing kanamycin (100 mg/ml). The culture was grown overnight at 28°C, then 50 µl of the culture was transferred into 5 ml of fresh LB media with kanamycin and rifampicin (100 mg/ml and 50 mg/ml, respectively). The cells were grown overnight at 28°C, and the culture was centrifuged at 3,000 rpm for 10 mins. Pelleted cells were resuspended in agroinfiltration buffer (10 mM MES, pH 5.85; 10 mM MgCl2; 150 µM Acetosyringone) at the optical density 1.0 at 600 nm (OD600 nm = 1.0). Following the incubation for at least 2 hours without shaking at room temperature, the suspension was infiltrated into the lower surface of fully expanded leaves of six weeks old *Nicotiana benthamiana* 16c plants using needleless syringes. The infiltrated plants were grown under 16h/8h of light/dark cycle until further analysis.

2.3.4 Examination of Fluorescence in Plants

Six weeks old *N. benthaminana* 16c plants were infiltrated with *A. tumefaciens* GV3101 cells transformed with pAI-GFP mixed with cells transformed with P0 constructs (pAI-P0AL, pAI-P0at, or pAI-P0ty) or other known VSRs (pPZP-P19 or pPZP-HC-Pro; Qu et al., 2003) or empty pAI vector in equal volumes (v/v, OD600nm = 1.0). The expression of the GFP transgene within this transgenic line (16c) can be silenced when extra copies of the GFP transcript are introduced via a binary vector (Voinnet et al., 1998). However, silencing of GFP induced this way can be suppressed by the simultaneous expression of VSRs (Voinnet et al., 1999). This method has been used to identify VSRs among virus-encoded proteins for decades (Brigneti et al., 1998; Voinnet et al., 1999; Qu et al., 2003; Cui et al., 2005; Li et al., 2014; Dong et al., 2016; Li et al., 2019; Sinha et al., 2021; Wang et al., 2022). ´Green fluorescence was observed under a long wavelength (365 nm) using a hand-held UV lamp raised 6 inches above the plants at four days post infiltration (dpi) in the dark room. The infiltrated leaves were collected at 4 dpi and examined using an

epifluorescence microscope, Echo Revolve (San Diego, CA, USA), with wavelengths specified by FITC cube (EX:470 ± 40 nm and EM:525 ± 50 nm).

2.3.5 Relative Expression Levels of GFP mRNA

The relative expression levels of GFP mRNA were evaluated by RT-qPCR using Luna® universal RT-qPCR system (New England Biolabs). Total RNA was extracted from 100 mg of leaf discs of infiltrated *N. benthamiana* (four discs of 0.9 cm in diameter). The samples were ground in liquid nitrogen using TissueLyser II (Qiagen, Hilden, Germany). The extraction was performed using RNeasy Plant Mini Kit (Qiagen) according to the manufacturer's protocol. RNA quality and concentration were evaluated using NanoDrop™ Lite Spectrophotometer (ThermoFisher Scientific). One-step RT-qPCR reactions were performed in a CFX Connect™ Real-time PCR detection system (BIO-RAD) with a total volume of 10 ml, using 2 ml of RNA (10 ng/ml). For the amplification of GFP, a pair of oligomers; MFA.Gq-PCR: FW (5`-GATGACGGGAACTACAAGAC -3`) and MFA.Gq-PCR: RV (5`-CGAGTACAACTATAACTCACAC -3`) were used. The reference gene, NbACTIN2, was used as the internal control and was amplified using a pair of NbACTIN2-FW (5`-CAATCCAGACACTGTACTTTCTCTC-3`) and NbACTIN2-RV (5`-AAGCTGCAGGTATCCATGAGACTA-3`) as previously described (Luo et al., 2019).

The cycling conditions include the reverse transcription at 55°C for 10 min, incubation at 95°C for 2 min, and 40 cycles of 95°C for 10 s and 60°C for 60 s. Three biological and technical replicates were performed for all treatments. Ct values were averaged for triplicates of each sample prior to calculating relative values using the 2−DDCt method (Livak and Schmittgen, 2001).

2.4 Results

2.4.1 CLRDV-AL P0 Suppresses RNA Silencing Mechanism in Host.

To verify the ability of the P0 protein encoded by CLRDV-AL (P0-AL) to suppress the RNA silencing, P0-AL was expressed along with a green fluorescent protein (GFP) in *Nicotiana benthamiana* 16c plants, a transgenic line that constitutively expresses GFP (Figure 1). When there is no suppression, the transiently expressed GFP triggers an RNA silencing response which degrades both endogenous and transient GFP mRNAs, and subsequently, the fluorescence level drops (Figure 1B; EV, top left). However, in the presence of suppressors, such degradation is

inhibited, and the level of GFP expression can be visualized under UV range light. In this assay, strong GFP fluorescence was observed in the presence of P19 or HC-Pro at four days post-infiltration (dpi) (Figure 1B; HC-Pro and P19, bottom right and left). P19 and HCPro are well-known strong VSRs encoded by Tomato bushy stunt virus and Tobacco etch virus, respectively (Anandalakshmi et al., 1998; Scholthof, 2006). Although P0-AL showed suppression activity of the RNA silencing, the GFP fluorescence level within the region of *N. benthamiana* 16c leaves co-infiltrated with GFP visualized by UV light was not comparable to the level shown by P19 or HC-Pro co-infiltration (Figure 1B; P0-AL, top right).

A similar pattern in the suppression of GFP fluorescence was observed upon the co-expression of GFP along with each VSR or EV in the individual leaves (Figure 1C). The visually assessed relative intensity of the GFP fluorescence suggested that the RNA silencing suppression potency of P0-AL is significantly weaker than that of P19 or HC-Pro because the fluorescence intensity was similar to the basal fluorescence from the non-infiltrated leaves (Figure 1C; P0-AL and Mock). To better evaluate the relative intensity of GFP fluorescence resulting from the suppression of RNA silencing, infiltrated leaf tissue patches were examined using a fluorescence microscope (Figure 1D). The relative fluorescence intensity calculated from more than 15 images per treatment using Region of Interest (ROI) on ImageJ and analyzed by one-way ANOVA test in R (see Materials and Methods) demonstrated significant difference ($p < 0.01$) in the fluorescence level of P0-AL-infiltrated patches compared to either HC-Pro- or P19-infiltrated patches (Figure 1E; denoted as ‘a’ for HC-Pro or P19, and as ‘b’ for P0-AL). According to the analysis, all three VSRs demonstrated significant ($p < 0.01$) suppressor activity relative to the empty vector (EV)-infiltrated control (Figure 1E; denoted as ‘c’ for EV control). However, it is noteworthy that the fluorescence level measured from P0-ALinfiltrated patches was not completely distinct from the basal level fluorescence measured from buffer-infiltrated *N. benthamiana* 16c plants (Figure 1E; denoted as ‘bc’ for 16c control). These results implied that the P0 protein of CLRDV-AL is not a potent silencing suppressor compared to other VSRs, such as P19 and HC-Pro, known for their strong silencing suppression.

2.4.2 $P0^{AL}$ is a Weak Viral Suppressor of RNA Silencing Like $P0^{at}$

Previously, the P0 protein encoded by an atypical strain of CLRDV (P0-at) was reported to function as a weaker VSR than the P0 protein encoded by a typical strain of CLRDV (P0-ty) by

a similar set of experiments described above (Agrofoglio et al., 2019). To evaluate the VSR potency of P0-AL compared to the P0 proteins from two other strains (P0-ty and P0-at), a similar set of qualitative and quantitative experiments and analysis shown in Figure 1 was performed (Figure 2). Each construct harboring the ORF of P0 from three different strains of CLRDV was co-infiltrated into the leaves of *N. benthamiana* 16c plants along with the GFP construct via agroinfiltration. When observed under the UV light at four dpi, non-infiltrated leaves showed the basal level of GFP fluorescence generated from their own GFP transgene expression (Figure 2A; Mock). On the contrary, the leaves co-infiltrated by the GFP construct with an empty vector did not show GFP fluorescence and looked rather red due to the autofluorescence from the chloroplasts (Figure 2A; EV). As expected from previous reports, the leaves co-infiltrated with P0-ty or P0-at showed a sharp contrast in fluorescence level (Figure 2A; P0-ty and P0-at).

Stronger fluorescence was observed from the leaves co-infiltrated with P0-ty, but less fluorescence was observed from the leaves co-infiltrated with P0-at. Upon the visual observation, the fluorescence level from the leaves co-infiltrated with P0-AL was even lower than the level of P0-at (Figure 2A: P0-AL). The relative intensities of the GFP fluorescence visually evaluated under UV light suggested that the RNA silencing suppression activity of P0-AL is weaker than P0-ty like P0-at. To evaluate the relative potency of the suppression of RNA silencing better, infiltrated leaf tissue patches were examined using a fluorescence microscope (Figure 2A; bottom row, see Supplementary Figure 1 for more representative images), and the relative fluorescence intensity was calculated from more than 15 images per treatment using ROI on ImageJ and analyzed by oneway ANOVA test in R (Figure 2B). The analysis demonstrated a significant difference ($p < 0.01$) in the fluorescence level from the patches infiltrated with three P0s individually compared to EV infiltrated patches (Figure 2B; denoted as ‘d’ for EV control).

The fluorescence level of the patches infiltrated with P0-ty was also significantly different and distinct from the other two sets of patches infiltrated with the other two P0s (Figure 2B; denoted as ‘a’ for P0-ty). However, the fluorescence level of the patches infiltrated with P0-at that was significantly different from the patches infiltrated with P0-ty (Figure 2B; denoted as ‘b’ for P0-at) was not completely distinct from the patches infiltrated with P0-AL (Figure 2B; denoted as ‘bc’ for P0-AL). Interestingly, according to the analysis, the fluorescence level of P0-AL-infiltrated patches did not show complete distinction from buffer-infiltrated *N. benthamiana* 16c

control (Figure 2B; denoted as ‘cd’ for 16c control). This implied that there was suppression activity for P0-AL, yet the suppression potency was not strong enough. This result is also in accordance with the result shown above (Figure 1E; denoted as ‘b’ and ‘bc’ for P0-AL and 16c control, respectively). Although the fluorescence of GFP under UV light is an indication of the level of silencing or its suppression, this can still be argued because silencing is the mechanism acting on the RNA, yet the analysis based on the observed florescence comes from the translated product of such RNA.

To further validate the observation from this chapter, the relative accumulation of GFP mRNA was analyzed by quantitative real-time PCR (Figure 2C). The GFP mRNA levels in the patches infiltrated with three P0s individually were all significantly higher, $p < 0.01$, than EV control patches (Figure 2C; significant difference was not noted within the graph). This was consistent with the analysis using the GFP fluorescence shown in Figure 2B. The GFP mRNA level in the patches infiltrated with P0-ty was significantly higher than the levels in the other two sets of patches infiltrated with P0-at or P0-AL. This was also in agreement with the analysis shown in Figure 2B. Remarkably, the GFP mRNA levels between the patches infiltrated with P0-at and P0-AL showed less significant difference (Figure 2C; $p < 0.05$), which was in line with the result shown in Figure 2B where P0-at and P0-AL were denoted as groups ‘b’ and ‘bc’, respectively. Overall, the analysis of relative GFP mRNA level by RT-qPCR (Figure 2C) supported the quantified GFP fluorescence level analyzed in Figure 2B. These results implied that the silencing suppressor potency of the P0 protein encoded by CLRDV-AL is comparable to the P0 protein encoded by CLRDV-at, which is weaker than the P0 protein encoded by CLRDV-ty.

2.5 Discussion

CLRDV induces a wide range of various symptoms, such as leaf drooping, wilting, reddening, stunting, and shortened internodes as well as asymptomatic infection which are commonly observed in the US (Agrofoglio et al., 2017; Avelar et al., 2019; Tabassum et al., 2020; Bag et al., 2021). The causes for diverse symptoms are not clearly understood and could be due to myriads of factors, such as abiotic factors, interactions between the virus and host, or a combination of both. Interaction between the virus and host also contributes to the resistance dynamic reported in the cotton-CLRDV pathosystem. Upon the rise of CBD in Brazil, deploying cultivars with a single dominant resistance gene, Rghv1, effectively mitigated the disease (Junior

et al., 2008). However, varieties carrying a single dominant resistance gene, Cbd (Fang et al., 2010), became susceptible to CLRDV-at in Argentina (Agrofoglio et al., 2019). Furthermore, the BRS-293 cultivar, which is moderately resistant to typical and atypical CLRDVs (Morello et al., 2010), was susceptible to prevalent CLRDV in the southeastern United States (Brown et al., 2019). Considered a crosstalk between plant immunity such as resistance and viral pathogenicity mediated by RNA silencing and VSR has been proposed (reviewed in Ding, 2010), it is noteworthy to mention that suppression of RNA silencing at variable degrees among different isolates within the same species or among different species within the same genus has been reported from several members of family Solemoviridae (Han et al., 2010; Kozlowska- Makulska et al., 2010; Fusaro et al., 2012; Delfosse et al., 2014; Zhuo et al., 2014; Cascardo et al., 2015; Agrofoglio et al., 2019). Thus, while it is not the sole factor, the characteristics of its VSR does contribute partially to the cryptic pathogenicity of CLRDV-AL.

In this study, the silencing suppression potency of the P0 protein encoded by CLRDV-AL was examined by using GFP co-infiltration assays on *N. benthamiana* 16c plants and analyzed the measure of suppression both in protein and RNA levels. This study demonstrated that CLRDV-AL P0 functioned as a local VSR (Figure 1), but the suppression level differed from cognate VSRs from other strains of CLRDV (Figure 2) or VSRs from other viruses (Figure 1). The alignment comparing the aa sequence of the P0-AL to the previously isolated strains from South American countries showed some mutations within the F-box domain known for VSR function (Agrofoglio et al., 2019). Figure 3 summarizes some notably divergent residues within its conserved F-box motif among three CLRDV strains used in this study. P0-AL has a valine (V) substitution which resembles an atypical strain (Figure 3; letter in red), and an arginine (R) substitution which resembles a typical strain (Figure 3; letter in blue). However, P0-AL also carries a unique phenylalanine (F) substitution that is found as either leucine (L) or isoleucine (I) in atypical or typical strains, respectively (Figure 3; letter in green). The collective difference in these residues among the three strains may contribute to the observation demonstrating that the P0 protein from CLRDV-AL displays yet another level of silencing suppression potency compared to two other P0s of different strains.

Previous study sought the correlation between the resistance-breaking trait of CLRDV-at and its VSR, P0-at, by comparing VSR potency between the P0 proteins from CLRDV-at and

CLRDV-ty (Agrofoglio et al., 2019). Agrofoglio et al. (2019) showed that an aa substitution, I to V, present in F-box motif was not sufficient to completely elucidate this question because the revertant P0-at, in which V residue has turned back to I, was still not able to restore the comparable suppression potency demonstrated by P0-ty. This results with P0-AL demonstrated a similar suppression potency to P0-at can be partially explained by the fact that P0-AL has the same substitution to V in that residue as P0-at. However, other substitutions unique in P0-AL from both P0-at and P0-ty may explain why P0-AL is not precisely at the same degree of VSR potency as P0-at (Figure 2B). Furthermore, it is known that the virus-encoded proteins interact among them during the virus infection within the host to expand their functional landscape and stability (Dao et al., 2020; Wang et al., 2022a; Wang et al., 2022b).

As presented, study was based on the transient expression of a single viral protein, it is worthy to note that the observed VSR potency could differ in the presence of the other CLRDV proteins under the viral context. CLRDV is a potentially threatening pest to the cotton industry due to its high mutation rate as a viral pathogen with an RNA genome and the tremendously effective transmission by insect vectors (Jones, 2009; Tarazi and Vaslin, 2022). Considering the economic significance of cotton in the United States, it is imperative to develop predictable strategies to manage potential new strains of CLRDV. Further molecular investigation on P0-AL to understand the cryptic nature of CLRDV-AL and its disease development will provide insight into how different CLRDV strains display a wide range of various disease symptoms and severity. Additionally, identifying host factors playing a role with the P0 protein during the virus infection will help specify the strategy to develop resistant varieties that can mitigate potential loss by CLRDV and sustainably manage resources for cotton growers in the United States and beyond.

2.6 References

Aboughanem-Sabanadzovic, N., Allen, T. W., Wilkerson, T. H., Conner, K. N., Sikora, E. J., Nichols, R. L., et al. (2019). First Report of Cotton Leafroll Dwarf Virus in upland cotton (*Gossypium hirsutum*) in Mississippi. *Plant Dis.* 103, 1798. doi: 10.1094/PDIS-01-19-0017-PDN

Agrofoglio, Y. C., Delfosse, V. C., Casse, M. F., Hopp, H. E., Kresic, I. B., and Distéfano, A. J. (2017). Identification of a new cotton disease caused by an atypical Cotton Leafroll Dwarf Virus in Argentina. *Phytopathology* 107, 369–376. doi: 10.1094/PHYTO-09-16-0349-R

Agrofoglio, Y. C., Delfosse Ab, V. C., Casse, M. F., Hopp, H. E., Bonacic Kresic, I., Ziegler-Graff, V., et al. (2019). P0 protein of Cotton Leafroll Dwarf Virus-atypical isolate is a weak RNA silencing suppressor and the avirulence determinant that breaks the cotton Cbd gene-based resistance. *Plant Pathol*. 68 (6), 1059–1071. doi: 10.1111/ppa.13031

Alabi, O. J., Isakeit, T., Vaughn, R., Stelly, D., Conner, K. N., Gaytán, B. C., et al. (2020). First report of Cotton Leafroll Dwarf Virus infecting upland cotton (*Gossypium hirsutum*) in Texas. *Plant Dis.* 104, 998. doi: 10.1094/PDIS-09-19-2008-PDN

Ali, A., and Mokhtari, S. (2020). First report of Cotton Leafroll Dwarf Virus infecting cotton (*Gossypium hirsutum*) in Kansas. *Plant Dis.* 104, 1880. doi: 10.1094/PDIS-12-19-2589-PDN

Ali, A., Mokhtari, S., and Ferguson, C. (2020). First report of Cotton Leafroll Dwarf Virus from cotton (*Gossypium hirsutum*) in Oklahoma. *Plant Dis.* 104, 2531. doi: 10.1094/PDIS-03-20-0479-PDN

Almasi, R., Miller, W. A., and Ziegler-Graff, V. (2015). Mild and severe Cereal Yellow Dwarf Viruses differ in silencing suppressor efficiency of the P0 protein. *Virus Res*. 208, 199–206. doi: 10.1016/j.virusres.2015.06.020

Anandalakshmi, R., Pruss, G. J., Ge, X., Marathe, R., Mallory, A. C., Smith, T. H., et al. (1998). A viral suppressor of gene silencing in plants. *Proc. Natl. Acad. Sci.* 95, 13079–13084. doi: 10.1073/pnas.95.22.13079

Avelar, S., Ramos-Sobrinho, R., Conner, K., Nichols, R. L., Lawrence, K., and Brown, J. K. (2020). Characterization of the complete genome and P0 protein for a previously unreported

genotype of Cotton Leafroll Dwarf Virus, an introduced polerovirus in the United States. *Plant Dis*. 104, 780–786. doi: 10.1094/PDIS-06-19-1316-RE

Avelar, S., Schrimsher, D. W., Lawrence, K., and Brown, J. K. (2019). First Report of Cotton Leafroll Dwarf Virus associated with cotton blue disease symptoms in Alabama. *Plant Dis.* 103, 592. doi: 10.1094/PDIS-09-18-1550-PDN

Bag, S., Roberts, P. M., and Kemerait, R. C. (2021). Cotton leafroll dwarf disease: An emerging virus disease on cotton in the U.S. *Crops Soils* 54, 18–22. doi: 10.1002/crso.20105

Brigneti, G., Voinnet, O., Li, W. X., Ji, L. H., Ding, S. W., and Baulcombe, D. C. (1998). Viral pathogenicity determinants are suppressors of transgene silencing in *Nicotiana benthamiana*. *EMBO J*. 17, 6739–6746. doi: 10.1093/emboj/17.22.6739

Brown, S., Conner, K., Hagan, A., Jacobson, A., Koebernick, J., Lawrence, K., et al. (2019). Report of a research review and planning meeting on Cotton Leafroll Dwarf Virus (Orange Beach, Alabama: Cotton Incorporated). Available at: https://www. cottoninc.com/cotton-production/ag-research/plant-pathology/cotton-leafroll-dwarfvirus-research/.

Cascardo, R. S., Arantes, I. L. G., Silva, T. F., Sachetto-Martins, G., Vaslin, M. F. S., and Corrêa, R. L. (2015). Function and diversity of P0 proteins among cotton leafroll dwarf virus isolates. *Virol. J.* 12, 123. doi: 10.1186/s12985-015-0356-7

Chohan, S., Perveen, R., Abid, M., Tahir, M. N., and Sajid, M. (2020). "Cotton diseases and their management," in Cotton production and uses: agronomy, crop protection, and postharvest technologies. Eds. S. Ahmad and M. Hasanuzzaman (Singapore: *Springer*), 239–270.

Clavel, M., Lechner, E., Incarbone, M., Vincent, T., Cognat, V., Smirnova, E., et al. (2021). Atypical molecular features of RNA silencing against the phloem-restricted polerovirus TuYV. *Nucleic Acids Res*. 49, 11274–11293. doi: 10.1093/nar/gkab802 Conner, K., Strayer-Scherer,

A., Hagan, A., Koebernick, J., Jacobson, A., Bowen, K., et al. (2021). "Cotton Leafroll Dwarf Virus," (Alabama: Alabama Cooperative Extension System). Available at: https://www.aces.edu/blog/topics/crop-production/cotton-leafroll-dwarf-virus/.

Cui, X., Li, G., Wang, D., Hu, D., and Zhou, X. (2005). A begomovirus DNAbencoded protein binds DNA, functions as a suppressor of RNA silencing, and targets the cell nucleus. *J. Virol.* 79, 10764–10775. doi: 10.1128/JVI.79.16.10764-10775.2005

Dao, T. N. M., Kang, S.-H., Bak, A., and Folimonova, S. Y. (2020). A non-conserved p33 protein of Citrus Tristeza Virus interacts with multiple viral partners. Mol. *Plant Microbe Interact.* 33, 859–870. doi: 10.1094/MPMI-11-19-0328-FI

Da Silva, A. K. F., Romanel, E., Silva, T., da, F., Castilhos, Y., Schrago, C. G., et al. (2015). Complete genome sequences of two new virus isolates associated with cotton blue disease resistance breaking in Brazil. *Arch. Virol.* 160, 1371–1374. doi: 10.1007/s00705-015-2380-8

Delfosse, V. C., Agrofoglio, Y. C., Casse, M. F., Kresic, I. B., Hopp, H. E., Ziegler-Graff, V., et al. (2014). The P0 protein encoded by cotton leafroll dwarf virus (CLRDV) inhibits local but not systemic RNA silencing. *Virus Res*. 180, 70–75. doi: 10.1016/j.virusres.2013.12.018

Ding, S.-W. (2010). RNA-based antiviral immunity. *Nat. Rev. Immunol.* 10, 632–644. doi: 10.1038/nri2824

Distéfano, A. J., Bonacic Kresic, I., and Hopp, H. E. (2010). The complete genome sequence of a virus associated with cotton blue disease, cotton leafroll dwarf virus, confirms that it is a new member of the genus Polerovirus. *Arch. Virol.* 155, 1849–1854. doi: 10.1007/s00705-010-0764-3

Dong, K., Wang, Y., Zhang, Z., Chai, L.-X., Tong, X., Xu, J., et al. (2016). Two amino acids near the N-terminus of Cucumber Mosaic Virus 2b play critical roles in the suppression of RNA silencing and viral infectivity. *Mol. Plant Pathol*. 17, 173–183. doi: 10.1111/mpp.12270

Edgar, R. C. (2004). MUSCLE: multiple sequence alignment with high accuracy and high throughput. *Nucleic Acids Res.* 32, 1792–1797. doi: 10.1093/nar/gkh340

Edula, S. R., Bag, S., Milner, H., Kumar, M., Suassuna, N. D., Chee, P. W., et al. (2023). Cotton leafroll dwarf disease: An enigmatic viral disease in cotton. *Mol. Plant Pathol.* 24, 513–526. doi: 10.1111/mpp.13335

Ellis, M. H., Stiller, W. N., Phongkham, T., Tate, W. A., Gillespie, V. J., Gapare, W. J., et al. (2016). Molecular mapping of bunchy top disease resistance in *Gossypium hirsutum* L. *Euphytica* 210, 135–142. doi: 10.1007/s10681-016-1713-3

Fang, D. D., Xiao, J., Canci, P. C., and Cantrell, R. G. (2010). A new SNP haplotype associated with blue disease resistance gene in cotton (*Gossypium hirsutum* L.). *Theor. Appl. Genet.* 120, 943–953. doi: 10.1007/s00122-009-1223-y

Faske, T. R., Stainton, D., Aboughanem-Sabanadzovic, N., and Allen, T. W. (2020). First Report of Cotton Leafroll Dwarf Virus from upland cotton (*Gossypium hirsutum*) in Arkansas. *Plant Dis*. 104,2742. doi: 10.1094/PDIS-12-19-2610-PDN

Ferguson, C., and Ali, A. (2022). Complete genome sequence of Cotton Leafroll Dwarf Virus infecting cotton in Oklahoma, USA. Microbiol. *Resour Announc* 11, e0014722. doi: 10.1128/mra.00147-22

Fusaro, A. F., Correa, R. L., Nakasugi, K., Jackson, C., Kawchuk, L., Vaslin, M. F. S., et al. (2012). The Enamovirus P0 protein is a silencing suppressor which inhibits local and systemic RNA silencing through AGO1 degradation. *Virology* 426, 178–187. doi: 10.1016/j.virol.2012.01.026

Galbieri, R., Boldt, A. S., Scoz, L. B., Rodrigues, S. M., Rabel, D. O., Belot, J. L., et al. (2017). Cotton blue disease in central-west Brazil: Occurrence, vector (*Aphis gossypii*) control levels and cultivar reaction. *Trop. Plant Pathol*. 42, 468–474. doi: 10.1007/s40858-017-0165-1

Han, Y.-H., Xiang, H.-Y., Wang, Q., Li, Y.-Y., Wu, W.-Q., Han, C.-G., et al. (2010). Ring structure amino acids affect the suppressor activity of melon aphid-borne yellows virus P0 protein. *Virology* 406, 21–27. doi: 10.1016/j.virol.2010.06.045

Iriarte, F. B., Dey, K. K., Small, I. M., Conner, K. N., O'Brien, G. K., Johnson, L., et al. (2020). First report of cotton leafroll dwarf virus in Florida. *Plant Dis*. 104, 2744. doi: 10.1094/PDIS-10-19-2150-PDN

Jones, R. A. C. (2009). Plant virus emergence and evolution: origins, new encounter scenarios, factors driving emergence, effects of changing world conditions, and prospects for control. *Virus Res.* 141, 113–130. doi: 10.1016/j.virusres.2008.07.028

Junior, O., Schuster, I., Pinto, R., Pires, E., Belot, J., Silvie, P., et al. (2008). Inheritance of resistance to cotton blue disease. *Pesquisa Agropecuária Bras*. 43, 661–665. doi: 10.1590/S0100-204X2008000500015

Kang, S.-H., Bak, A., Kim, O.-K., and Folimonova, S. Y. (2015). Membrane association of a nonconserved viral protein confers virus ability to extend its host range. *Virology* 482, 208–217. doi: 10.1016/j.virol.2015.03.047

King, A. M. Q., Adams, M. J., Carstens, E. B., and Lefkowitz, E. J. (2012). "Family - Luteoviridae," in Virus Taxonomy (San Diego: *Elsevier*), 1045–1053.

Kozlowska-Makulska, A., Guilley, H., Szyndel, M. S., Beuve, M., Lemaire, O., Herrbach, E., et al. (2010). P0 proteins of European beet-infecting poleroviruses display variable RNA silencing suppression activity. *J. Gen. Virol*. 91, 1082–1091. doi: 10.1099/vir.0.016360-0

Li, Z., He, Y., Luo, T., Zhang, X., Wan, H., Ur Rehman, A., et al. (2019). Identification of key residues required for RNA silencing suppressor activity of p23 protein from a mild strain of Citrus Tristeza Virus. *Viruses* 11, 782. doi: 10.3390/v11090782

Li, F., Huang, C., Li, Z., and Zhou, X. (2014). Suppression of RNA silencing by a plant DNA virus satellite requires a host calmodulin-like protein to repress RDR6 expression. *PloS Pathog.* 10, e1003921. doi: 10.1371/journal.ppat.1003921

Li, F., and Wang, A. (2019). RNA-targeted antiviral immunity: more than just RNA silencing. *Trends Microbiol*. 27, 792–805. doi: 10.1016/j.tim.2019.05.007

Lin, J., Guo, J., Finer, J., Dorrance, A., Redinbaugh, M. G., and Qu, F. (2014). The bean pod mottle virus RNA2-encoded 58K protein is required in cis for RNA2 accumulation. *J. Virol*. 88, 3213–3222. doi: 10.1128/JVI.03301-13

Livak, K. J., and Schmittgen, T. D. (2001). Analysis of relative gene expression data using real-time quantitative PCR and the 2(-Delta Delta C(T)) Method. *Methods* 25, 402–408. doi: 10.1006/meth.2001.1262

Luo, C., Wang, Z. Q., Liu, X., Zhao, L., Zhou, X., and Xie, Y. (2019). Identification and analysis of potential genes regulated by an Alphasatellite (TYLCCNA) that contribute to host resistance

against Tomato Yellow Leaf Curl China Virus and its Betasatellite (TYLCCNV/TYLCCNB) Infection in *Nicotiana benthamiana*. *Viruses* 11, 442–442. doi: 10.3390/v11050442

Mahas, J. W., Hamilton, F. B., Roberts, P. M., Ray, C. H., Miller, G. L., Sharman, M., et al. (2022). Investigating the effects of planting date and *Aphis gossypii* management on reducing the final incidence of cotton leafroll dwarf virus. *Crop Prot.* 158, 106005. doi: 10.1016/j.cropro.2022.106005

Morello, C., Suassuna, N., Farias, F., Lamas, F., Pedrosa, M., Ribeiro, J., et al. (2010). BRS 293: A midseason high-yielding upland cotton cultivar for Brazilian savanna. *Crop Breed. Appl. Biotechnol*. 10, 180–182. doi: 10.12702/1984-7033.v10n02a13

Nishiguchi, M., and Kobayashi, K. (2011). Attenuated plant viruses: preventing virus diseases and understanding the molecular mechanism. *J. Gen. Plant Pathol*. 77, 221– 229. doi: 10.1007/s10327-011-0318-x

Parkash, V., Sharma, D. B., Snider, J., Bag, S., Roberts, P., Tabassum, A., et al. (2021). Effect of cotton leafroll dwarf virus on physiological processes and yield of individual cotton plants. *Front. Plant Sci*. 12. doi: 10.3389/fpls.2021.734386

Price, T., Valverde, R., Singh, R., Davis, J., Brown, S., and Jones, H. (2020). First report of cotton leafroll dwarf virus in Louisiana. *Plant Health Prog*. 21, 142–143. doi: 10.1094/PHP-03-20-0019-BR

Qu, F., Ren, T., and Morris, T. J. (2003). The Coat Protein of Turnip Crinkle Virus suppresses posttranscriptional gene silencing at an early initiation step. *J. Virol*. 77, 511–522. doi: 10.1128/JVI.77.1.511-522.2003

Ramos-Sobrinho, R., Adegbola, R. O., Lawrence, K., Schrimsher, D. W., Isakeit, T., Alabi, O. J., et al. (2021). Cotton Leafroll Dwarf Virus US genomes comprise divergent subpopulations and harbor extensive variability. *Viruses* 13, 2230. doi: 10.3390/v13112230

Scholthof, H. (2006). The Tombusvirus-encoded P19: from irrelevance to elegance. Nat. Rev. *Microbiol*. 4, 405–411. doi: 10.1038/nrmicro1395

Sharma, P., and Ikegami, M. (2010). Tomato leaf curl Java virus V2 protein is a determinant of virulence, hypersensitive response and suppression of posttranscriptional gene silencing. *Virology* 396, 85–93. doi: 10.1016/j.virol.2009.10.012

Silva, T., Corrêa, R., Castilho, Y., Silvie, P., Bélot, J.-L., and Vaslin, M. (2008). Widespread distribution and a new recombinant species of Brazilian virus associated with cotton blue disease. *Virol. J*. 5, 123. doi: 10.1186/1743-422X-5-123

Sinha, K. V., Das, S. S., and Sanan-Mishra, N. (2021). Overexpression of a RNA silencing suppressor, B2 protein encoded by Flock House virus, in tobacco plants results in tolerance to salt stress. *Phytoparasitica* 49, 299–316. doi: 10.1007/s12600-020-00847-y

Smirnova, E., Firth, A. E., Miller, W. A., Scheidecker, D., Brault, V., Reinbold, C., et al. (2015). Discovery of a small non-AUG-initiated ORF in Poleroviruses and Luteoviruses that is required for long-distance movement. *PloS Pathog*. 11, e1004868. doi: 10.1371/journal.ppat.1004868

Sõmera, M., Fargette, D., Hébrard, E., Sarmiento, C. ICTV report consortium (2021). ICTV virus taxonomy profile: Solemoviridae 2021. *J. Gen. Virol*. 102, 001707. doi: 10.1099/jgv.0.001707

Tabassum, A., Bag, S., Suassuna, N. D., Conner, K. N., Chee, P., Kemerait, R. C., et al. (2021). Genome analysis of cotton leafroll dwarf virus reveals variability in the silencing suppressor protein, genotypes and genomic recombinants in the USA. *PloS One* 16, e0252523. doi: 10.1371/journal.pone.0252523

Tabassum, A., Roberts, P. M., and Bag, S. (2020). Genome sequence of Cotton Leafroll Dwarf Virus infecting cotton in Georgia, USA. *Microbiol. Resour Announc* 9, e00812–e00820. doi: 10.1128/MRA.00812-20

Tarazi, R., and Vaslin, M. F. S. (2022). The viral threat in cotton: how new and emerging technologies accelerate virus identification and virus resistance breeding. *Front. Plant Sci*. 13. doi: 10.3389/fpls.2022.851939

Thiessen, L. D., Schappe, T., Zaccaron, M., Conner, K., Koebernick, J., Jacobson, A., et al. (2020). First report of Cotton Leafroll Dwarf Virus in cotton plants affected by cotton leafroll dwarf disease in North Carolina. *Plant Dis*. 104, 3275. doi: 10.1094/PDIS-02-20-0335-PDN

Voinnet, O., Vain, P., Angell, S., and Baulcombe, D.C. (1998). Systemic spread of sequence-specific transgene RNA degradation in plants is initiated by localized introduction of ectopic promoterless DNA. *Cell* 95, 177–187. doi: 10.1016/S0092-8674(00)81749-3

Voinnet, O., Pinto, Y. M., and Baulcombe, D. C. (1999). Suppression of gene silencing: A general strategy used by diverse DNA and RNA viruses of plants. Proc. *Natl. Acad. Sci. U.S.A.* 96, 14147–14152. doi: 10.1073/pnas.96.24.14147

Wang, L., Fan, P., Jimenez-Gongora, T., Zhang, D., Ding, X., Medina-Puche, L., et al. (2022a). The V2 protein from the Geminivirus Tomato Yellow Leaf Curl Virus largely associates to the endoplasmic reticulum and promotes the accumulation of the viral C4 protein in a silencing suppression-independent manner. *Viruses* 14, 2804. doi: 10.3390/v14122804

Wang, H., Greene, J., Mueller, J., Conner, K., and Jacobson, A. (2020). First report of Cotton Leafroll Dwarf Virus in cotton fields of South Carolina. *Plant Dis.* 104, 2532. doi: 10.1094/PDIS-03-20-0635-PDN

Wang, Y., Liu, H., Wang, Z., Guo, Y., Hu, T., and Zhou, X. (2022). P25 and P37 proteins encoded by firespike leafroll-associated virus are viral suppressors of RNA silencing. *Front. Microbiol*. 13, 964156. doi: 10.3389/fmicb.2022.964156

Wang, L., Tan, H., Medina-Puche, L., Wu, M., Gomez, B. G., Gao, M., et al. (2022b). Combinatorial interactions between viral proteins expand the potential functional landscape of the tomato yellow leaf curl virus proteome. *PloS Pathog.* 18, e1010909. doi: 10.1371/journal.ppat.1010909

Wang, L., Tian, P., Yang, X., Zhou, X., Zhang, S., Li, C., et al. (2021). Key amino acids for Pepper Vein Yellows Virus P0 protein pathogenicity, gene silencing, and subcellular localization. *Front. Microbiol*. 12, 1653–1653. doi: 10.3389/fmicb.2021.680658

Xiao, Q., Li, W., Kai, Y., Chen, P., Zhang, J., and Wang, B. (2019). Occurrence prediction of pests and diseases in cotton on the basis of weather factors by long short term memory network. *BMC Bioinf*. 20, 688. doi: 10.1186/s12859-019-3262-y

Xiao-Yan, Z., Yuan-Yuan, L., Wang, Y., Jia-Lin, Y., and Cheng-Gui, H. (2021). Comparative analysis of biological characteristics among P0 proteins from different Brassica Yellows Virus genotypes. *Biology* 10, 1076. doi: 10.3390/biology10111076

Zhuo, T., Li, Y.-Y., Xiang, H.-Y., Wu, Z.-Y., Wang, X.-B., Wang, Y., et al. (2014). Amino acid sequence motifs essential for P0-mediated suppression of RNA silencing in an isolate of potato leafroll virus from Inner Mongolia. *Mol. Plant Microbe Interact*. 27, 515–527. doi: 10.1094/MPMI-08-13-0231-R

Ziegler-Graff, V. (2020). Molecular insights into host and vector manipulation by plant viruses. *Viruses* 12, 263. doi: 10.3390/v12030263

Figures

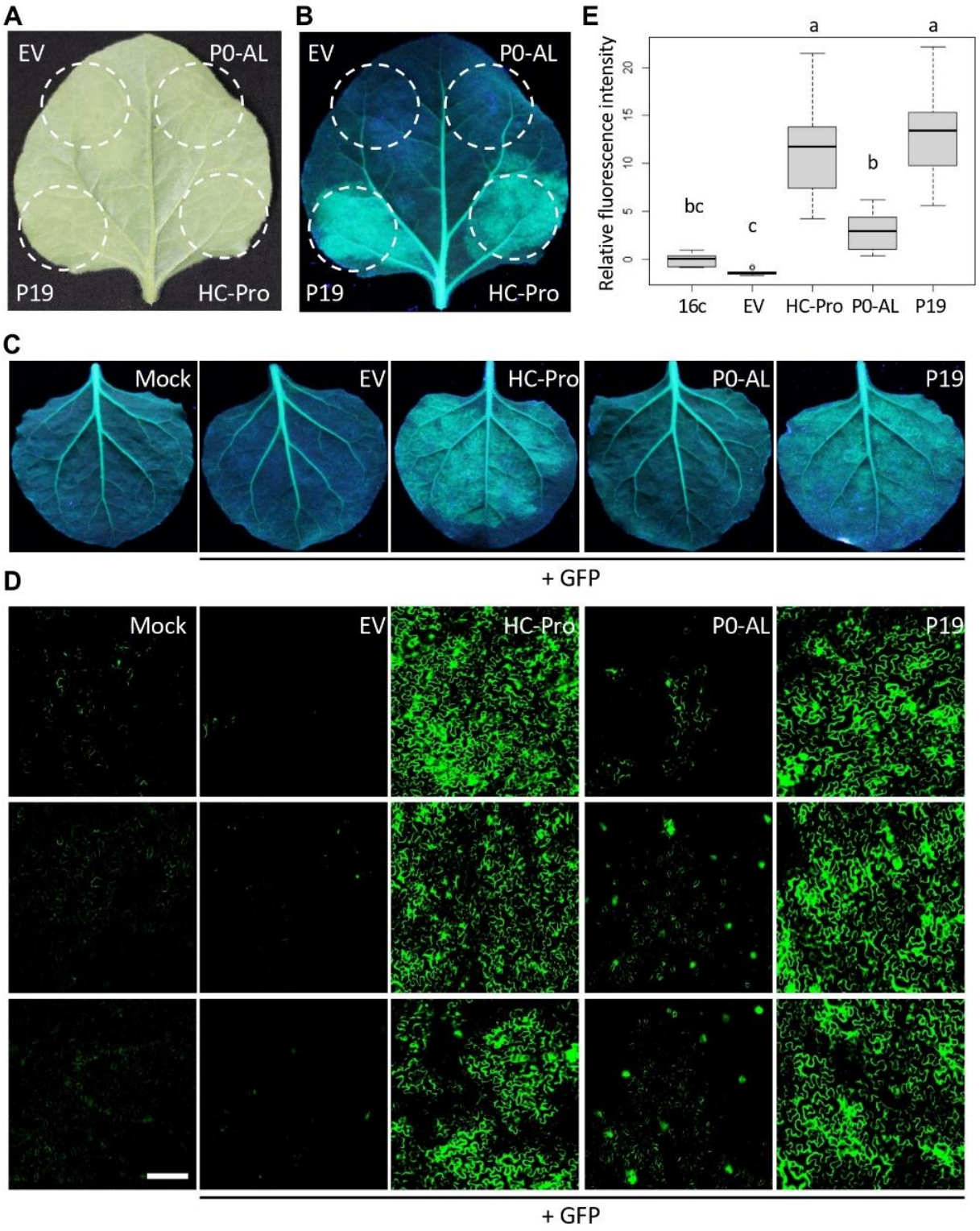
A
EV
P0-AL
P19
HC-Pro
B
EV
P0-AL
P19
HC-Pro
E
Relative fluorescence intensity
0
5
10
15
20
a
a
b
bc
c
16c
EV
HC-Pro
P0-AL
P19
C
Mock
EV
HC-Pro
P0-AL
P19
+ GFP
D
Mock
EV
HC-Pro
P0-AL
P19
+ GFP

Figure 1: P0 protein of CLRDV-AL is a weak local VSR

Potency of P0 protein of CLRDV-AL as a viral suppressor of RNA silencing (VSR) was compared to the known VSRs, such as P19 or HC-Pro, by co-expressing GFP and each VSR in GFP-transgenic *N. benthamiana* (16c) plants by Agroinfiltration. Images were taken at 4 days post infiltration (dpi) under the natural light **(A)** and UV light **(B, C)**. The same leaf is shown for panels **(A, B)** EV, empty vector. **(D)** Infiltrated leaf tissue shown in panel **(C)** was examined using a fluorescence microscope. Three representative images per treatment were shown. Scale bar = 180 µm. **(E)** The fluorescence intensity was calculated using Region of Interest (ROI) on ImageJ. The relative intensity was analyzed by one-way ANOVA test in R and shown as a box and whisker plot. Each box plot depicts the interquartile range (middle 50% of the data), the lower and upper edge show the first and third quartile (25th and 75th percentile respectively), median (horizontal line within the box). The whiskers are the contributions within the 1.5 interquartile range; open circles beyond these whiskers are considered as outliers; significant differences, $p < 0.01$, were denoted by letters.

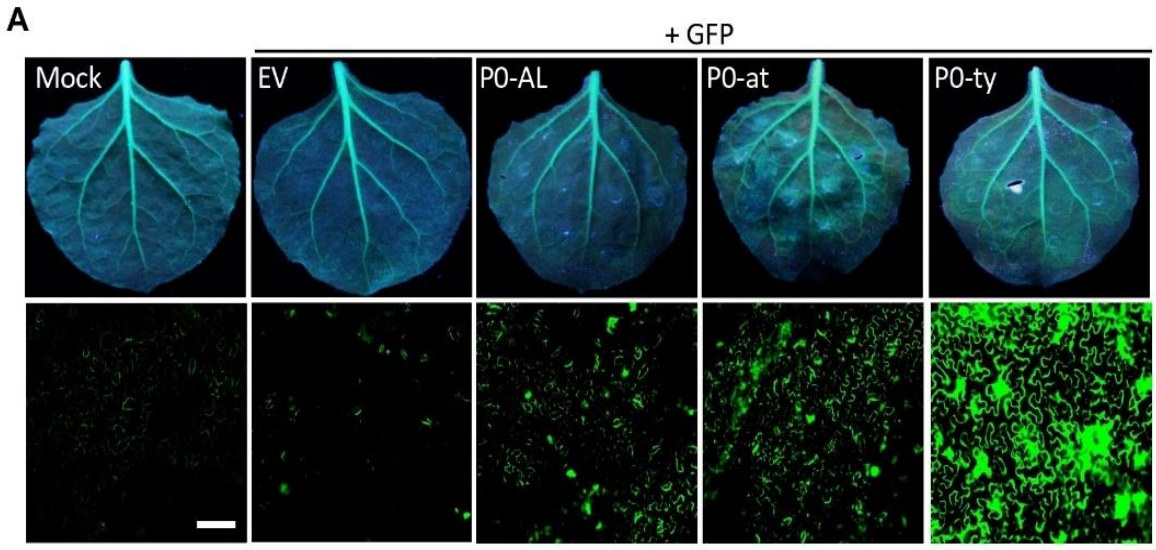
A
+ GFP
Mock
EV
P0-AL
P0-at
P0-ty

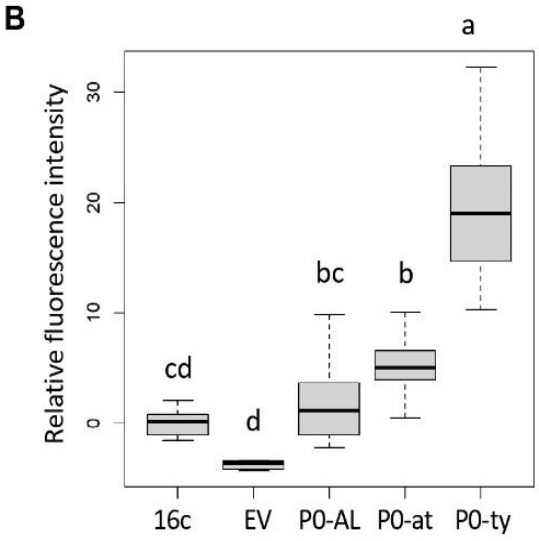
B
Relative fluorescence intensity
0
10
20
30
a
bc
b
cd
d
16c
EV
P0-AL
P0-at
P0-ty

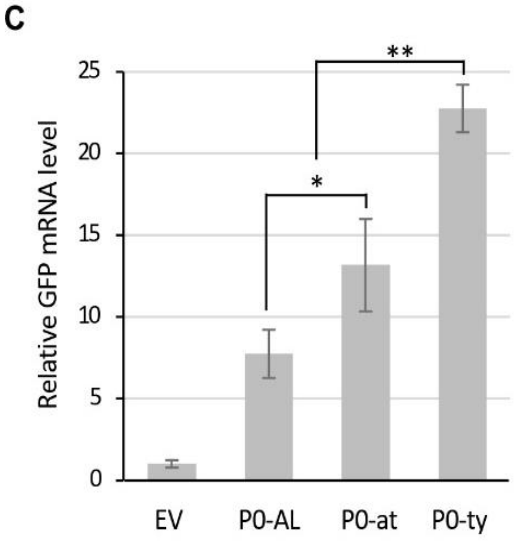
C
Relative GFP mRNA level
0
5
10
15
20
25
**
*
EV
P0-AL
P0-at
P0-ty

Figure 2: Comparison of VSR potency among the P0s encoded by three CLRDV strains.

The suppressor of RNA silencing activity of the P0 proteins from CLRDV-AL, CLRDV-ty, and CLRDV-at was compared by co-expressing GFP and each P0 in GFP-transgenic *N. benthamiana* (16c) plants by Agroinfiltration. Images were taken at 4 dpi under the UV light (**A**, top row) and using a fluorescence microscope (**A**, bottom row). Scale bar = 180 µm. Mock; non-infiltrated *N. benthamiana* 16c plant, EV; empty vector. See Supplementary Figure 1 for more fluorescence microscopy images. Note that the leaves shown for Mock and EV are the same images used in Figure 1C as this set of Agroinfiltration was performed concurrently. **(B)** The fluorescence intensity was calculated using Region of Interest (ROI) on ImageJ. The relative intensity was analyzed by one-way ANOVA test in R and shown as a box and whisker plot. Significant differences were denoted by letters. **(C)** GFP mRNA levels in tissues co-infiltrated with a set shown in **(A)** were analyzed by RT-qPCR. Error bars indicate the standard deviation of the means of Ct values in three biological repeats using *actin2* reference gene and $2^{-\Delta\Delta Ct}$ method. Statistically significant differences determined by Student's t-test, $p < 0.05$ or < 0.01, were denoted by asterisks (* or **, respectively). Note that all P0s showed significant difference ($p < 0.01$) from EV, but not noted.


CLRDV-at MLNLIICRVSSAALVRRASPSVKSNQVDFLHFITQLQQYLIFCNSPDLNPFHNGFNESFL
CLRDV-AL MLNLIICRISSAALIRHASASVSNNQVDFLHFLTQLPEYLIFCHSPEHNPFQNVFNESFL
CLRDV-ty MLNLIICRISSAALIRHASASVSNNQVDFLFFLTQLPEYLTFCNSPELNPFHDGFNESFL
CLRDV-at LRSLLFLLPFLVGGISSSRFALPRGLRADFMALSRATKYMPTVTEYKGNYIVALHLPSCR
CLRDV-AL LRSLLFLLPFFVRGISSSRFALPRGLRADFMALSRATKYMPTVTEFEGNYIVALHLPSRR
CLRDV-ty LRSLLFLLPFIIRGISSSRFALPRGIRADFMALSRATKYMPTVTDFKGNYLVALHLPSRR
CLRDV-at ATGRATRERFATRSLVENNWLEFEHLCTRGYEYFKRFTRLLAGEVRECPQERWTVRPSCV
CLRDV-AL ATGRATRERFATRSLVENNRLEFEYLCTRGYKYFQRFAQVLAGEVRECSQERWTVRPSCV
CLRDV-ty ATGRATRERFAIRSLVENNRLEFEYLCTRGYEYFKRFAQTLAGEVRECPQERWTVRPSCM
CLRDV-at GLRALAIRLMDLVPGDEPLSNRSGHRLSVLVHNLYGDDASLSFWRIARFPDSSYYHFDDE
CLRDV-AL GLRALAIRLLELVPGDEPLSDGSGRRLSVLVHNLYGSGASLSFWRIARFPDSSFYFFDDE
CLRDV-ty GLRALAIRLMDLVPGDEPLSNRSGHRLSVLVHNLYGDGASLSFWRIARFPDSSYYHFDDE
CLRDV-at GGVGLLHQSQIQQLLCEGESS
CLRDV-AL GGVGLLYQSQIQQLLCEGESS
CLRDV-ty GGVGLLYQSQIQQLLCEGESS

Figure 3: Alignment of the P0s encoded by CLRDV-AL, CLRDV-ty, and CLRDV-at.

Amino acid (aa) sequences of the P0 proteins from three CLRDV strains were aligned. Notable divergence in P0-AL, within the F-box motif (shown in a box with black line) linked to RNA silencing suppressor activity, from atypical, typical, or both are noted in blue, red, or green, respectively. Consensus symbols show sequence similarities based on Percent Accepted Mutations (PAM) 250 scoring matrix. '*'; indicates aa fully conserved aa residues. ':'; indicates conservation between groups of strongly similar properties. '.'; indicates conservation between groups of weakly similar properties.

Supplementary Figure

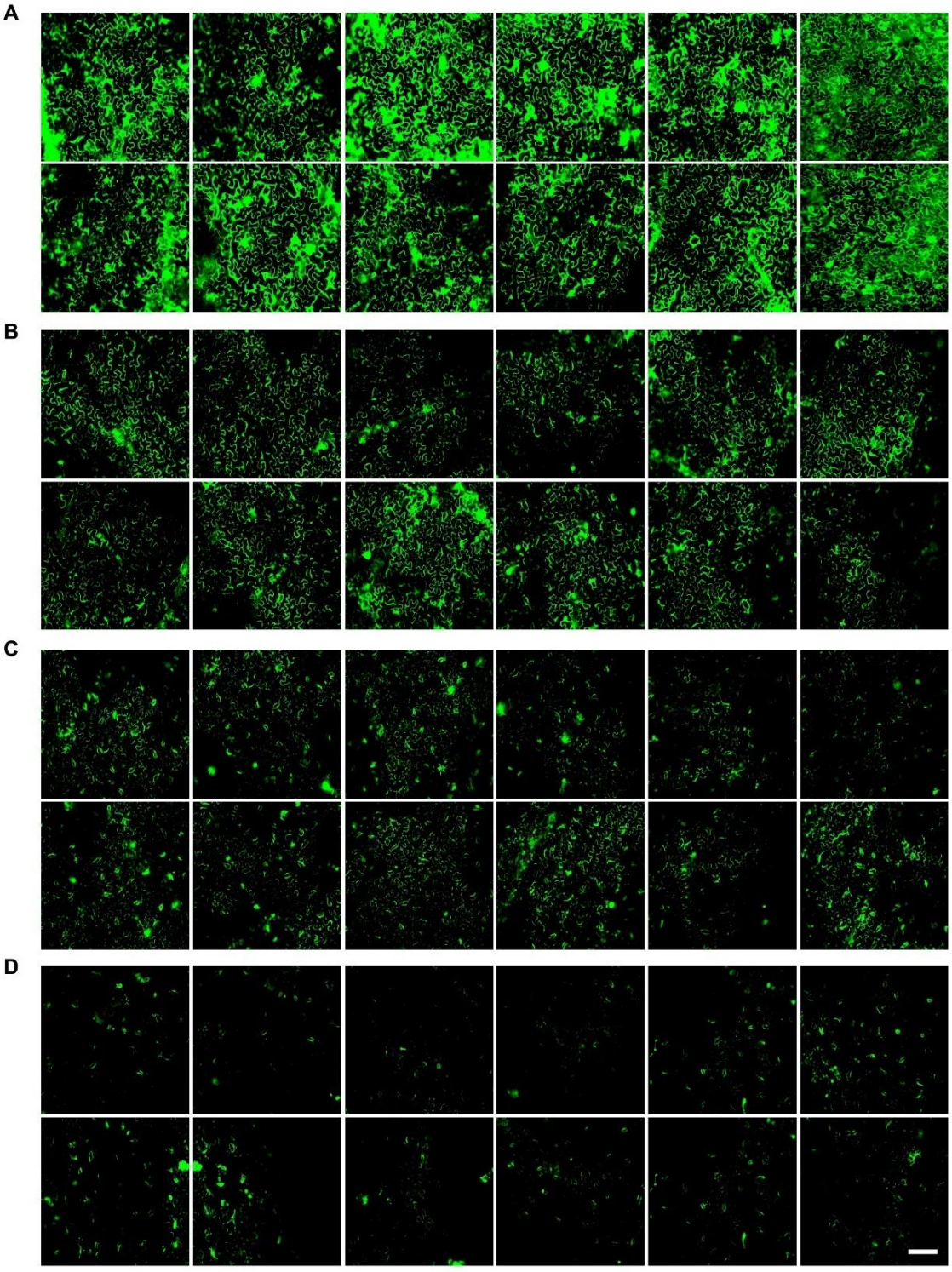

Supplementary Figure 1: Infiltrated leaf tissue showing GFP silencing inhibition from Figure 2A was examined using a fluorescence microscope. Representative images used for the analysis of relative fluorescence intensity (Figure 2B) are shown. (**A**; P0-ty, **B**; P0-at, **C**; P0-AL, **D**; EV). Scale bar = 180 µm.

Chapter 3

Predictive Amino Acid Mutation Reveals an Amplified RNA Silencing Suppressor Potency of a New Cotton Infecting Polerovirus

3.1 Abstract

The P0 proteins encoded by Cotton leafroll dwarf virus (CLRDV) serve as suppressors of RNA silencing (VSR), countering host defenses and influencing pathogenicity and disease severity. CLRDV P0 proteins, including a newly isolated strain characterized by its cryptic pathogenicity and weaker P0 suppressor, share a VSR-associated F-box-like motif. This study investigated the role of specific amino acid (aa) residues within the F-box-like motif through a comparative analysis of P0 proteins among CLRDV strains, elucidating their implications for virulence, VSR potency, and intracellular localization. Analysis of various single aa substitution mutants within the F-box-like motif to understand their influence on P0's VSR potency revealed that specific mutations can significantly affect P0's ability to suppress RNA silencing, emphasizing the crucial role of the F-box-like motif. Subcellular localization examinations indicated that the P0 proteins associate with the endoplasmic reticulum (ER), which may be linked to their VSR function. Additionally, different CLRDV strains exhibited variations in nuclear localization, further influencing their VSR potency. The study also observed the induction of hypersensitive response (HR)-like symptoms and the accumulation of reactive oxygen species by P0 proteins, suggesting their role as pathogenicity factors. These results indicated that specific mutations significantly affect functions of multifaceted P0 protein, highlighting the F-box-like motif's crucial role. This study highlighted the importance of further molecular investigations to elucidate how different CLRDV strains manifest various disease symptoms and severity. This is crucial considering the global economic importance of cotton and the potential emergence of more threatening CLRDV isolates.

3.2 Introduction

Cotton leafroll dwarf virus (CLRDV) is a newly emerging virus in the United States that has had a significant impact on cotton production in other countries (Agrofoglio et al., 2017; Avelar et al., 2019; Bag et al., 2021; Distéfano et al., 2010; Edula et al., 2023; Parkash et al., 2021). CLRDV belongs to the family *Solemoviridae* and the genus *Polerovirus*, which consists of plant viruses expressing their proteins through complex translation strategies from the genome (reviewed in Delfosse et al., 2021; Avelar et al., 2020; Correa et al., 2005; Smirnova et al., 2015; Sõmera et al., 2021). CLRDV has a monopartite, positive-sense, single-stranded RNA genome with a length of 5.7 kb (Avelar et al., 2020). The genome comprises seven open reading frames (ORFs) (Figure 1A) (Distéfano et al., 2010; King et al., 2012). ORF 0 encodes the P0 protein, a viral suppressor of RNA silencing (VSR), which plays a role in countering plants' RNA silencing mechanism (Agrofoglio et al., 2019; Akinyuwa et al., 2023; Cascardo et al., 2015; Delfosse et al., 2014). ORF 1 and ORF 1-2 produce P1 and P1-P2 that are responsible for replication through leaky scanning and ribosomal frameshift, respectively (Cornish et al., 2005; Delfosse et al., 2021; Tabassum et al., 2021). ORF 3 encodes the P3 protein, serving as a major coat protein involved in the encapsidation (Kaplan et al., 2007; Lee et al., 2005; Terradot et al., 2001). ORF 4 is embedded within the ORF 3 and is translated through leaky scanning to produce the P4 protein (Hofius et al., 2001; Lee et al., 2002; Xia et al., 2012). ORF3a encodes the P3a protein using a non-canonical start codon located upstream of ORF3 (DeBlasio et al., 2018; Smirnova et al., 2015; Zhang et al., 2018). Both P3a and P4 proteins are involved in the virus movement (Smirnova et al., 2015; Xia et al., 2012; Zhang et al., 2018). ORF 3-5 encodes the P3-P5 protein through translational readthrough, and is essential for aphid transmission and virus accumulation in the host (Peter et al., 2009, 2008; Rodriguez-Medina et al., 2015; Tabassum et al., 2021).

Among the proteins commonly produced by members of genus *Polerovirus*, the P0 protein has been extensively studied due to its pivotal role in countering the host's antiviral defense system, RNA silencing (Agrofoglio et al., 2019; Almasi et al., 2015; Delfosse et al., 2014; Sun et al., 2020; K.-D. Wang et al., 2023, L. Wang et al., 2021). RNA silencing involves the recognition and subsequent degradation of viral double-stranded RNA (Hammond, 2005; Li and Wang, 2019; Voinnet, 2005). Host factors participating in this process include an endonuclease called Dicer, responsible for generating siRNA, and the Argonaut (AGO) protein, which processes the target

(Blevins et al., 2006; Derrien et al., 2018; Li and Wang, 2019; Pazhouhandeh et al., 2006). However, plant viruses have evolved their own proteins to interfere with this process. In the case of the members of the genus *Polerovirus*, this interference is accomplished through the P0 proteins (Agrofoglio et al., 2019; Akinyuwa et al., 2023; Bortolamiol-Bécet et al., 2018; Delfosse et al., 2014; Fusaro et al., 2012; Kozlowska-Makulska et al., 2010; Li et al., 2019; Sun et al., 2020; Wang et al., 2018, 2021a). Consequently, the P0 protein is often associated with virus pathogenicity and symptom development (Agrofoglio et al., 2019; Liang et al., 2023; Rashid et al., 2019; Wang et al., 2015, 2023, 2021a). Interestingly, despite being the most divergent ORF within the genome, P0 retains a conserved region referred to as the F-box-like motif in its N-terminal proximity (Figure 1B; Baumberger et al., 2007; Cascardo et al., 2015; LaTourrette et al., 2021; Pazhouhandeh et al., 2006; Wang et al., 2018). In previous studies using mutant P0s with amino acid (aa) substitutions, this motif has been shown to be involved in VSR activity, intracellular location, and interactions with host proteins (Bortolamiol et al., 2007; Correa et al., 2013; Derrien et al., 2012, 2018; Li et al., 2019; Pazhouhandeh et al., 2006; Rashid et al., 2019; Sun et al., 2018, 2020; Wang et al., 2023, 2021a; Zhuo et al., 2014).

Two previously reported CLRDV strains, CLRDV-ty and CLRDV-at, exhibit variations in their pathogenicity levels and their ability to overcome resistance (Agrofoglio et al., 2019, 2017; da Silva et al., 2015; Delfosse et al., 2014; Galbieri et al., 2017). A study using an aa substitution that reverted a single aa within the F-box-like motif in CLRDV-at to that found in CLRDV-ty demonstrated an enhancement in its VSR potency and pathogenicity compared to the wild-type (WT) CLRDV-at (Agrofoglio et al., 2019, 2017; Delfosse et al., 2014; Tabassum et al., 2021). Similar changes in symptom development, VSR potency, intracellular localization, and viral pathogenicity resulting from aa substitution within the F-box-like motif were also reported in other members of the genus *Polerovirus* (Rashid et al., 2019; Sun et al., 2020; Wang et al., 2018, 2023, 2021a; Zhuo et al., 2014). Interestingly, the results from chapter 2 reported that the cryptic pathogenicity displayed by a new strain of CLRDV, recently isolated from the U.S. and designated as CLRDV-AL (Avelar et al., 2020, 2019), could be due to relatively weaker P0 protein activity as a VSR compared to other strains (Akinyuwa et al., 2023). That study discussed the three different aa residues within CLRDV-AL's F-box-like motif compared to CLRDV-ty and CLRDV-at. However, it remained speculative, and the underlying function of this difference has not been demonstrated.

This chapter aimed to identify specific aa residues associated with the characteristics of the P0 protein encoded by CLRDV-AL ($P0^{AL}$). A series of mutant P0 proteins with aa substitutions within the F-box-like motif was generated using site-directed mutagenesis. This study demonstrated how mutations or reversions within this conserved motif could exert significant changes on the protein's VSR potency, intracellular localization, and pathogenicity. Moreover, this chapter engaged in a comprehensive discussion regarding identified aa residues compared other members of genus Polerovirus. The findings from this chapter could offer insights into the potential new variants of CLRDV that might present a greater threat to cotton industry.

3.3 Materials and Methods

3.3.1 CLRDV P0 Constructs

The cDNA constructs of the ORF 0 from three different CLRDV strains (-ty, -at, and -AL) placed under the CaMV 35S promoter sequence in the binary plasmid pAIDEE (pAI-P0^{ty}, pAI-P0^{at}, and pAI-P0^{AL}, respectively) were previously described (Akinyuwa et al., 2023).

3.3.2 Generation of P0^{AL} Mutant Constructs

The cDNA constructs expressing a series of mutant P0^{AL,} which carry a single aa substitution mutation within the F-box-like motif were constructed by Q5 site-directed mutagenesis kit (New England Biolabs, Ipswich, MA, USA). To generate pAI-P0^{L68A}, pAI-P0^{P69A}, and pAI-P0^{V72I}, pairs of oligomers were designed as per the manufacturer's protocol (Table 1) and used to amplify the cDNA encompassing the entire plasmid with the P0 sequence with the targeted mutation using the pGEMT-P0^{AL}, a cDNA of P0^{AL} coding sequence cloned into pGEM-T plasmid (Promega, Madison, WI, USA), as a template. The final products were verified by sequencing at Psomagen Inc. (Rockville, MD, USA) and amplified using a pair of oligomers, P0^{AL}.FW.*Apa*I and P0^{AL}.RV.*Xba*I (Table 1). The amplified product was separated in 0.8% agarose gel by electrophoresis, and the target DNAs were purified using DNA Clean & Concentrator®-5 Kit (Zymo Research, Irvine, CA, USA). The purified DNAs were digested using *Apa*I and *Xba*I restriction endonucleases (New England BioLabs, Ipswich, MA, USA) and ligated into the corresponding region of the binary plasmid pAIDEE (pAI; (Lin et al., 2014) digested with the same restriction endonucleases using T4 DNA ligase (Promega, Madison, WI, USA). Constructs were transformed into *E. coli* NEB® DH 5-alpha competent cells (New England Biolabs, Ipswich, MA, USA) and the resulting transformants were screened on Luria–Bertani (LB) agar plates containing kanamycin (100 µg/µl). Final products were verified by sequencing at Psomagen Inc. (Rockville, MD, USA). The cDNA constructs expressing a series of mutant P0^{AL} (P0^{L68A}, P0^{P69A}, P0^{F71I}, P0^{F71L}) were made using the cDNAs of ORF 0 synthesized and cloned into a pUC57mini plasmid (Genscript, Piscataway, NJ, USA) with the corresponding site mutation. The synthesized products were digested with *Kpn*I and *Apa*I restriction endonucleases (New England BioLabs, Ipswich, MA, USA. The excised fragments were separated in 1.5% agarose gel by electrophoresis

and purified from the gel using Zymoclean Gel DNA Recovery Kit (Zymo Research, Irvine, CA, USA). The purified DNAs were ligated into the corresponding region of the wild-type pAI-P0^{AL}, which was digested with the same restriction endonucleases using T4 DNA ligase (Promega, Madison, WI, USA). Constructs were transformed into *E. coli* NEB® DH 5-alpha competent cells and the resulting transformants were screened on LB agar plates containing kanamycin (100 µg/µl). Final products were verified by sequencing at Psomagen Inc. (Rockville, MD, USA).

3.3.3 Generation of the Green Fluorescent Protein-tagged Constructs

To generate the green fluorescent protein (GFP)-tagged set of selected clones (P0^{ty}:GFP, and P0^{at}:GFP, P0^{AL}:GFP, and P0^{V72I}:GFP), overlap-extension polymerase chain reaction (OE-PCR) was performed as previously described (Kang et al., 2018). The overlap was achieved by two PCR fragments with overhangs; one contains the 3´ end of P0 with an extension into the 5´ region of the GFP ORF, and the other contains the 5´ end of GFP with an extension into P0 3´ (Carrasco et al., 2007). The stop codon of the P0 was deleted to allow readthrough to the GFP ORF (Figure 1C). The first product, the P0-GFP fragment was generated by fusing the 3´ end of P0 or its mutants (P0^{V72I}:GFP) in front of the GFP ORF using PCR with a pair of oligomers, P0^{AL}.FW.*Apa*I and P0:GFP-RV (Table 1). For P0^{at}:GFP fragment, a pair of oligomers, P0^{at}.FW.*Apa*I and P0:GFP-RV, was used (Table 1). The full-length cDNA clones of GFP, P0^{AL}, P0^{V72I}, P0^{ty}, and P0^{at} placed under the CaMV 35S promoter sequence in the binary vector pAI were used to amplify the different fragments of the latter fragments (P0^{AL}:GFP, P0^{V72I}:GFP, P0^{ty}:GFP, and P0^{at}:GFP). The OE-PCR was performed to generate overlap fragments using two pairs of oligomers; P0^{AL}.FW.*Apa*I and GFP.RV.*Xba*I for P0^{AL}:GFP, P0^{V72I}:GFP, P0^{ty}:GFP, and P0^{at}.FW.*Apa*I and GFP.RV.*Xba*I for P0^{at}:GFP (Table 1). The overlap fragments were subsequently digested with *Xba*I and *Apa*I restriction endonucleases before ligating into the pAI plasmid. The remaining GFP-tagged P0 mutants (P0^{L68A}:GFP, P0^{P69A}:GFP, P0^{F71I}:GFP, and P0^{F71L}:GFP) were generated similarly as described above (See Materials and Methods 2.2) except that pAI-P0^{AL}:GFP was used as a backbone for the ligation. Constructs were transformed into *E. coli* NEB® DH 5-alpha competent cells (Ipswich, MA, USA) and the transformants were screened on LB plates containing kanamycin (100 µg/µl). Final products were verified by sequencing at Psomagen Inc. (Rockville, MD, USA).

3.3.4 Agroinfiltration

Agroinfiltration of the constructs was conducted as previously described (Kang et al., 2015). Briefly, *Agrobacterium tumefaciens* strain GV3101 was transformed with the plasmid constructs by the heat shock method. The resulting transformants were screened on LB agar plates containing kanamycin and rifampicin (100 mg/ml and 50 mg/ml, respectively). A single colony was selected and inoculated in 3 ml liquid LB media containing kanamycin (100 mg/ml). The cells were grown overnight at 28^{o}C, then 50 µl of the culture was transferred into 5 ml of fresh LB media with kanamycin and rifampicin (100 µg/µl and 50 µg/µl, respectively). The cells were grown overnight at 28^{o}C, and the culture was centrifuged at 3,000 rpm for 10 mins. Pelleted cells were resuspended in agroinfiltration buffer (10 mM MES, pH 5.85; 10 mM $MgCl_2$; 150 µM Acetosyringone) at the optical density (OD_{600nm}) 1.0 or 0.5. Following the incubation for at least 2 hours without shaking at room temperature, the suspension was infiltrated into the lower surface of fully expanded leaves of six weeks old *Nicotiana benthamiana* plants using needleless syringes. The infiltrated plants were grown under 16h/8h of light/dark cycle until further analysis.

3.3.5 Examination of Fluorescence in Plants

Six weeks old *N. benthaminana* 16c plants were co-infiltrated with equal volumes of *A. tumefaciens* cells containing pAI-P0^{AL}, pAI-P0^{ty}, pAI-P0^{at}, pAI-P0^{L68A}, pAI-P0^{P69A}, pAI-P0^{F71I}, pAI-P0^{F71L}, and pAI-P0^{V72I} or empty vector mixed with pAI-GFP. The expression of GFP transgene was observed under a long wavelength (365 nm) using a hand-held UV lamp raised 6 inches above the plants at four days post infiltration (dpi) in the dark room. The infiltrated leaves were collected at 5 dpi and examined using a fluorescence microscope with wavelengths specified by FITC cube (EX:470±40 and EM:525±50) on Echo Revolve (San Diego, CA, USA).

3.3.6 Intracellular Localization

pAI-P0^{AL}:GFP, pAI-P0^{ty}:GFP, pAI-P0^{at}:GFP, pAI-P0^{L68A}:GFP, pAI-P0^{P69A}:GFP, pAI-P0^{F71I}:GFP, pAI-P0^{F71L}:GFP, and pAI-P0^{V72I}:GFP were infiltrated in *N. benthamiana* plants. Mesophyll cells of the leaves were observed at 5 dpi using an Echo Revolve fluorescence

microscope (San Diego, CA, USA) with FITC cube (EX:470±40 and EM:525±50) and TxRED cube (EX:560±40 and EM:630±75) for the detection of GFP and RFP fluorescence, respectively. Images were captured using 20x objectives.

3.3.7 Relative Expression Levels of GFP mRNA

The relative expression levels of GFP mRNA were evaluated by RT-qPCR using the Luna® universal RT-qPCR system (New England Biolabs, Ipswich, MA, USA). Total RNA was extracted from 100 mg of leaf discs of infiltrated *N. benthamiana* (seven discs of 0.9 cm in diameter). The samples were ground in liquid nitrogen using TissueLyser II (Qiagen, Hilden, Germany). The extraction was performed using the RNeasy Plant Mini Kit (Qiagen, Hilden, Germany) according to the manufacturer's protocol. RNA quality and concentration were evaluated using a NanoDrop^{TM} Lite Spectrophotometer (ThermoFisher Scientific, Waltham, MA, USA). One-step RT-qPCR reactions were performed in a total volume of 10 µl, using 2 µl of RNA (10 ng/µl). The amplification of GFP was done using a pair of oligomers, MFA.Gq-PCR:FW and MFA.Gq-PCR:RV. The reference gene, *NbACTIN2*, was used as the internal control and was amplified using a pair of oligomers, *NbACTIN*2-FW and *NbACTIN*2-RV, as previously described (Luo et al., 2019). The cycling conditions include the reverse transcription at 55^{o}C for 10 min, incubation at 95^{o}C for 2 min, and 40 cycles of 95 ^{o}C for 10 s and 60 ^{o}C for 60 s. Three biological and technical replicates were performed for all treatments. Ct values were averaged for triplicates of each sample before calculating relative values using the $2^{-\Delta\Delta Ct}$ method (Livak and Schmittgen, 2001).

3.3.8 Histochemical Staining

3,3´-diaminobenzidine (DAB) staining was performed to detect reactive oxygen species (ROS) as previously described (Kang et al., 2019). *N. benthamiana* leaves infiltrated as described in Materials and Methods 2.4 at OD_{600nm} = 0.5 were detached and washed three times with double distilled water. Then, the leaves were incubated overnight in 1 mg/ml DAB-HCl (Sigma-Aldrich, St. Louis, MO, USA) prepared in boric acid buffer (50 mM, pH 7.6). The leaves were subsequently incubated in 95% ethanol with three changes before the images were taken. Relative DAB stain

intensity was analyzed by measuring infiltrated patches' pixel intensity using regions of interest (ROI) with ImageJ software (Schindelin et al., 2012).

3.4 Results

3.4.1 A Single Amino Acid Substitution Enhances RNA Silencing Suppression Potency of CLRDV $P0^{AL}$

From previous study (Akinyuwa et al., 2023), it was reported that the P0 protein encoded by CLRDV-AL ($P0^{AL}$) acts as a weak VSR and hypothesized its potential correlation with the cryptic traits of the virus during host infection. While $P0^{AL}$ shares a conserved F-box-like motif with other CLRDV strains (Figure 1B), there are notable differences in specific aa residues when compared to CLRDV-ty and CLRDV-at (Akinyuwa et al., 2023). It was postulated that these divergent residues might contribute to the distinctive characteristics of $P0^{AL}$ and the cryptic traits of CLDRV-AL. To investigate this, a series of constructs that express $P0^{AL}$ mutants were generated, each carrying a single amino acid substitution at specific residues within the F-box-like motif (Figure 1C; pAI-$P0^{L68A}$, pAI-$P0^{P69A}$, pAI-$P0^{F71I}$, pAI-$P0^{F71L}$, and pAI-$P0^{V72I}$), and compared their VSR potency to that of the WT $P0^{AL}$ (Figure 2). Each construct harboring the ORF of P0 from $P0^{AL}$, $P0^{ty}$, and the five mutants was co-infiltrated into the leaves of *N. benthamiana* 16C plants along with the pAI-GFP, which expresses a free GFP, via agroinfiltration. Upon observation under the UV light at five dpi, non-infiltrated leaves showed a basal level of GFP fluorescence generated from their own GFP transgene expression (Figure 2A; Mock). However, leaves co-infiltrated with a free GFP construct and an empty vector did not exhibit GFP fluorescence and appeared red due to chloroplast autofluorescence (Figure 2A; EV). As previously reported (Akinyuwa et al. 2023), the leaves co-infiltrated with $P0^{ty}$ and $P0^{AL}$ exhibited a marked difference in GFP fluorescence levels. Strong GFP fluorescence was observed in leaves co-infiltrated with $P0^{ty}$, while leaves co-infiltrated with $P0^{AL}$ displayed less GFP fluorescence (Figure 2A; $P0^{ty}$ and $P0^{AL}$). Among the $P0^{AL}$ mutants, three ($P0^{P69A}$, $P0^{F71I}$, and $P0^{F71L}$) showed little to no GFP fluorescence, resembling the control infiltration using the empty vector. The green fluorescence in the leaves co-infiltrated with $P0^{L68A}$ remained at a level similar to that observed with $P0^{AL}$. Notably, the leaves co-infiltrated with $P0^{V72I}$ displayed strong GFP fluorescence, comparable to the level of green fluorescence observed in the leaves co-infiltrated with $P0^{ty}$ (Figure 2A; V72I). The relative intensities of the GFP fluorescence, visually evaluated under UV light, indicated that the substitution at aa residue 72 of $P0^{AL}$ increased the VSR potency of $P0^{AL}$ to a level similar to that of $P0^{ty}$.

To further evaluate the efficiency of RNA silencing suppression among the mutants, the patches of the infiltrated leaves were examined using a fluorescence microscope for quantitative analysis (Figure 2B, see Supplementary Figure 1 for more representative images). The relative fluorescence intensity was calculated from more than 13 images per treatment using ROI on ImageJ and analyzed by one-way ANOVA test in R (Figure 2C). The analysis revealed no significant difference in the GFP fluorescence within the infiltrated patches of three P0 mutants ($P0^{P69A}$, $P0^{F71I}$, and $P0^{F71L}$) compared to the control patch (EV) (Figure 2C; denoted as 'd'). Their green fluorescence levels were even lower than those analyzed from buffer-infiltrated *N. benthamiana* 16c control (Figure 3C; 16c, denoted as 'c'), suggesting that these three mutant P0s failed to suppress RNA silencing. There was no significant difference in the green fluorescence levels between the patches infiltrated with $P0^{L68A}$ and $P0^{AL}$ (Figure 2C; denoted as 'b'), which is consistent with the results observed under the UV light. The green fluorescence level of the patches infiltrated with $P0^{V72I}$ was similar to that of $P0^{ty}$, and their fluorescence levels were significantly different ($p < 0.01$) than the other groups (Figure 2C; denoted as 'a'). To further validate this observation, the relative accumulation of GFP mRNA was analyzed by quantitative real-time PCR (Figure 2D). In line with the results in Figure 2C, the relative GFP mRNA levels were divided into three groups. The highest levels of GFP mRNA were detected in the tissue infiltrated with $P0^{ty}$ or $P0^{V72I}$, aligning with the result shown in Figure 2C, where $P0^{V72I}$ was denoted as a group 'a' along with $P0^{ty}$. Following this, $P0^{AL}$ and $P0^{L68A}$ formed an intermediate group, corresponding to the group 'b' in Figure 2C. The tissue infiltrated with $P0^{P69A}$, $P0^{F71I}$, or $P0^{F71L}$ showed the lowest amount of GFP mRNA, similar to the control, EV This aligns with the 'd' group as noted in Figure 2C. These results collectively suggested that a single aa substitution, changing V (valine) to I (isoleucine) within the F-box-like motif, restored the VSR potency of $P0^{AL}$ to a level comparable to that demonstrated by the P0 protein of CLRDV-ty.

3.4.2 F-box-motif Modulates HR-like Response Triggered by CLRDV P0

Many poleroviral P0 proteins have been previously reported to induce hypersensitive response-like (HR-like) reactions, including the formation of necrotic lesions and the accumulation of reactive oxygen species (ROS) (Liang et al., 2023; Mangwende et al., 2009; Wang et al., 2015, 2021b; Zhang et al., 2021). To determine if CLRDV P0 proteins elicit similar responses in plants,

N. benthamiana leaves were infiltrated with the P0 constructs from three different strains (Figure 1C; pAI-P0^{AL}, pAI-P0^{at}, pAI-P0^{ty}) using agroinfiltration (Figure 3). Within three days post-infiltration (dpi), leaf patches expressing the P0 proteins began displaying HR-like necrotic lesions, which were observed up to 8 dpi (Figure 3A). However, the necrotic phenotype triggered by all three P0 proteins at 8 dpi was less severe than what was shown by the P38 protein of Turnip crinkle virus (P/C) that triggered a more robust programmed cell death response (Kant et al., 2015). Interestingly, among the three P0s, P0^{ty} induced a more pronounced necrotic lesion response than the P0 proteins from the atypical and Alabama strains. To investigate whether the cell death phenotype associated with the P0 proteins was also linked to ROS accumulation, agroinfiltrated leaves were collected at 3 dpi and subjected to treatment with DAB to detect hydrogen peroxide (Figure 3B). The staining revealed brown pigmentation in all constructs within the infiltrated patches (white dotted circles). Notably, the intensity of the brown pigmentation was visibly stronger in patches infiltrated with P0^{ty} or P/C compared to the patches infiltrated with P0^{at} or P0^{AL}. For a more precise assessment of the relative ROS production among these patches, the intensity of the DAB staining was measured (Figure 3E). The analysis indicated that P0^{ty} triggered a similar amount of ROS accumulation to that induced by P/C (Figure 3E; denoted as 'a'), which was higher than the accumulation resulting from P0^{AL} or P0^{at} (Figure 3E; denoted as 'b'). These results suggest that CLRDV P0 proteins can induce HR-like responses and ROS accumulation, implying that P0 proteins may serve as pathogenicity factors.

A previous study on *Pepper Vein Yellows Virus* (PeVYV) demonstrated that aa substitutions within the F-box-like motif altered P0's capacity to induce HR-like response and ROS accumulation (Wang et al., 2021b). To investigate whether the F-box-like motif within CLRDV P0 proteins is similarly responsible for the phenotypes observed above, *N. benthamiana* leaves were infiltrated with the P0 constructs featuring five single aa substitutions as described above. The agroinfiltrated plants were maintained for up to 8 dpi (Figure 3C). Similar to what was observed with P0^{AL}, mild necrotic lesions were developed within the infiltrated patches expressing the mutant P0 proteins. Interestingly, more rapid lesion development was observed on the leaf patch infiltrated with P0^{P69A}. To determine the presence of accumulated ROS, DAB staining was conducted on the agroinfiltrated leaves collected at 3 dpi (Figure 3D). Upon visual examination, there appeared to be subtle difference in the intensity of brown pigmentation among the P0 mutants. For more precise assessment, the relative ROS accumulation was analyzed using ImageJ

software (Figure 3F). As expected, the quantitative measurement revealed differences in ROS production among the mutant P0 proteins. Two mutants, $P0^{P68A}$ and $P0^{V72I}$, which demonstrated relatively higher VSR potency (Figure 2), accumulated a slightly lower amount of ROS than $P0^{AL}$. In contrast, three mutants, $P0^{P69A}$, $P0^{F71I}$, and $P0^{F71L}$, which exhibited little or no VSR potency (Figure 2), accumulated more ROS than $P0^{AL}$. These results suggest that aa residues within the F-box-like motif of the CLRDV P0 protein play an important role in its ability to induce ROS accumulation and HR-like lesions. Furthermore, the observed correlation between the phenotypes analyzed in Figure 2 and Figure 3, particularly with respect to the same aa substitution mutations, highlights the significance of VSR potency for the P0 protein as a potential pathogenicity factor.

3.4.3 F-box-like Motif Plays a Role in the Intracellular Localization of CLRDV P0

Understanding the intracellular localization of virus proteins provides insight to unravel their functions and roles in the viral infection cycle. The subcellular localization of poleroviral P0 proteins has elucidated some key mechanisms of the P0 in viral infection (Wang et al., 2018, 2021b). To extend the understanding of CLRDV-encoded P0 proteins, this chapter examined the subcellular localization of CLRDV P0 protein by expressing it fused to the GFP ORF at its C-terminal end. The P0 proteins of three CLRDV stains (Figure 1C; $P0^{AL}$:GFP, $P0^{ty}$:GFP, $P0^{at}$:GFP) and aa substitution mutants of $P0^{AL}$ (Figure 1C; $P0^{L68A}$:GFP, $P0^{P69A}$:GFP, $P0^{F71I}$:GFP, $P0^{F71L}$:GFP, $P0^{V72I}$:GFP) were constructed and expressed in *N. benthamiana* plants by agroinfiltration along with a pAI:GFP (Figure 4). Upon the observation using a fluorescence microscope, the green fluorescence from pAI:GFP expressing a free GFP was evenly distributed along the cell membrane and within the nucleus (Figure 4A; panel GFP). However, marked differences was observed from examined localization patterns of the green fluorescence emitted by the GFP-fused P0 proteins from the three CLRDV strains. as they displayed uneven and discontinuous These P0 proteins exhibited irregular and intermittent green fluorescence along the cell membrane (Figure 4A; panels ty, at, and AL). Interestingly, there was noteable difference in the fluorescence pattern of $P0^{AL}$:GFP from $P0^{ty}$:GFP or $P0^{at}$:GFP. In contrast to $P0^{ty}$:GFP or $P0^{at}$:GFP, the green fluorescence from $P0^{AL}$:GFP was seen as multiple speckles that accumulated along the cell membrane (Figure 4A; AL, white triangles) and formed intense aggregates within the cytoplasm (Figure 4A; AL, red triangles). Furthermore, $P0^{AL}$:GFP did not display prominent nuclear fluorescence, which was

observed in the case of $P0^{ty}$:GFP and $P0^{at}$:GFP (Figure 4A; ty and at, yellow triangles). Among the five mutants of $P0^{AL}$ tagged with GFP, four of them exhibited a similar green fluorescence pattern to that of wild-type $P0^{AL}$:GFP. These mutants displayed large, intense aggregates within the cytoplasm and multiple speckles along the cell membrane, resembling the pattern observed with P0AL:GFP (Figure 4A; L68A, P69A, F71I, and F71L). Conversely, $P0^{V72I}$:GFP displayed a different pattern. Its fluorescence was more akin to that of $P0^{ty}$:GFP or $P0^{at}$, characterized by pronounced nuclear fluorescence and fewer speckles along the cell membrane (Figure 4A; V72I, yellow triangles).

The intriguing subcellular localization patterns observed for CLRDV P0 proteins, characterized by multiple speckles and aggregates, prompted us to investigate the mechanisms underlying their function as VSR. Previous studies have revealed that the subcellular localization of poleroviral P0 proteins can influence their role in the degradation of AGO proteins when they are excluded from the endoplasmic reticulum (ER) membrane (Derrien et al., 2012; Michaeli et al., 2019a). To explore this further with CLRDV P0s, a similar approach was conducted by co-expressing GFP-fused P0 proteins from the three CLRDV strains (ty, at, and AL) along with a red fluorescent protein-tagged ER marker (RFP-ER), then observed the fluorescence in two different channels using a fluorescence microscope (Figure 4B). In the cells displaying both green and red fluorescence, indicating the co-expression of two infiltrated plasmid constructs, several bright orange spots were observed (Figure 4B; white triangles). These orange spots were not readily found in the leaves co-infiltrated with RFP-ER and a free GFP construct, implying that GFP was targeted to ER when fused to CLRDV P0s. These results align with previous studies that investigated other members of the genus *Polerovirus*, suggesting that CLRDV P0 proteins suppress RNA silencing through their association with the ER membrane, where they possibly interact with the host proteins to facilitate the degradation of AGO proteins.

3.5 Discussion

This chapter examined the properties of the F-box-like motif present in the suppressor of RNA silencing encoded by a newly isolated cotton-infecting Polerovirus, CLRDV-AL. This was achieved by using a series of mutant proteins with single aa substitutions. These aa substitutions were selected based on the variation found among three different strains of CLRDV (Akinyuwa et al., 2023). Through the five P0 mutants ($P0^{L68A}$, $P0^{P69A}$, $P0^{F71I}$, $P0^{F71L}$, and $P0^{V71I}$), this chapter demonstrated how a single aa alteration within the F-box-motif could lead to modifications in the protein's function.

The leucine (L) at the aa position 68 is conserved among CLRDVs and most members in the genus *Polerovirus*. In this study, $P0^{L68A}$, substituting this L with alanine showed minimal impact on the overall VSR potency (Figure 2). It suggests that this residue may not play a significant role in the mechanism of RNA silencing suppression by P0. In contrast, the substitution of Proline (P) at aa position 69 to alanine ($P0^{P69A}$) resulted in a complete loss of VSR potency (Figure 2). This can be attributed to the importance of P for maintaining the structural integrity and stability of the protein, as noted in previous studies (Kumar et al., 1998; Pemberton et al., 2012). Similar loss of VSR potency induced by the change of these two aa residues was also reported from the P0 proteins of *Maize yellow dwarf virus*-RMV2 (Wang et al., 2018), *Potato leafroll virus* (Zhuo et al., 2014), and PEVYV (Wang et al., 2021b). More notable case relates to the substitution at the aa position 72, converting V to I, which is the aa present in $P0^{ty}$, a stronger VSR among three CLRDVs (Akinyuwa et al., 2023). Remarkably, $P0^{V72I}$ demonstrated a robust silencing suppression potency similar to that of $P0^{ty}$. This suggests that a naturally occurring mutation at this residue during viral replication in the field could give rise to a variant with increased VSR potency, potentially causing more severe disease (Ramos-Sobrinho et al., 2021; Tabassum et al., 2021). It is noteworthy , and also concerning, that a variant carrying the same substitution at this residue has recently been isolated in Texas, resulting in severe symptoms in the host (Tabassum et al., 2021). However, the enhancement in VSR potency appears to depend on the other residues within the F-box-like motif. A prior study involving P0 proteins from CLRDV-ty and CLRDV-at conducted by Agrofoglio et al. (2019) introduced the same mutation on the aa position 72 and the VSR potency was compared. In that study, a change from V to I on $P0^{at}$ enhanced the VSR potency. However, it was a slight increase, unlike what was shown by $P0^{AL}$

carrying the same substitution ($P0^{V72I}$) here, suggesting that other residues within the motif may also influence and collaborate in determining the overall VSR function of the P0 protein. The results from two other mutants, $P0^{F71I}$ and $P0^{F71L}$, which exhibited little to no suppression activity, further support the hypothesis that the VSR potency of the P0 protein is not solely determined by a single amino acid at position 72.

A previous study that delved into the function of aa residues within the F-box-like motif of PeVYV P0 revealed that a specific aa, leucine, positioned at the start of the motif, played a critical role in inducing programmed cell death when expressed in the host (Wang et al., 2015). This is the same leucine found at aa position 68 in $P0^{AL}$ (figure 1C). The results from this chapter align with it, an observed reduction in the formation of HR-like lesions and the accumulation of reactive oxygen species (ROS) (Figure 3). However, in this chapter, which involved more mutants targeting additional aa residues, $P0^{V72I}$ induced less necrosis, much like $P0^{L68A}$. On the contrary, the necrosis triggered by three mutants ($P0^{P69A}$, $P0^{F71I}$, and $P0^{F71L}$) that exhibited little to no VSR activity was more severe compared to $P0^{AL}$ and approached the levels induced by $P0^{ty}$ or $P0^{at}$. It's important to note that it is yet premature to draw any conclusions regarding a direct correlation between the functions of specific residues within the F-box-like motif in both suppressing RNA silencing and inducing an HR-like response. Further investigations are needed, such as comprehensive surveys involving multiple residue substitution mutants or examinations of the interactions between the P0 protein and host proteins involved in the RNA silencing pathway, to gain a deeper understanding of these mechanisms.

The mechanism of RNA silencing suppression by the P0 protein has been extensively explored in other members of the genus *Polerovirus*. In these studies, it has been shown that P0 proteins effectively seize a host factor, SKP1, to degrade AGO proteins (Baumberger et al., 2007; Csorba et al., 2010; Derrien et al., 2012). Notably, in two poleroviruses, *Beet western yellows virus* (BWYV) and *Turnip yellows virus* (TuYV), it has been demonstrated that their P0 proteins interact with ER membrane-bound AGO1, subsequently form vesicles (Derrien et al., 2012; Michaeli et al., 2019). Additionally, BWYV P0 triggers the removal of unloaded AGO1 from the nucleus (Csorba et al., 2010), while TuYV P0 degrades AGO4, which predominantly localizes in the soluble fraction (Li et al., 2016; Michaeli et al., 2019). Results from this chapter, as shown in Figure 4B, indicate that the P0 proteins from three different CLRDV strains share an association

with the endoplasmic reticulum (ER), suggesting a conserved mechanism of RNA silencing suppression common to them, irrespective of the strain. However, it's important to note that the prominent nuclear accumulation observed in $P0^{ty}$, $P0^{at}$, and $P0^{V72I}$ (Figure 4A) implies that nuclear localization may have contributed to differentiating their VSR potency, potentially making them more effective than $P0^{AL}$ and the other $P0^{AL}$ mutants.

It is evident from these results that the collective variation within the F-box-like motif of the P0 proteins among the three strains of CLRDV contributes to the difference in the levels of silencing suppression potency and pathogenicity. However, it is not clear whether there is a correlation between VSR potency and subcellular localization, and whether this leads to the altered pathogenicity of the virus. As an RNA virus, CLRDV is prone to frequent mutations and the potential emergence of new isolates that can cause more severe disease in cotton. Given the global economic significance of cotton, it is imperative to elucidate the pathogenicity mechanism of CLRDV through further molecular investigations of the P0 protein and the host factors involved with it. This will help us understand how different CLRDV strains display a wide range of disease symptoms and severity.

3.6 References

Agrofoglio, Y.C., Delfosse, V.C., Casse, M.F., Hopp, H.E., Bonacic Kresic, I., Ziegler-Graff, V., Distéfano, A.J., 2019. P0 protein of cotton leafroll dwarf virus-atypical isolate is a weak RNA silencing suppressor and the avirulence determinant that breaks the cotton Cbd gene-based resistance. *Plant Pathology* 68, 1059–1071. doi: 10.1111/ppa.13031

Agrofoglio, Y.C., Delfosse, V.C., Casse, M.F., Hopp, H.E., Kresic, I.B., Distéfano, A.J., 2017. Identification of a new cotton disease caused by an atypical cotton leafroll dwarf virus in Argentina. *Phytopathology* 107, 369–376. doi: 10.1094/PHYTO-09-16-0349-R

Akinyuwa, M.F., Price, B.K., Martin, K.M., Kang, S.-H., 2023. A newly isolated cotton-infecting Polerovirus with cryptic pathogenicity encodes a weak suppressor of RNA silencing. *Frontiers in Agronomy* 5, 2673-3218. doi: 10.3389/fagro.2023.1235168

Almasi, R., Miller, W.A., Ziegler-Graff, V., 2015. Mild and severe cereal yellow dwarf viruses differ in silencing suppressor efficiency of the P0 protein. *Virus Research* 208, 199–206. doi: 10.1016/j.virusres.2015.06.020

Avelar, S., Ramos-Sobrinho, R., Conner, K., Nichols, R.L., Lawrence, K., Brown, J.K., 2020. Characterization of the complete genome and P0 protein for a previously unreported genotype of cotton leafroll dwarf virus, an introduced polerovirus in the United States. *Plant Disease* 104, 780–786. doi: 10.1094/PDIS-06-19-1316-RE/ASSET/IMAGES/LARGE/PDIS-06-19-1316-RE_T2

Avelar, S., Schrimsher, D.W., Lawrence, K., Brown, J.K., 2019. First report of Cotton Leafroll Dwarf Virus associated with Cotton Blue Disease symptoms in Alabama. *Plant Dis.* 103, 592. doi: 10.1094/PDIS-09-18-1550-PDN.

Bag, S., Roberts, P.M., Kemerait, R.C., 2021. Cotton Leafroll Dwarf Disease: An emerging virus disease on cotton in the U.S. *Crops & Soils* 54, 18–22. doi: 10.1002/crso.20105

Baumberger, N., Tsai, C.-H., Lie, M., Havecker, E., Baulcombe, D.C., 2007. The Polerovirus silencing suppressor P0 targets ARGONAUTE proteins for degradation. *Curr Biol* 17, 1609–1614. doi: 10.1016/j.cub.2007.08.039

Blevins, T., Rajeswaran, R., Shivaprasad, P.V., Beknazariants, D., Si-Ammour, A., Park, H.-S., Vazquez, F., Robertson, D., Meins, F., Hohn, T., Pooggin, M.M., 2006. Four plant Dicers mediate viral small RNA biogenesis and DNA virus induced silencing. *Nucleic Acids Res* 34, 6233–6246. doi: 10.1093/nar/gkl886

Bologna, N.G., Iselin, R., Abriata, L.A., Sarazin, A., Pumplin, N., Jay, F., Grentzinger, T., Dal Peraro, M., Voinnet, O., 2018. Nucleo-cytosolic shuttling of ARGONAUTE1 prompts a revised model of the plant microRNA pathway. *Mol Cell* 69, 709-719.e5. doi: 10.1016/j.molcel.2018.01.007

Bortolamiol, D., Pazhouhandeh, M., Marrocco, K., Genschik, P., Ziegler-Graff, V., 2007. The Polerovirus F box protein P0 targets ARGONAUTE1 to suppress RNA silencing. *Curr Biol* 17, 1615–1621. doi: 10.1016/j.cub.2007.07.061

Bortolamiol-Bécet, D., Monsion, B., Chapuis, S., Hleibieh, K., Scheidecker, D., Alioua, A., Bogaert, F., Revers, F., Brault, V., Ziegler-Graff, V., 2018. Phloem-triggered virus-induced gene silencing using a recombinant Polerovirus. *Frontiers in Microbiology* 9. 1664-302X. doi: 10.3389/fmicb.2018.02449

Carrasco, P., Daròs, J.A., Agudelo-Romero, P., Elena, S.F., 2007. A real-time RT-PCR assay for quantifying the fitness of tobacco etch virus in competition experiments. *Journal of Virological Methods* 139, 181–188. doi: 10.1016/j.jviromet.2006.09.020

Cascardo, R.S., Arantes, I.L.G., Silva, T.F., Sachetto-Martins, G., Vaslin, M.F.S., Corrêa, R.L., 2015. Function and diversity of P0 proteins among cotton leafroll dwarf virus isolates. *Virology Journal* 12, 123. doi: 10.1186/s12985-015-0356-7

Cornish, P.V., Hennig, M., Giedroc, D.P., 2005. A loop 2 cytidine-stem 1 minor groove interaction as a positive determinant for pseudoknot-stimulated –1 ribosomal frameshifting. Proceedings of the *National Academy of Sciences* 102, 12694–12699. doi: 10.1073/pnas.0506166102

Correa, R., Silva, T., Simoes-Araujo, J., Barroso, P., Vidal, M., Vaslin, M., 2005. Molecular characterization of a virus from the family *Luteoviridae* associated with cotton blue disease. *Archives of virology* 150, 1357–67. doi: 10.1007/s00705-004-0475-8.

Correa, R.L., Bruckner, F.P., De Souza Cascardo, R., Alfenas-Zerbini, P., 2013. The role of F-Box proteins during viral infection. *International Journal of Molecular Sciences* 14, 4030–4049. doi: 10.3390/ijms14024030

Csorba, T., Lózsa, R., Hutvágner, G., Burgyán, J., 2010. Polerovirus protein P0 prevents the assembly of small RNA-containing RISC complexes and leads to degradation of ARGONAUTE1. *Plant J* 62, 463–472. doi: 10.1111/j.1365-313X.2010.04163.x

da Silva, A.K.F., Romanel, E., Silva, T. da F., Castilhos, Y., Schrago, C.G., Galbieri, R., Bélot, J.-L., Vaslin, M.F.S., 2015. Complete genome sequences of two new virus isolates associated with cotton blue disease resistance breaking in Brazil. *Arch Virol* 160, 1371–1374. doi: 10.1007/s00705-015-2380-8

DeBlasio, S.L., Xu, Y., Johnson, R.S., Rebelo, A.R., MacCoss, M.J., Gray, S.M., Heck, M., 2018. The interaction dynamics of two Potato Leafroll Virus movement proteins affects their localization to the outer membranes of mitochondria and plastids. *Viruses* 10, 585. doi: 10.3390/v10110585

Delfosse, V.C., Agrofoglio, Y.C., Casse, M.F., Kresic, I.B., Hopp, H.E., Ziegler-Graff, V., Distéfano, A.J., 2014. The P0 protein encoded by cotton leafroll dwarf virus (CLRDV) inhibits local but not systemic RNA silencing. *Virus Res* 180, 70–75. doi: 10.1016/j.virusres.2013.12.018

Delfosse, V.C., Barrios Barón, M.P., Distéfano, A.J., 2021. What we know about poleroviruses: Advances in understanding the functions of polerovirus proteins. *Plant Pathology* 70, 1047–1061. doi: 10.1111/ppa.13368

Derrien, B., Baumberger, N., Schepetilnikov, M., Viotti, C., De Cillia, J., Ziegler-Graff, V., Isono, E., Schumacher, K., Genschik, P., 2012. Degradation of the antiviral component ARGONAUTE1 by the autophagy pathway. *Proc Natl Acad Sci U S A* 109, 15942–15946. doi: 10.1073/pnas.1209487109

Derrien, B., Clavel, M., Baumberger, N., Iki, T., Sarazin, A., Hacquard, T., Ponce, M.R., Ziegler-Graff, V., Vaucheret, H., Micol, J.L., Voinnet, O., Genschik, P., 2018. A suppressor screen for AGO1 degradation by the viral F-Box P0 protein uncovers a role for AGO DUF1785 in sRNA duplex unwinding. *The Plant Cell* 30, 1353–1374. doi: 10.1105/tpc.18.00111

Distéfano, A.J., Bonacic Kresic, I., Hopp, H.E., 2010. The complete genome sequence of a virus associated with cotton blue disease, cotton leafroll dwarf virus, confirms that it is a new member of the genus Polerovirus. *Arch Virol* 155, 1849–1854. doi: 10.1007/s00705-010-0764-3

Edula, S.R., Bag, S., Milner, H., Kumar, M., Suassuna, N.D., Chee, P.W., Kemerait, R.C., Hand, L.C., Snider, J.L., Srinivasan, R., Roberts, P.M., 2023. Cotton leafroll dwarf disease: An enigmatic viral disease in cotton. *Molecular Plant Pathology* 24, 513–526. doi: 10.1111/mpp.13335

Fusaro, A.F., Correa, R.L., Nakasugi, K., Jackson, C., Kawchuk, L., Vaslin, M.F.S., Waterhouse, P.M., 2012. The Enamovirus P0 protein is a silencing suppressor which inhibits local and systemic RNA silencing through AGO1 degradation. *Virology* 426, 178–187. doi: 10.1016/j.virol.2012.01.026

Galbieri, R., Boldt, A.S., Scoz, L.B., Rodrigues, S.M., Rabel, D.O., Belot, J.L., Vaslin, M., da Franca Silva, T., Kobayasti, L., Chitarra, L.G., 2017. Cotton blue disease in central-west Brazil: Occurrence, vector (*Aphis gossypii*) control levels and cultivar reaction. Trop. *plant pathol*. 42, 468–474. doi: 10.1007/s40858-017-0165-1

Hammond, S.M., 2005. Dicing and slicing: the core machinery of the RNA interference pathway. *FEBS Lett* 579, 5822–5829. doi: 10.1016/j.febslet.2005.08.079

Hofius, D., Herbers, K., Melzer, M., Omid, A., Tacke, E., Wolf, S., Sonnewald, U., 2001. Evidence for expression level-dependent modulation of carbohydrate status and viral resistance by the potato leafroll virus movement protein in transgenic tobacco plants. *The Plant Journal* 28, 529–543. doi: 10.1046/j.1365-313X.2001.01179.x

Kang, S.-H., Atallah, O.O., Sun, Y.-D., Folimonova, S.Y., 2018. Functional diversification upon leader protease domain duplication in the Citrus Tristeza Virus genome: Role of RNA sequences and the encoded proteins. *Virology* 514, 192–202. doi: 10.1016/j.virol.2017.11.014

Kang, S.-H., Bak, A., Kim, O.-K., Folimonova, S.Y., 2015. Membrane association of a nonconserved viral protein confers virus ability to extend its host range. *Virology* 482, 208–217. 10.1016/j.virol.2015.03.047

Kang, S.H., Sun, Y.D., Atallah, O.O., Huguet-Tapia, J.C., Noble, J.D., Folimonova, S.Y., 2019. A long non-coding RNA of Citrus Tristeza Virus: Role in the virus interplay with the host immunity. *Viruses* 11. doi: 10.3390/V11050436

Kaplan, I.B., Lee, L., Ripoll, D.R., Palukaitis, P., Gildow, F., Gray, S.M., 2007. Point mutations in the potato leafroll virus major capsid protein alter virion stability and aphid transmission. *J Gen Virol* 88, 1821–1830. doi: 10.1099/vir.0.82837-0

King, A.M.Q., Adams, M.J., Carstens, E.B., Lefkowitz, E.J. (Eds.), 2012. Family - Luteoviridae, in: Virus Taxonomy. *Elsevier, San Diego*, pp. 1045–1053. doi: 10.1016/B978-0-12-384684-6.00090-2

Kozlowska-Makulska, A., Guilley, H., Szyndel, M.S., Beuve, M., Lemaire, O., Herrbach, E., Bouzoubaa, S., 2010. P0 proteins of European beet-infecting poleroviruses display variable RNA silencing suppression activity. *J Gen Virol* 91, 1082–1091. doi: 10.1099/vir.0.016360-0

Kumar, T.K., Samuel, D., Jayaraman, G., Srimathi, T., Yu, C., 1998. The role of proline in the prevention of aggregation during protein folding in vitro. *Biochem Mol Biol Int* 46, 509–517. doi: 10.1080/15216549800204032

LaTourrette, K., Holste, N.M., Garcia-Ruiz, H., 2021. Polerovirus genomic variation. *Virus Evol* 7, veab102. doi: 10.1093/ve/veab102

Lee, L., Kaplan, I.B., Ripoll, D.R., Liang, D., Palukaitis, P., Gray, S.M., 2005. A surface loop of the potato leafroll virus coat protein is involved in virion assembly, systemic movement, and aphid transmission. *J Virol* 79, 1207–1214. doi: 10.1128/JVI.79.2.1207-1214.2005

Lee, L., Palukaitis, P., Gray, S.M., 2002. Host-Dependent Requirement for the Potato leafroll virus 17-kDa Protein in Virus Movement. *MPMI* 15, 1086–1094. doi: 10.1094/MPMI.2002.15.10.1086

Li, F., Wang, A., 2019. RNA-targeted antiviral immunity: More than just RNA silencing. *Trends in Microbiology* 27, 792–805. doi: 10.1016/j.tim.2019.05.007

Li, Shengben, Le, B., Ma, X., Li, Shaofang, You, C., Yu, Y., Zhang, B., Liu, L., Gao, L., Shi, T., Zhao, Y., Mo, B., Cao, X., Chen, X., 2016. Biogenesis of phased siRNAs on membrane-bound polysomes in Arabidopsis. *eLife* 5, e22750. doi: 10.7554/eLife.22750

Li, Y., Sun, Q., Zhao, T., Xiang, H., Zhang, Xiaoyan, Wu, Z., Zhou, C., Zhang, Xin, Wang, Y., Zhang, Y., Wang, X., Li, D., Yu, J., Dinesh-Kumar, S.P., Han, C., 2019. Interaction between Brassica Yellows Virus silencing suppressor P0 and plant SKP1 facilitates stability of P0 in vivo against degradation by proteasome and autophagy pathways. *New Phytol* 222, 1458–1473. doi: 10.1111/nph.15702

Liang, K.-L., Liu, J.-Y., Bao, Y.-Y., Wang, Z.-Y., Xu, X.-B., 2023. Screening and identification of host factors interacting with the virulence factor P0 encoded by Sugarcane Yellow Leaf Virus by Yeast Two-Hybrid assay. *Genes* 14, 1397. doi: 10.3390/genes14071397

Lin, J., Guo, J., Finer, J., Dorrance, A.E., Redinbaugh, M.G., Qu, F., 2014. The Bean Pod Mottle Virus RNA2-encoded 58-kilodalton protein P58 is required in cis for RNA2 accumulation. *Journal of Virology* 88, 3213–3222. doi: 10.1128/jvi.03301-13

Livak, K.J., Schmittgen, T.D., 2001. Analysis of relative gene expression data using real-time quantitative PCR and the 2(-Delta Delta C(T)) Method. *Methods* 25, 402–408. doi: 10.1006/meth.2001.1262

Luo, C., Wang, Z.Q., Liu, X., Zhao, L., Zhou, X., Xie, Y., 2019. Identification and analysis of potential genes regulated by an alphasatellite (TYLCCNA) that contribute to host resistance against Tomato Yellow Leaf Curl China Virus and its betasatellite (TYLCCNV/TYLCCNB) infection in *Nicotiana benthamiana. Viruses* 11, 442–442. doi: 10.3390/V11050442

Mangwende, T., Wang, M.-L., Borth, W., Hu, J., Moore, P.H., Mirkov, T.E., Albert, H.H., 2009. The P0 gene of Sugarcane Yellow Leaf Virus encodes an RNA silencing suppressor with unique activities. *Virology* 384, 38–50. doi: 10.1016/j.virol.2008.10.034

Michaeli, S., Clavel, M., Lechner, E., Viotti, C., Wu, J., Dubois, M., Hacquard, T., Derrien, B., Izquierdo, E., Lecorbeiller, M., Bouteiller, N., De Cilia, J., Ziegler-Graff, V., Vaucheret, H., Galili, G., Genschik, P., 2019b. The viral F-box protein P0 induces an ER-derived autophagy degradation pathway for the clearance of membrane-bound AGO1. *Proceedings of the National Academy of Sciences* 116, 22872–22883. doi: 10.1073/pnas.1912222116

Parkash, V., Sharma, D.B., Snider, J., Bag, S., Roberts, P., Tabassum, A., West, D., Khanal, S., Suassuna, N., Chee, P., 2021. Effect of Cotton Leafroll Dwarf Virus on physiological processes and yield of individual cotton plants. *Front Plant Sci* 12, 734386. doi: 10.3389/fpls.2021.734386

Pazhouhandeh, M., Dieterle, M., Marrocco, K., Lechner, E., Berry, B., Brault, V., Hemmer, O., Kretsch, T., Richards, K.E., Genschik, P., Ziegler-Graff, V., 2006. F-box-like domain in the polerovirus protein P0 is required for silencing suppressor function. *Proc. Natl. Acad. Sci. U.S.A.* 103, 1994–1999. doi: 10.1073/pnas.0510784103

Pemberton, T.A., Still, B.R., Christensen, E.M., Singh, H., Srivastava, D., Tanner, J.J., 2012. Proline: mother nature's cryoprotectant applied to protein crystallography. *Acta Crystallogr D Biol Crystallogr* 68, 1010–1018. doi: 10.1107/S0907444912019580

Peter, K.A., Gildow, F., Palukaitis, P., Gray, S.M., 2009. The C terminus of the polerovirus p5 readthrough domain limits virus infection to the phloem. *J Virol* 83, 5419–5429. doi: 10.1128/JVI.02312-08

Peter, K.A., Liang, D., Palukaitis, P., Gray, S.M., 2008. Small deletions in the Potato Leafroll Virus readthrough protein affect particle morphology, aphid transmission, virus movement and accumulation. *J Gen Virol* 89, 2037–2045. doi: 10.1099/vir.0.83625-0

Ramos-Sobrinho, R., Adegbola, R.O., Lawrence, K., Schrimsher, D.W., Isakeit, T., Alabi, O.J., Brown, J.K., 2021. Cotton Leafroll Dwarf Virus US genomes comprise divergent subpopulations and harbor extensive variability. *Viruses* 13, 2230. doi: 10.3390/v13112230

Rashid, M.-O., Zhang, X.-Y., Wang, Y., Li, D.-W., Yu, J.-L., Han, C.-G., 2019. The three essential motifs in P0 for suppression of RNA silencing activity of Potato Leafroll Virus are required for virus systemic infection. *Viruses* 11, 170. doi: 10.3390/v11020170

Rodriguez-Medina, C., Boissinot, S., Chapuis, S., Gereige, D., Rastegar, M., Erdinger, M., Revers, F., Ziegler-Graff, V., Brault, V., 2015. A protein kinase binds the C-terminal domain of the readthrough protein of Turnip yellows virus and regulates virus accumulation. *Virology* 486, 44–53. doi: 10.1016/j.virol.2015.08.031

Schindelin, J., Arganda-Carreras, I., Frise, E., Kaynig, V., Longair, M., Pietzsch, T., Preibisch, S., Rueden, C., Saalfeld, S., Schmid, B., Tinevez, J.-Y., White, D.J., Hartenstein, V., Eliceiri, K.,

Tomancak, P., Cardona, A., 2012. Fiji: an open-source platform for biological-image analysis. *Nat Methods* 9, 676–682. doi: 10.1038/nmeth.2019

Smirnova, E., Firth, A.E., Miller, W.A., Scheidecker, D., Brault, V., Reinbold, C., Rakotondrafara, A.M., Chung, B.Y.W., Ziegler-Graff, V., 2015. Discovery of a small non-AUG-initiated ORF in Poleroviruses and Luteoviruses that is required for long-distance movement. *PLOS Pathogens* 11, e1004868–e1004868.

Sõmera, M., Fargette, D., Hébrard, E., Sarmiento, C., 2021. ICTV virus taxonomy profile: Solemoviridae 2021. *J Gen Virol* 102, 001707. doi: 10.1099/jgv.0.001707

Sun, Q., Li, Y.Y., Wang, Y., Zhao, H.H., Zhao, T.Y., Zhang, Z.Y., Li, D.W., Yu, J.L., Wang, X.B., Zhang, Y.L., Han, C.G., 2018. Brassica Yellows Virus P0 protein impairs the antiviral activity of NbRAF2 in *Nicotiana benthamiana. Journal of Experimental Botany* 69, 3127–3139. doi: 10.1093/jxb/ery131

Sun, Q., Zhuo, T., Zhao, T., Zhou, C., Li, Y., Wang, Y., Li, D., Yu, J., Han, C., 2020. Functional characterization of RNA silencing suppressor P0 from Pea Mild Chlorosis Virus. *International Journal of Molecular Sciences* 21, 7136. doi: 10.3390/ijms21197136

Sun, Y.D., Folimonova, S.Y., 2019. The p33 protein of Citrus Tristeza Virus affects viral pathogenicity by modulating a host immune response. *New Phytologist* 221, 2039–2053. doi: 10.1111/nph.15482

Tabassum, A., Bag, S., Suassuna, N.D., Conner, K.N., Chee, P., Kemerait, R.C., Roberts, P., 2021. Genome analysis of cotton leafroll dwarf virus reveals variability in the silencing suppressor protein, genotypes and genomic recombinants in the USA. *PLoS One* 16, e0252523. doi: 10.1371/journal.pone.0252523

Terradot, L., Souchet, M., Tran, V., Giblot Ducray-Bourdin, D., 2001. Analysis of a three-dimensional structure of Potato Leafroll Virus coat protein obtained by homology modeling. *Virology* 286, 72–82. doi: 10.1006/viro.2001.0900

Voinnet, O., 2005. Induction and suppression of RNA silencing: insights from viral infections. *Nat Rev Genet* 6, 206–220. doi: 10.1038/nrg1555

Wang, F., Zhao, X., Dong, Q., Zhou, B., Gao, Z., 2018. Characterization of an RNA silencing suppressor encoded by Maize Yellow Dwarf Virus-RMV2. *Virus Genes* 54, 570–577. doi: 10.1007/s11262-018-1565-0

Wang, K.-D., Dughbaj, M.A., Nguyen, T.T.V., Nguyen, T.Q.Y., Oza, S., Valdez, K., Anda, P., Waltz, J., Sacco, M.A., 2023. Systematic mutagenesis of Polerovirus protein P0 reveals distinct and overlapping amino acid functions in *Nicotiana glutinosa*. *Virology* 578, 24–34. doi: 10.1016/j.virol.2022.11.005

Wang, K.-D., Empleo, R., Nguyen, T.T.V., Moffett, P., Sacco, M.A., 2015. Elicitation of hypersensitive responses in *Nicotiana glutinosa* by the suppressor of RNA silencing protein P0 from poleroviruses. *Molecular Plant Pathology* 16, 435–448. doi: 10.1111/mpp.12201

Wang, L., Tian, P., Yang, Xiuling, Zhou, X., Zhang, S., Li, C., Yang, Xuehui, Liu, Y., 2021a. Key amino acids for Pepper Vein Yellows Virus P0 protein pathogenicity, gene silencing, and subcellular localization. *Frontiers in Microbiology* 12, 1653–1653. doi: 10.3389/fmicb.2021.680658

Xia, Z., Cao, R., Sun, K., Zhang, H., 2012. The movement protein of Barley Yellow Dwarf Virus-GAV self-interacts and forms homodimers in vitro and in vivo. *Arch Virol* 157, 1233–1239. doi: 10.1007/s00705-012-1288-9

Zhang, X.-Y., Li, Y.-Y., Wang, Y., Li, D.-W., Yu, J.-L., Han, C.-G., 2021. Comparative analysis of biological characteristics among P0 proteins from different Brassica Yellows Virus genotypes. *Biology (Basel)* 10, 1076. doi: 10.3390/biology10111076

Zhang, X.-Y., Zhao, T.-Y., Li, Y.-Y., Xiang, H.-Y., Dong, S.-W., Zhang, Z.-Y., Wang, Y., Li, D.-W., Yu, J.-L., Han, C.-G., 2018. The conserved Proline18 in the Polerovirus P3a is important for Brassica Yellows Virus systemic infection. *Front Microbiol* 9, 613. doi: 10.3389/fmicb.2018.00613

Zhuo, T., Li, Y.-Y., Xiang, H.-Y., Wu, Z.-Y., Wang, X.-B., Wang, Y., Zhang, Y.-L., Li, D.-W., Yu, J.-L., Han, C.-G., 2014. Amino acid sequence motifs essential for P0-mediated suppression of RNA silencing in an isolate of Potato Leafroll Virus from Inner Mongolia. *MPMI* 27, 515–527. doi: 10.1094/MPMI-08-13-0231-R

Figures

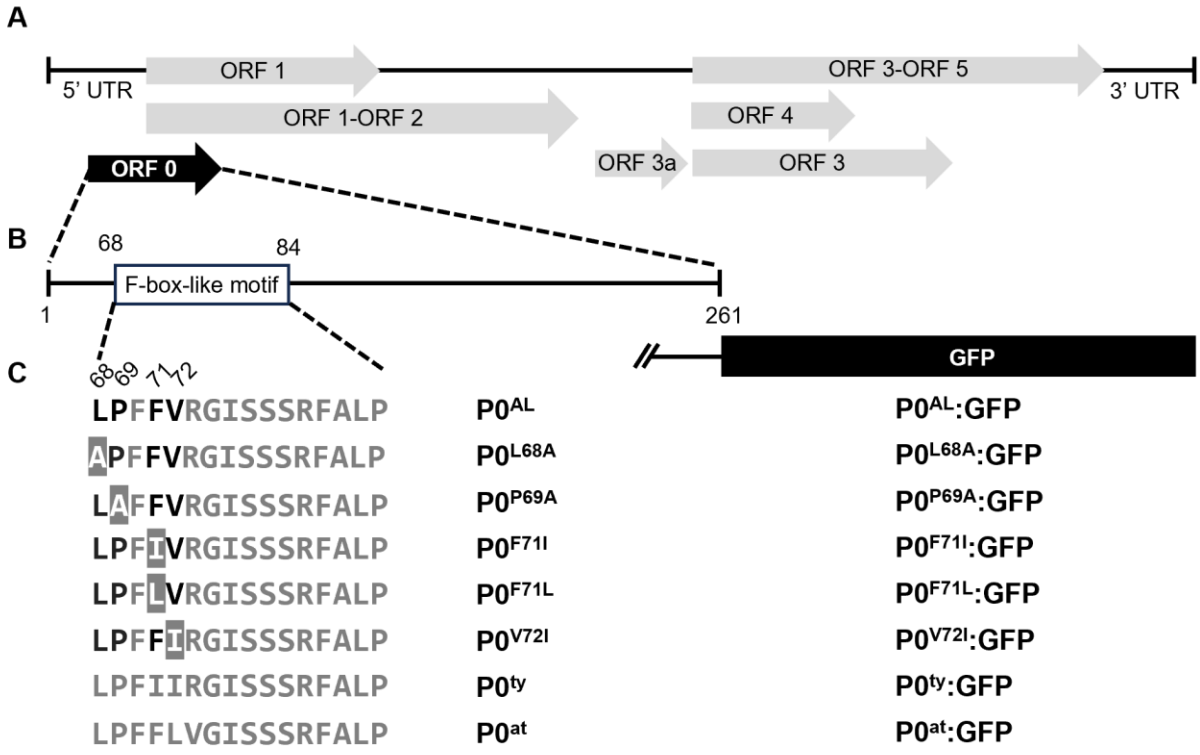

Figure 1*:* CLRDV P0 cDNA constructs.

(A) A schematic representation of the CLRDV-AL genome. Open reading frames (ORFs) are represented as gray and black arrowhead boxes. **(B)** A schematic diagram of an F-box-like motif within the ORF 0. Amino acid (aa) residue positions corresponding to both ends of the motif are shown. **(C)** The aa substitutions within the F-box-like motif of CLRDV P0 protein are identified as white letters on a gray background. Corresponding aa residue positions are shown. Another set of constructs with the same mutations fused with GFP ORF immediately after the 3' end of the P0 ORF (aa position 261) is depicted on the right.

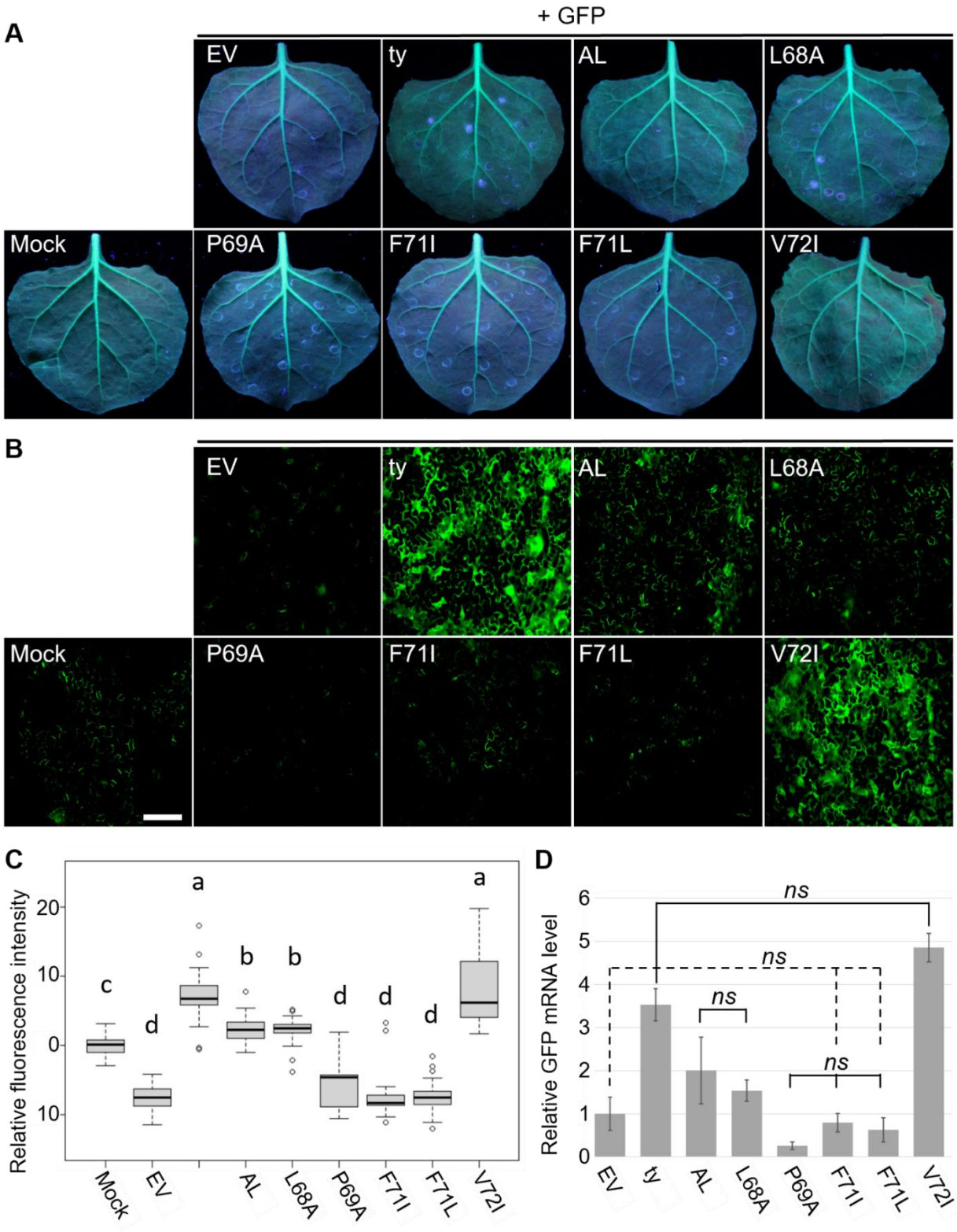
A
+ GFP
EV
ty
AL
L68A
Mock
P69A
F71I
F71L
V72I
B
EV
ty
AL
L68A
Mock
P69A
F71I
F71L
V72I
C
Relative fluorescence intensity
20
10
0
10
a
b
b
c
d
d
d
d
a
Mock
EV
AL
L68A
P69A
F71I
F71L
V72I
D
Relative GFP mRNA level
6
5
4
3
2
1
0
ns
ns
ns
ns
EV
ty
AL
L68A
P69A
F71I
F71L
V72I

Figure 2*:* Comparison of VSR potency among CLRDV P0s with single amino acid (aa) mutation within the F-box-like motif.

RNA silencing suppression activity of the P0 proteins from CLRDV-AL, CLRDV-ty, and five CLRDV-AL mutants ($P0^{L68A}$, $P0^{P69A}$, $P0^{F71I}$, $P0^{F71L}$, and $P0^{V72I}$) were compared by co-expressing GFP and each P0 in GFP-transgenic *N. benthamiana* (16c) plants by Agroinfiltration. Images were taken at 5 dpi under the UV light (**A**) and using a fluorescence microscope (**B**). Scale bar = 180 µm. Mock; non-infiltrated *N. benthamiana* 16c plant, EV; empty vector. **(C)** The green fluorescence intensity was calculated using the Region of Interest (ROI) on ImageJ. The relative intensity was analyzed by one-way ANOVA in R and depicted as a box and whisker plot. Each boxplot represents the interquartile range (middle 50% of the data), the lower and upper edges show the first and third quartile (25th and 75th percentile, respectively), and the median (horizontal line within the box). The whiskers are the contributions within the 1.5 interquartile range; open circles beyond these whiskers are considered outliers; significant differences, $p < 0.01$, were denoted by letters. **(D)** GFP mRNA levels in tissues co-infiltrated with a set shown in (A) were analyzed by RT-qPCR. Error bars indicate the standard deviation of the means of Ct values in three biological repeats using the *actin2* reference gene and $2^{-\Delta\Delta Ct}$ method. Statistically significant differences were determined by Student's t-test. Non-significant groups are indicated (*ns*). Each non-significant group is significantly different from the other at $p < 0.01$, but not noted.

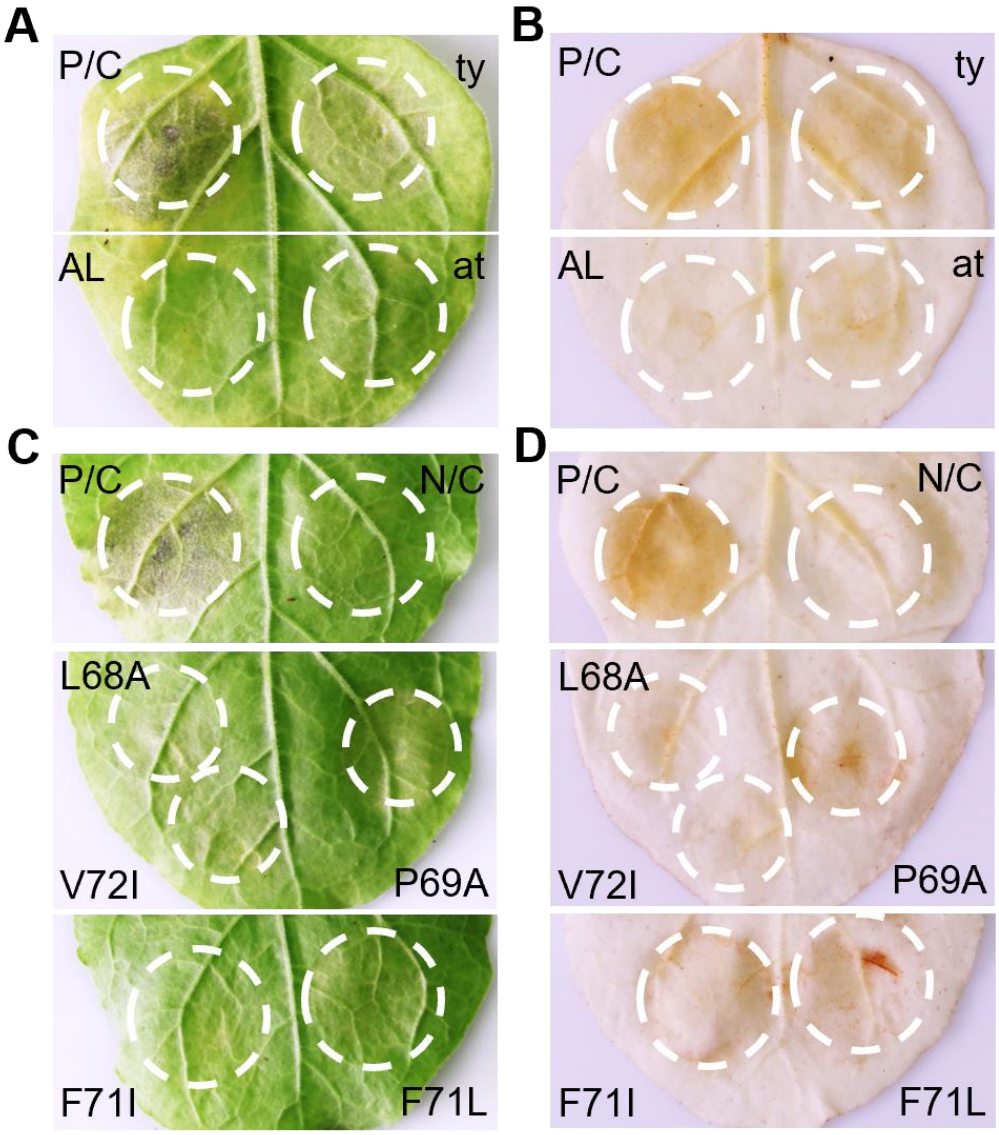
A
P/C
ty
AL
at
B
P/C
ty
AL
at
C
P/C
N/C
L68A
V72I
P69A
F71I
F71L
D
P/C
N/C
L68A
V72I
P69A
F71I
F71L

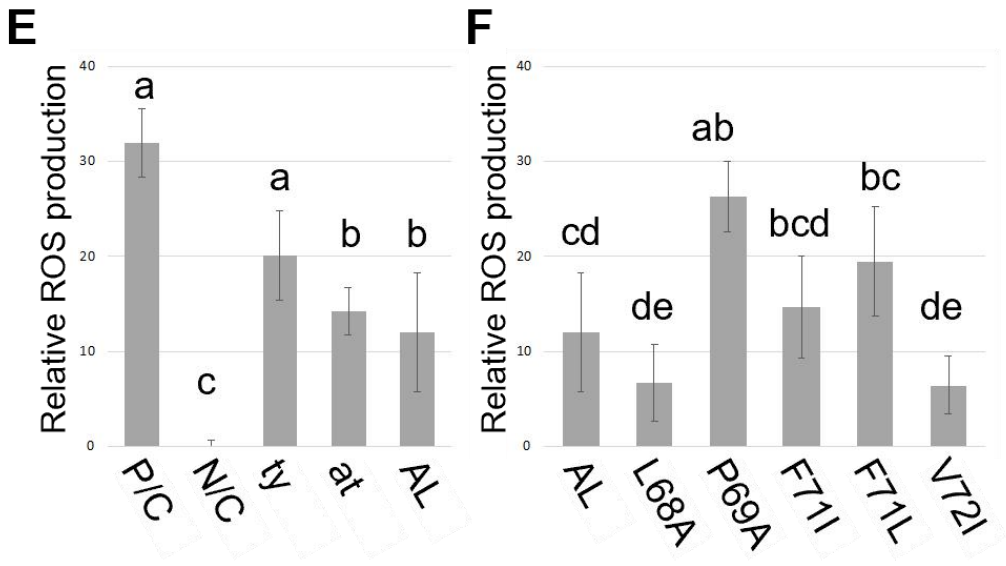
E
Relative ROS production
40
30
20
10
0
a
c
a
b
b
P/C
N/C
ty
at
AL
F
Relative ROS production
40
30
20
10
0
cd
de
ab
bcd
bc
de
AL
L68A
P69A
F71I
F71L
V72I

Figure 3: The P0 proteins of CLRDV and its mutants trigger an HR-like response and accumulate reactive oxygen species (ROS).

The P0 proteins from three CLRDV strains (**A** and **B**) and the aa substitution mutants of $P0^{AL}$ (**C** and **D**) were transiently expressed in *Nicotiana benthamiana* by agroinfiltration. Left panels (A and C) are bright field images showing necrotic phenotype within the infiltrated patches (white dotted circle). Images were taken at 8 dpi. Right panels (B and D) are infiltrated *N. benthamiana* leaves treated by 3,3´-diaminobenzidine (DAB) staining to demonstrate ROS accumulation within the infiltrated patches (white dotted circle). Images were taken at 3 dpi. Relative ROS production (**E** and **F**) was analyzed by measuring the color intensity of DAB staining using the ROI on ImageJ. Values are means from at least three independent patches per treatment. Error bars are standard deviation. Statistically significant differences, $p < 0.01$, determined by one-way ANOVA are denoted by letters.

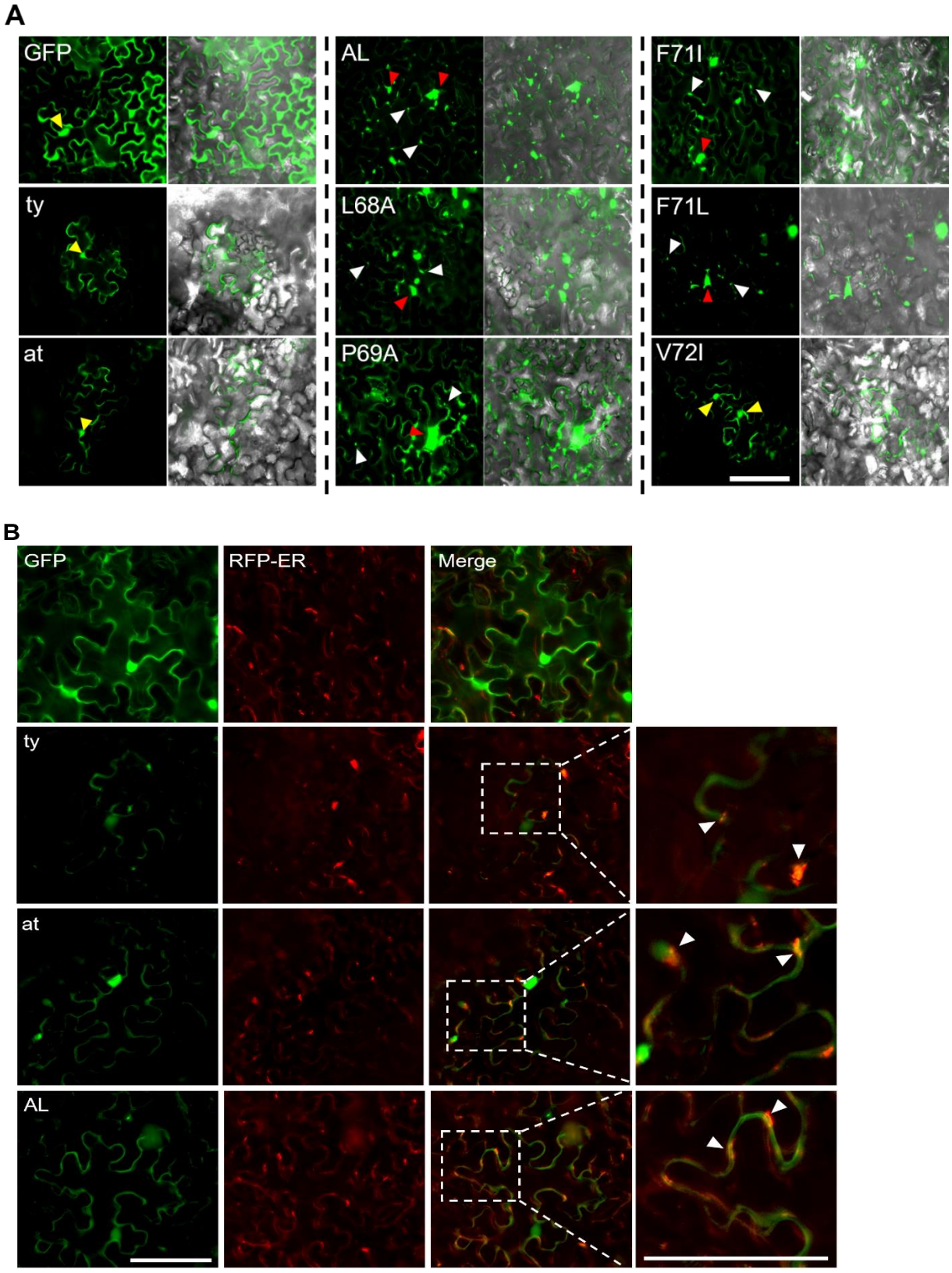
A
GFP
ty
at
AL
L68A
P69A
F71I
F71L
V72I
B
GFP
RFP-ER
Merge
ty
at
AL

Figure 4: Intracellular localization of the P0 proteins.

(A) The P0 proteins from three CLRDV strains (ty, at, and AL) and the amino acid (aa) substitution mutants of $P0^{AL}$ (L68A, P69A, F71I, F71L, and V72I) fused to the green fluorescent protein (GFP) were transiently expressed in *Nicotiana benthamiana* leaves by agroinfiltration. Each set of images consists of two panels showing the GFP channel (left) and the GFP channel merged with the trans channel (right). Yellow, red, and white triangles point to nuclei, aggregates, and speckles, respectively. **(B)** The P0 proteins from three CLRDV strains (ty, at, and AL) fused to GFP were transiently expressed in *N. benthamiana* by agroinfiltration along with the red fluorescent protein (RFP)-tagged endoplasmic reticulum (ER) cellular marker (RFP-ER). Zoomed-in images on the far-right column correspond to the dotted square in the 'Merge' panels. White triangles point to the co-localized fluorescent molecules. Representative images were shown from four independent agroinfiltration sets for A and B panels. Images were taken at 5 days post infiltration. Scale bars = 100 µm.

Supplementary Figure

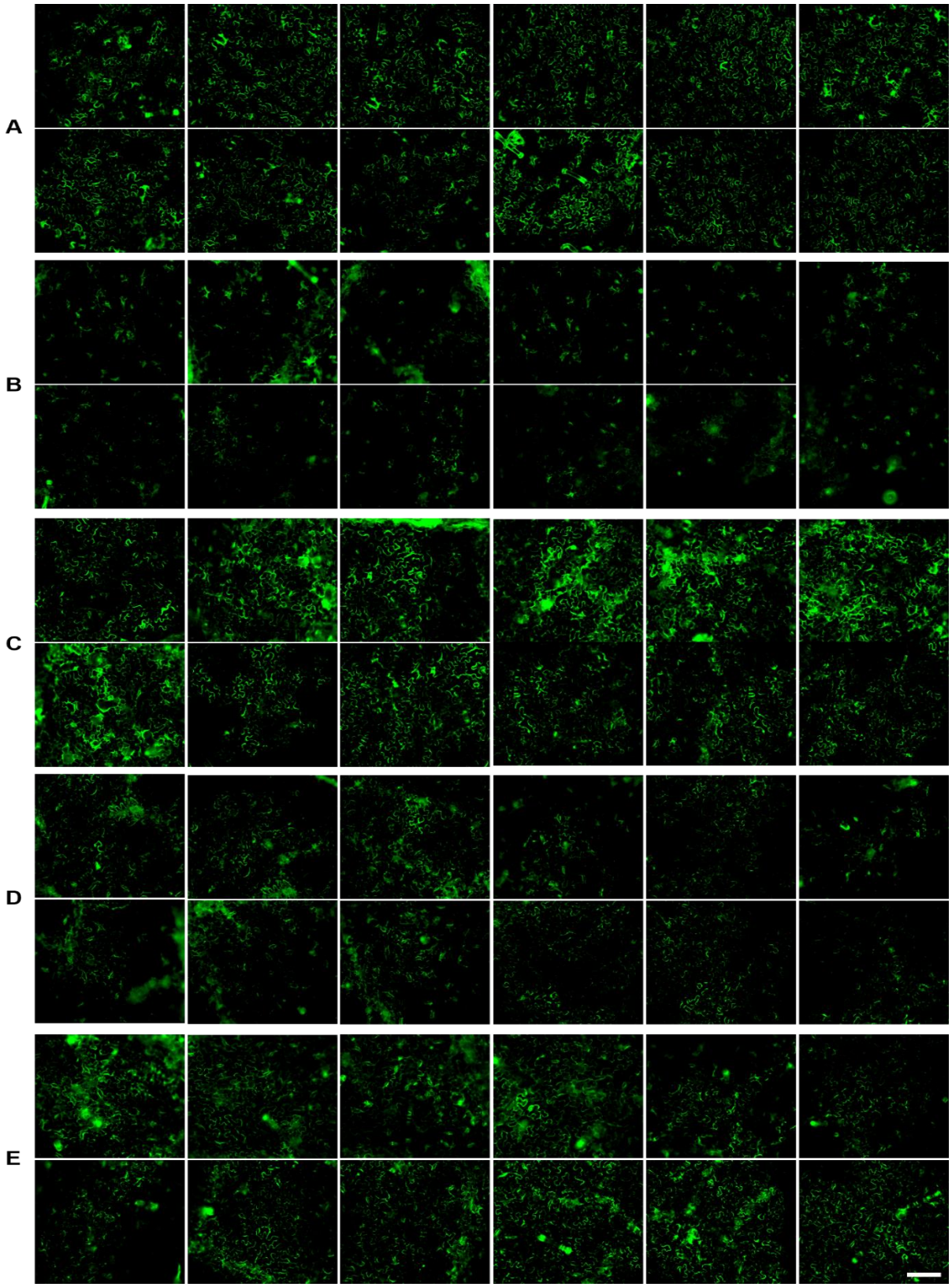

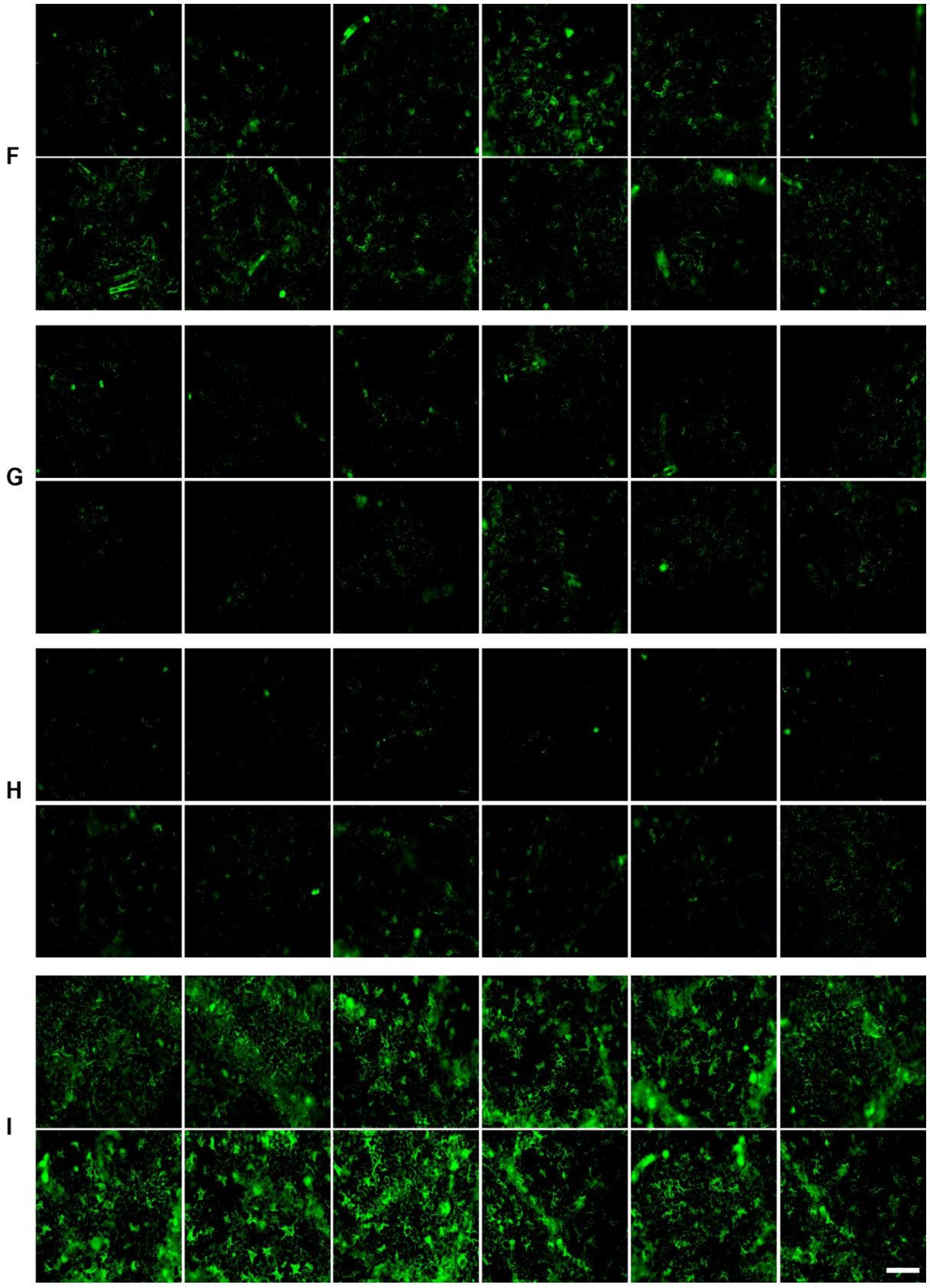
F
G
H
I

Supplementary Figure 1: Infiltrated leaf tissue showing suppression of GFP silencing from Figure 2A was examined using a fluorescence microscope. Representative images used to analyze relative green fluorescence intensity (Figure 2B) are shown. (**A**; 16C, **B**; GFP, **C**; $P0^{ty}$, **D**; $P0^{AL}$, **E**; $P0^{L68A}$, **F**; $P0^{P69A}$, **G**; $P0^{F71I}$, **H**; $P0^{F71L}$, **I**; $P0^{V72I}$). Scale bar = 180 μm.

Tables

Table 1: List of oligomers used for the generation of constructs and RT-qPCR assay.

Name	Sequence (5′ to 3′)	References
Q-5 site-directed mutagenesis		
pAI-P0^{L68A}:FW	TCTTTTTCTC**GCT**CCATTCTTCG	
pAI-P0^{L68A}:RV	AGAGAACGAAGGAGAAAAGA	This study,
pAI-P0^{P69A}:FW	TTTTCTCCTT**GCA**TTCTTCGTTA	Materials and
pAI-P0^{P69A}:RV	AGAAGAGAACGAAGGAGAAA	Methods 2.2
pAI-P0^{V72I}:FW	TCCATTCTTC**ATT**AGGGGAATTT	and 2.3
pAI-P0^{V72I}:RV	AGGAGAAAAAGAAGAGAACG	
Non-tagged P0s		
P0^{AL}.FW.*Apa*I	ACTA*GGGCCC*AACAATGTTGAATTTGATCATCT GC	This study,
P0^{AL}.RV.*Xba*I	GGAC*TCTAGA*TCAACTGCTTTCTCCTTCAC	Materials and
P0^{at}.FW.*Apa*I	ACTA*GGGCCC*AACAATGTTGAACTTGATTATCT GC	Methods 2.2
GFP-tagged P0s		
P0:GFP-FW	TATGTGAAGGAGAAAGCAGTATGGCTAGCAAAG GAGAAGA	This study,
P0:GFP-RV	TCTTCTCCTTTGCTAGCCATACTGCTTTCTCCTTC ACATA	Materials and Methods 2.3
GFP.RV.*Xba*I	GTAC*TCTAGA*CTATTTGTAGAGCTCATCC	
Sequence verification		
pAI SEQ FW	CCTCGAGAATTCTCAACACAAC	Akinyuwa et
pAI SEQ RV	GCTCAACACATGAGCGAAACCC	al., 2023
Quantitative mRNA analysis		
MFA.Gq-PCR:FW	GATGACGGGAACTACAAGAC	Akinyuwa et
MFA.Gq-PCR:RV	CGAGTACAACTATAACTCACAC	al., 2023
*NbACTIN*2-FW	CAATCCAGACACTGTACTTTCTCTC	Luo et al., 2019
*NbACTIN*2-RV	AAGCTGCAGGTATCCATGAGACTA	

The amino acid substitution mutation-inducing nucleotides through Q-5 site-directed mutagenesis are indicated in **bold** characters. Restriction endonuclease (*Xba*I and *Apa*I) recognition sequences are *italicized and underlined*.

Appendices

Preliminary characterization of CLRDV-AL proteins

The molecular characterization of CLRDV-AL proteins is crucial to understand protein functions and its role in viral infection cycle. Considering that cryptic trait of CLRDV-AL and its observed sequence variation from other known strains in South America, dissecting the function of each of its encoded proteins would serve as a preliminary resource to developing a resistant variety or other innovative molecular biological control method for this virus in the U.S.

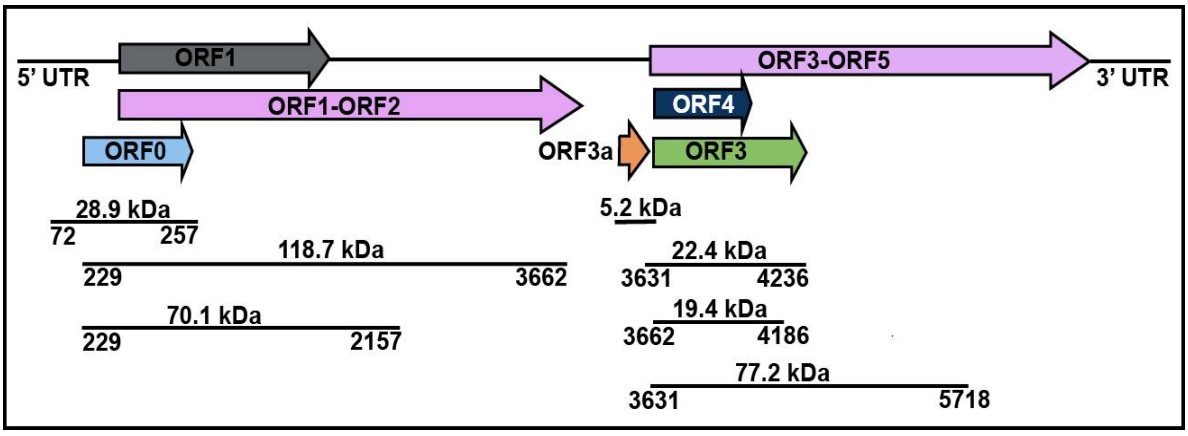

Figure 1: Schematic representation of CLRDV-AL genome structure and organization.

CLRDV-AL ORFs are portrayed as arrowhead boxes. ORF 0; encodes P0, a viral suppressor of RNA silencing. ORF1 and ORF2 encode P1 and P1-P2, involved in RNA dependent RNA polymerase (RdRp), ORF 3a and ORF 4 encode P3a and P4 responsible for virus movement. Finally, ORF 3 and ORF3-5 encode P3 and P3-5 proteins involved in major and minor coat proteins. Modified from Avelar et al., 2020.

DDO						
	P0	**P1**	**P3**	**P3a**	**P3a***	**P4**
P0	+	+	+	+	+	+
P1						
P3	+		+	+	+	+
P3a	+	+	+		+	
P3a*	+	+	+		+	+
P4	+	+	+		+	+

QDO and QDO/X/A						
	P0	**P1**	**P3**	**P3a**	**P3a***	**P4**
P0	-	-	-	-	-	-
P1						
P3	-		+	-	-	-
P3a	-	-	-		-	
P3a*	-	-	-		-	-
P4	-	-	-		-	-

Figure 2: CLRDV-AL protein interactome.

Saccharomyces cerevisiae Y2HGold small scale co-transformation with potential pairs of CLRDV-AL proteins was performed via GAL4-based Yeast two hybrid (YTH) system (Matchmaker Gold, Clontech Laboratories, Inc.). The constructs were cloned into pGBKT7 (pBD) and pGADT7 (pAD) plasmids and grown on selective agar media to test for their interaction via the yeast growth driven by the reporter gene(s) on the quadruple drop-out (QDO) selective media and the double drop-out media (DDO) enforced with Aureobasidin A. following the manufacturer's description. +; yeast growth present, demonstrating an interaction between two proteins, -; yeast growth not present, indicating absence of interaction between two proteins. Cell growth on DDO indicates both pAD and pBD plasmid co-transformation while growth on more stringent media (QDO and QDO/X/A) shows protein-protein interaction. As seen in P3 and P3 coat protein interaction. P3a* signifies P3a construct with canonical start codon (AUG). Note that this method does not identify the potential interaction of proteins that localize on a membrane.

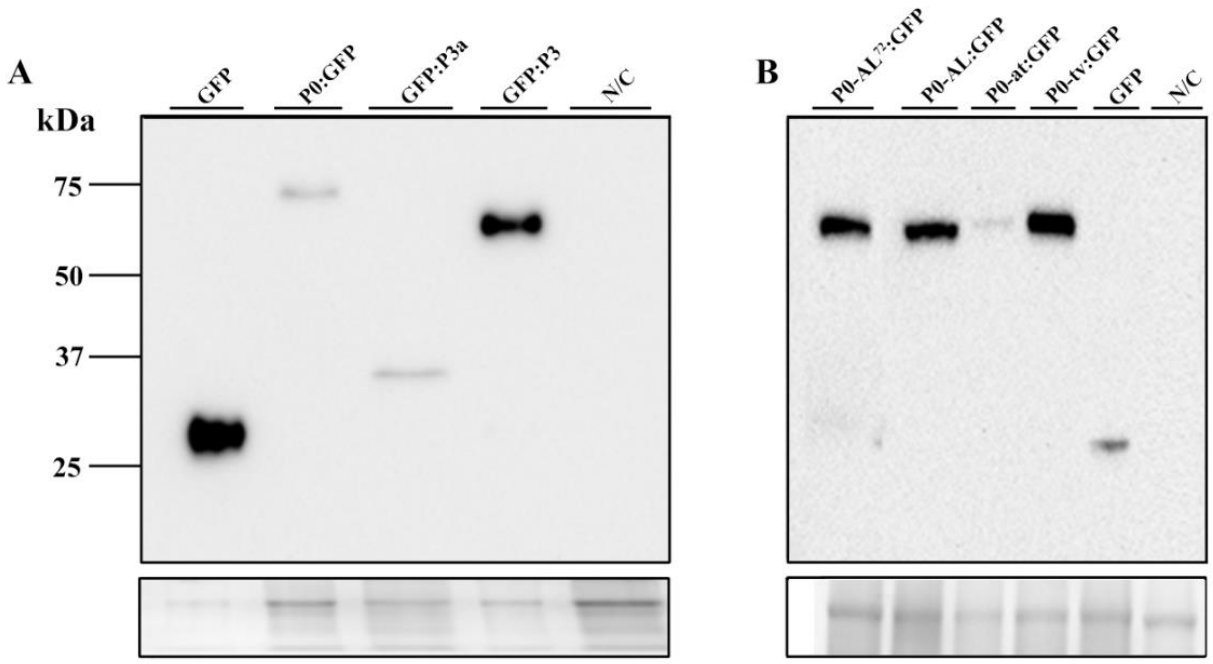

Figure 3: Western blot analysis of the leaves shown on the left panel.

(A) Protein expression of selected CLRDV-AL proteins tagged with GFP at the N terminal and C terminal ends (GFP:P3a, GFP:P3, and P0:GFP respectively), GFP and non-infiltrated (N/C) controls were detected using an anti-GFP antibody. (B) CLRDV VSR proteins (P0) from three strains $P0^{at}$, $P0^{ty}$, $P0^{AL}$, and $P0^{V72I}$; a mutant derivative of $P0^{AL}$ where Valine was substituted with Isoleucine and controls. Total protein was extracted from the infiltrated leaves of *N. benthamiana.* *S*amples were ground in lysis buffer (50Mm Tris-HCL, 1mM EDTA, 150mM NaCl, and 5% glycerol). The mixture was centrifuged at 15,000xg for 15 mins at 4^{o}C. This resulted in supernatant that was denatured in 6X loading dye at 100^{o}C for 10 mins prior to the loading into an SDS-PAGE gel for the separation. Coomassie blue stained gel image (3A; bottom) shows the protein separation before the transfer to PVDF membrane.

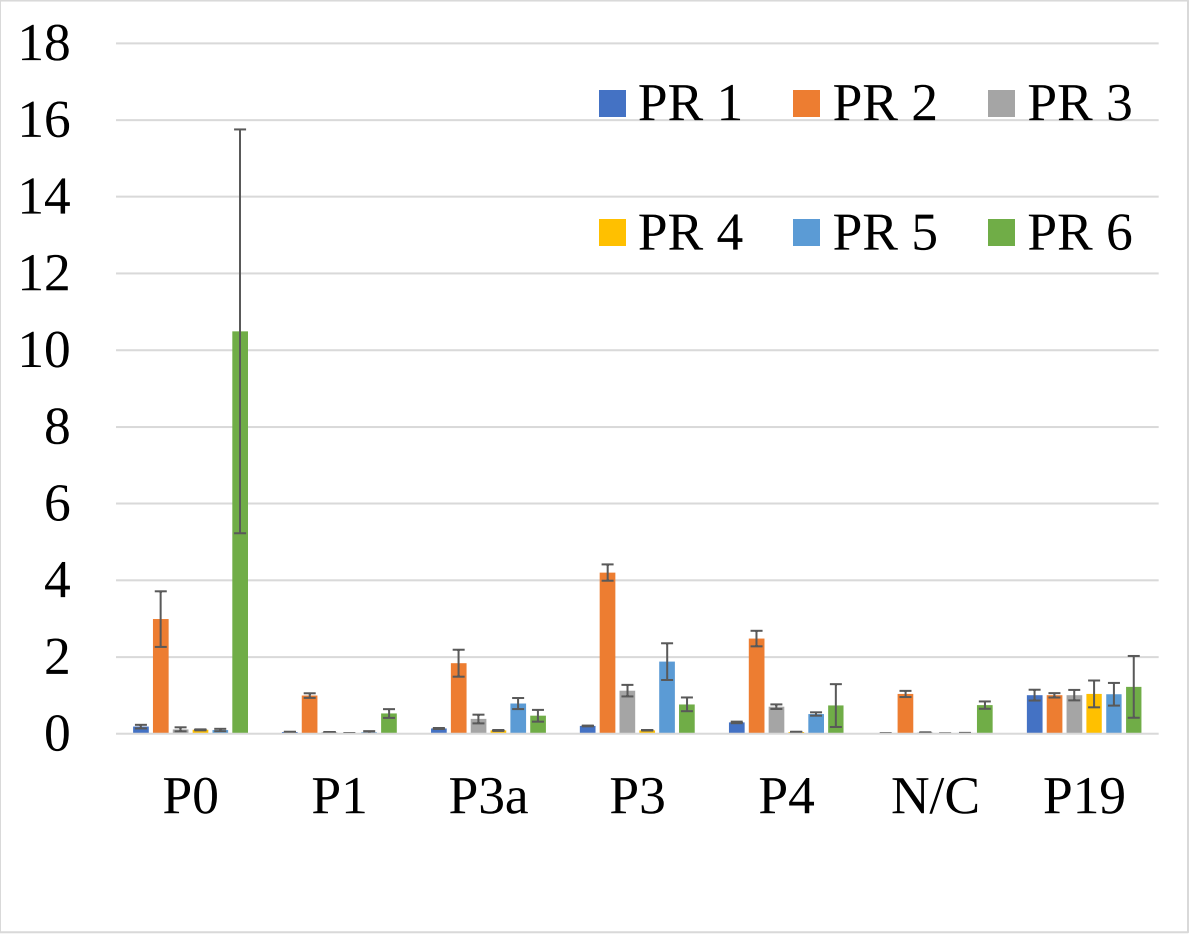

Figure 4: Differentially regulated pathogenicity-related (PR) genes.

Increased accumulation of *PR*-2 and *PR*-6 genes was observed. RT-qPCR analysis of *PR* genes (*PR*1–*PR*6) accumulation in CLRDV-AL protein infiltrated wild type (4C) *N. benthamiana* plants compared to P19 or buffer infiltrated (N/C) plants at 5 dpi. RNA extraction and one-step RT-qPCR was performed as described in Chapter 2 (See 2.3.5). Pairs of oligomers were used *PR* 1 -FW (5`- CCGCCTTCCCTCAACTCAAC-3`) and *PR* 1-RV (5`- GCACAACCAAGACGTACTGAG -3`) (Nie et al., 2021), *PR* 2-FW (5`- GCAGCAGACGATGTAATGATGG -3`) and *PR* 2-RV (5`- TCCACAAGCCTAGTGAGCCTC) (Jiang et al., 2021), *PR* 3-FW (5`- CAGGAGGGTATTGCTTTGTTAGG -3`) and *PR* 3-RV (5`- CGTGGGAAGATGGCTTGTTGTC -3`), *PR* 4-FW (5`- GGCCAAGATTCCTGTGGTAGAT -3`) and *PR* 4-RV (5`- CACTGTTGTTTGAGTTCCTGTTCCT -3`) (Nie et al., 2021), *PR* 5-FW5`- CCGAGGTAATTGTGAGACTGGAG -3`) and *PR* 5-RV (5`-

CCTGATTGGGTTGATTAAGTGCA -3`) (Guo et al., 2019), and *PR* 6-FW (5`-GGAGAGTCTGATCCTAGAAATCC -3`) and *PR* 6-RV (5`-GATGATGGAACTTTTGTTTGTGAAGGA- 3`). Bars shown are the means and standard deviation of Ct values analyzed using *actin* reference gene and $2^{-\Delta\Delta Ct}$ method (See Chapter 2).

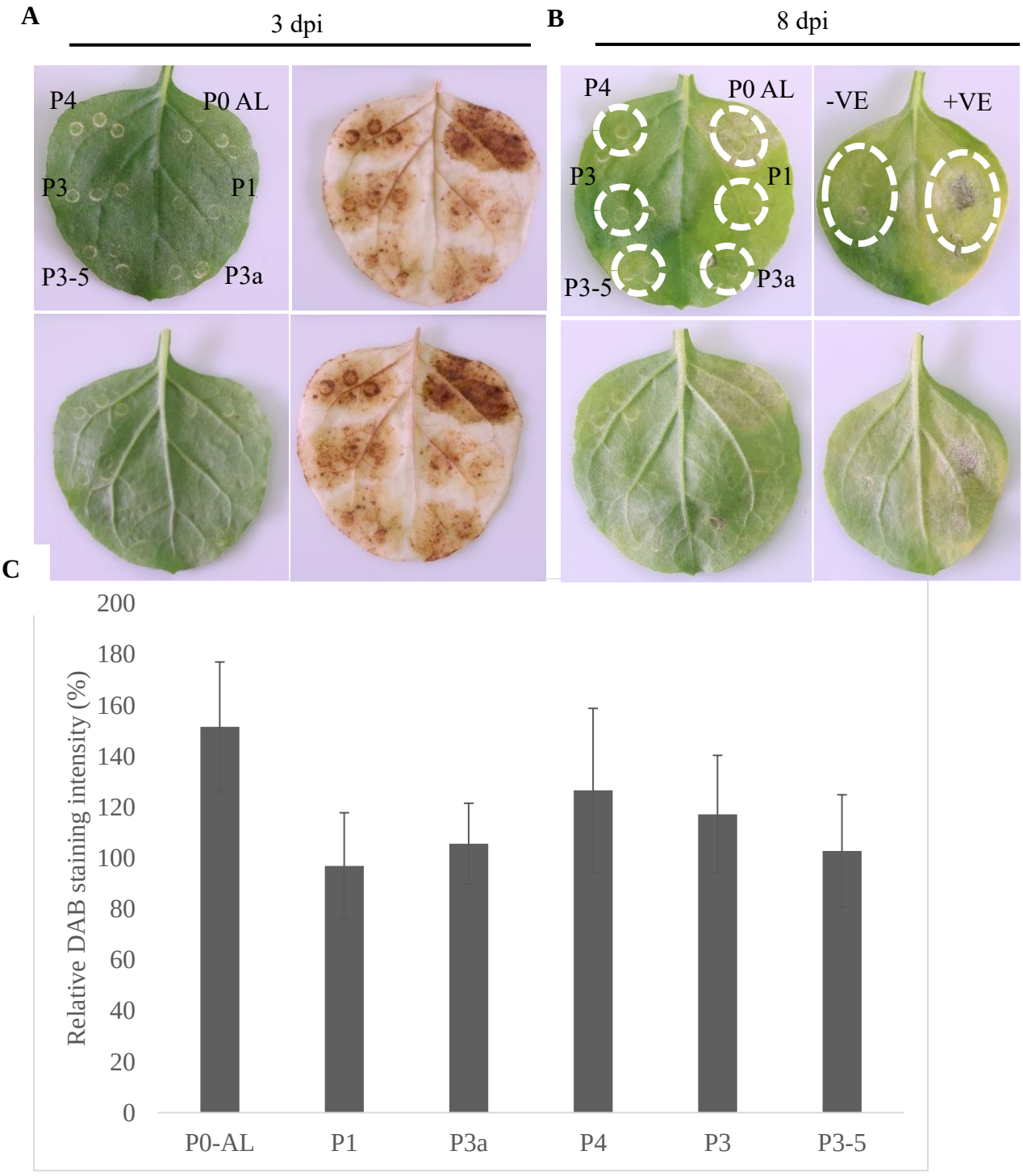
A
3 dpi
B
8 dpi
P4
P0 AL
P3
P1
P3-5
P3a
-VE
+VE
C
Relative DAB staining intensity (%)
200
180
160
140
120
100
80
60
40
20
0
P0-AL
P1
P3a
P4
P3
P3-5

Figure 5: CLRDV-AL proteins trigger HR-like and accumulate reactive oxygen species (ROS) with DAB staining.

CLRDV-AL proteins were individually expressed in *N. benthamiana* using agroinfiltration. (A) Infiltrated *N. benthamiana* leaves with bright field images and leaves treated with 3,3´ -diaminobenzidine (DAB) staining to demonstrate ROS accumulation within the infiltrated patches (white dotted circle). Images were taken at 3 dpi. Strong lesions were observed in the spot co-infiltrated with CLRDV-AL P0 and P19. Note that P0 protein is a viral suppressor of RNA silencing (VSR) of CLRDV-AL. (B) Bright field images showing necrotic phenotype within the infiltrated patches (white dotted circle). Images were taken at 8 dpi. (C) Relative ROS production was analyzed as described in Chapter 2. Statistically significant differences, $p < 0.01$, determined by one-way ANOVA are denoted by letters.

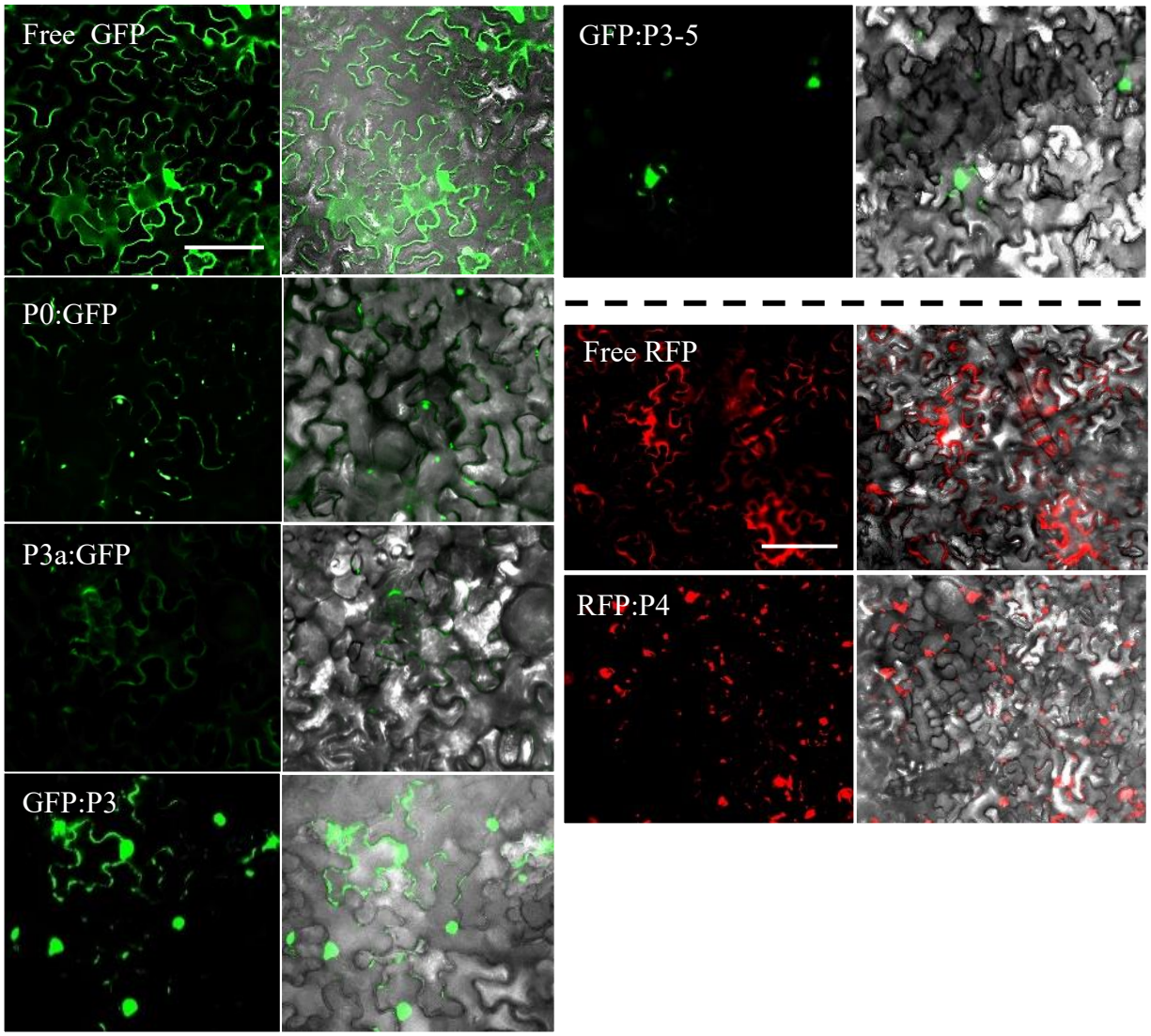
Free GFP
P0:GFP
P3a:GFP
GFP:P3
GFP:P3-5
Free RFP
RFP:P4

Figure 6: Subcellular localization of proteins encoded by CLRDV-AL in *N. benthamiana* leaves.

Proteins encoded by CLRDV-AL (P0, P3a, P3, P3-5) fused to the green fluorescent protein (GFP) and P4 fused to red fluorescent protein (RFP) were transiently expressed in *N. benthamiana* leaves by agroinfiltration individually expressed in the host cell (See Chapter 3). Each set of images consists of two panels showing the GFP or RFP channels (left) and the GFP or RFP channel merged with the trans channel (right). Fluorescence accumulation at different subcellular locations was observed. Note that the P0 protein was tagged by GFP on the C-terminal end, but other proteins were tagged on the N-terminal end. Scale bar = 100 µm.